Kuila, Debasish

KINETIC AND THERMODYNAMIC ASPECTS OF METALLO - N-ALKYLPORPHYRINS

City University of New York PH.D. 1984

PLEASE NOTE:

In all cases this material has been filmed in the best possible way from the available copy. Problems encountered with this document have been identified here with a check mark __✓__.

1. Glossy photographs or pages _____
2. Colored illustrations, paper or print _____
3. Photographs with dark background _____
4. Illustrations are poor copy __✓__
5. Pages with black marks, not original copy _____
6. Print shows through as there is text on both sides of page _____
7. Indistinct, broken or small print on several pages __✓__
8. Print exceeds margin requirements _____
9. Tightly bound copy with print lost in spine _____
10. Computer printout pages with indistinct print _____
11. Page(s) _____ lacking when material received, and not available from school or author.
12. Page(s) _____ seem to be missing in numbering only as text follows.
13. Two pages numbered _____. Text follows.
14. Curling and wrinkled pages _____
15. Other _____

KINETIC AND THERMODYNAMIC ASPECTS OF METALLO-N-ALKYLPORPHYRINS

by

Debasish Kuila

A dissertation submitted to the Graduate Faculty in Chemistry in partial fulfillment of the requirements for the degree of Doctor of Philosophy, The City University of New York.

1984

This manuscript has been read and accepted for the Graduate Faculty in Chemistry in satisfaction of the dissertation requirement for the degree of Doctor of Philosophy.

10/6/83
date

Chairman of Examining Comittee

10/6/83
date

Executive Officer

Thomas C. Stevens

Jacqueline Barton

Supervisory Committee

The City University of New York

Abstract

KINETIC AND THERMODYNAMIC ASPECTS OF METALLO-N-ALKYLPORPHYRINS

by

Debasish Kuila

Advisor: Professor David K. Lavallee

The occurrence of N-substituted porphyrins in animals and the possibility of using these compounds for therapy have stimulated an interest in their kinetic and thermodynamic properties. In the kinetic section of the dissertation, the dealkylation reactions which produce non-N-substituted metalloporphyrins are discussed. A variety of thermodynamic properties are presented in the subsquent chapters.

The nature of the solvent medium and nucleophile cause a pronounced effect on the dealkylation reactions of Cu(II) complexes of N-substituted porphyrins. The reactions are much slower in water than in acetonitrile(by about 100-fold) and dichloromethane(by about 10-fold). Amines are much better nucleophiles than pyridine or chloride ions. Porphy-

rin ring substituents have no mazor effect on the dealkylation reaction. However, the N-substituent has a profound effect. For example, under the similar conditions, the p-nitrobenzyl moiety is cleaved about 100 times faster than the methyl group and 1000 times faster than the ethyl group. Such carbocation-stabilizing substituents,therefore,should be useful in the rapid synthesis of radiolabelled metallo-non-N-alkylporphyrins.

Thermodynamic features of N-substituted porphyrin complexes which have been investigated include structural, electrochemical, epr and XPS properties. Comparisons of N-aryl(i.e. N-phenyl) and N-alkyl complexes show that the geometries in the solid state, electrochemical properties and spectroscopic properties are generally very similar. Large differences are evident, however, when N-substituted and non-N-substituted complexes are compared. For example, redox potentials greatly favor the reduced form of metallo-N-alkylporphyrins(Fe(II) and Mn(II)) and the cyclic voltammograms are highly reversible or quasi-reversible for non-N-substituted species. The reduction of Cu(II) to Cu(I) is evident in the voltammogram and is strongly affected by axial ligations.

DEDICATED

TO

MY PARENTS

ACKNOWLEDGEMENTS

I would first like to thank my mentor Professor David K. Lavallee for his help, guidance, admirable patience and criticism throughout the course of this work.

I am grateful to my colleagues and friends to make this work possible. I am thankful to Dr. Jon Doi, Bob Cavallo, Willio Gaillard and Dr. Douglas Miller for their help during the course of this work. I especially thank my friend A. Sudhakar for his generous help throughout this project work.

Support for this work from the National Institute of Health is greatfully acknowledged.

TABLE OF CONTENTS

Page

LIST OF TABLES

LIST OF ILLUSTRATIONS

CHAPTER 1

INTRODUCTION

Porphyrins, porphyrin derivatives and porphyrin-like materials are involved in reversible oxygen binding, electron transport, photosynthesis, and metabolic control and regulation in biological systems.[1-4] A wide variety of species with the basic porphyrin skeleton are known, including natural porphyrins: heme-derived hemeproteins; chlorophyll derivatives, vitamin B_{12} (a corrin), bile pigments (linear tetrapyrroles) and synthetic analogs: octa-alkylporphyrins, meso-porphyrins, tetrabenzo-porphyrins, N-alkylporphyrins; N-arylporphyrins, N-aminoporphyrins, azaporphyrins; tetra, tri, di and monophtalocyanines, homoporphyrins, carbon or nitrogen inserted metalloporphyrins, oxoporphyrins, quatrenes, and heterocyclic analogs: chlorins, bacteriochlorins, phlorins, porphyrinogens (reduced analogs), and metallo-derivatives.

N-alkyl or N-arylporphyrins and their metallo-derivatives have different properties from their non-N-alkylated analogs. In this dissertation I shall mainly discuss two aspects of the chemistry of N-alkylated porphyrins:

A. The kinetics of dealkylation of metallo-N-alkyl porphyrins.

B. The thermodynamic properties of metallo-N-alkyl porphyrins and comparisons with the metallo-non-N- alkylporphyrins.

Before I discuss these two aspects, it will be worthwhile to review several aspects of the field of N-alkyl and

N-aryl porphyrins.

From the synthesis of first N-alkylporphyrin N-methyl-etioporphyrin-I by McEwen[5,6] in 1936, until recently, little attention has been given to the chemistry of N-alkyl porphyrins. McEwen and others were simply interested in the effects of steric deformation on the properties of porphyrin.[6] Figure 1 shows that a porphyrin with a methyl group on the nitrogen, is nonplanar.[7] The first crystal structure of free base N-methyl porphyrin, reported recently by Lavallee and Anderson[8], shows the proposed nonplanarity (Figure 2).

Great interest in N-alkylporphyrin chemistry has been aroused by the finding that liver heme is converted into N-alkyl porphyrins by drugs with unsaturated side chains and certain dihydropyridines. The mechanisms for formation of green pigments (modified porphyrins or N-alkyl porphyrins) are different in two cases: (a) Destruction of cytochrome P-450 by drugs containing an allyl group[9] (barbiturates) and simple molecules like ethylene,[10,11] vinyl fluoride, vinyl bromide, fluoroxene (2,2,2-trifluoroethyl vinyl ether), acetylene[11b] (see Figure 3) is accompanied by the formation of a monooxygenated derivative of the drug bound onto one of the pyrrole nitrogen atoms of liver heme. (b) An alkyl group of certain dihydropyridines gets transferred to one of the nitrogens of heme during their metabolism by cytochrome P-450.

In case (a) different mechanisms have been proposed but all contend that N-alkylation of heme takes place through a transient species generated during the catalytic transfer of

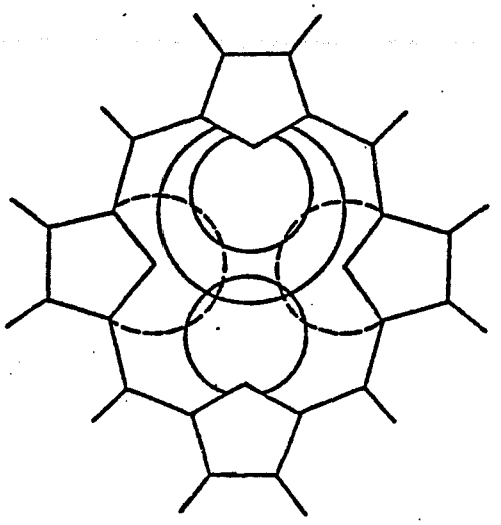

Figure 1. A schematic diagram of N-methyletioporphyrin-I: The small continuous circles represent van der walls radii of hydrogen (1.2Å). The large circle is the corresponding radius of CH_3 (2.0Å). The broken circles correspond to the radii of the ring nitrogens (1.5Å).

Figure 2. The structure of N-methyl-5,10,15,20-tetrakis-(p-bromophenyl)-porphyrin ($N\text{-}CH_3HTPPBr_4$) obtained from x-ray diffraction. In the top figure, hydrogen atoms have been rescaled for clarity, and the thermal ellipsoids are drawn at the 50% probability level. The picture at the bottom gives a side-on view of the $N\text{-}CH_3HTPPBr_4$ molecule indicating the relative orientations of the pyrrole rings. The hydrogen atom on nitrogen is strongly indicated to be across from the pyrrole bearing the methyl group. (Taken from Lavallee, D.K. and Anderson, O.P., J. Am. Chem. Soc. 1982, 104, 4707-08).

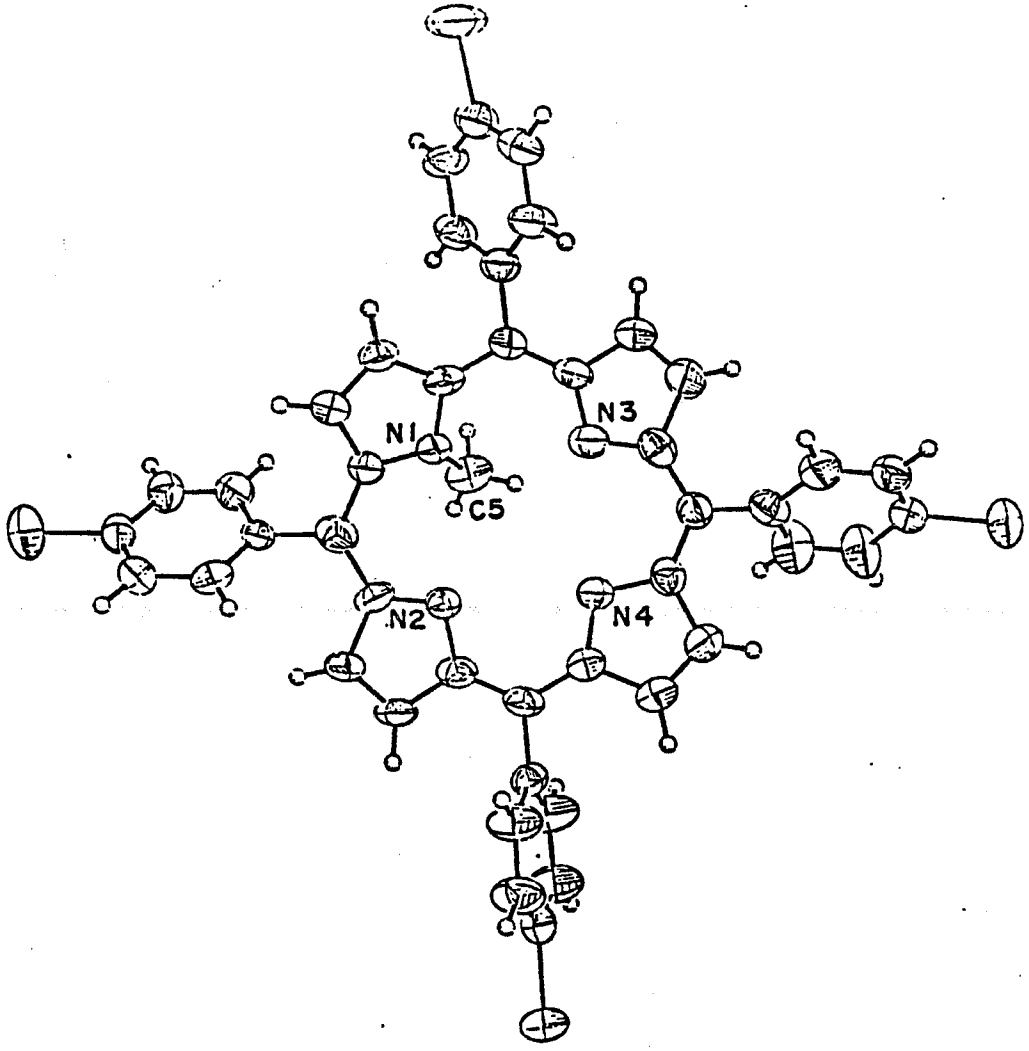
N1
N2
N3
N4
C5

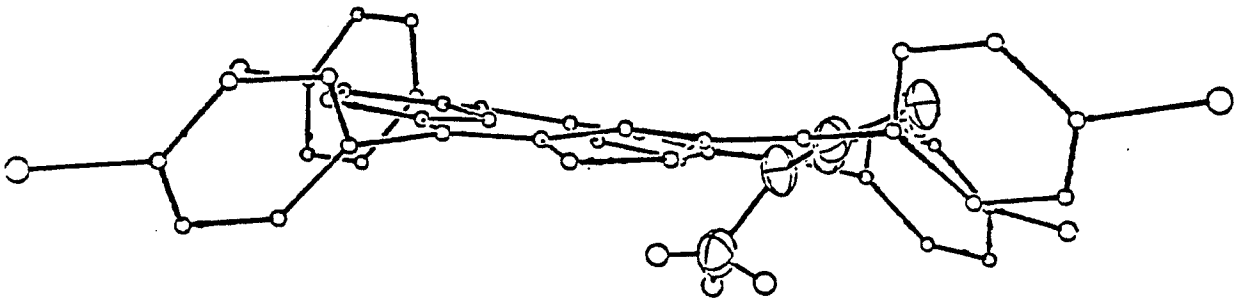

Figure 3. The alkylation of prosthetic heme of cytochrome P-450 by interaction of vinyl halides (top), acetylene (middle), and ethylene (bottom). The prosthetic heme is represented by an iron and four nitrogens in a quadrilateral. The orientation of the olefin shown here is that which leads to the isolated heme adduct and not that which is necessarily electronically favored. The actual oxidation states of iron will depend on electron delocalization (Taken from Ortiz de Montellano,P.R.; Kunze,K.L.; Beilan,H.S. and Wheeler, C., Biochem., 1982, 21, 1331-39 and the bottom one is adapted from Ortiz de Montellano,P.R.; Beilan, H.S.; Kunze, K.L. and Mico,B.A., J.Biol. Chem., 1981, 256,4395-99).

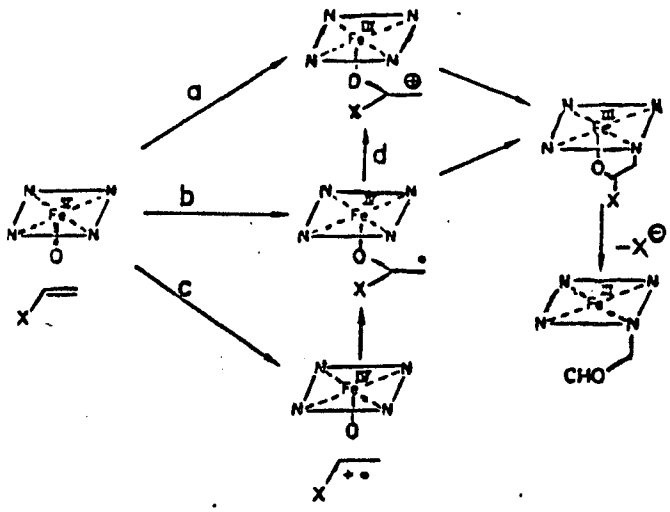
a
b
c
d
CHO

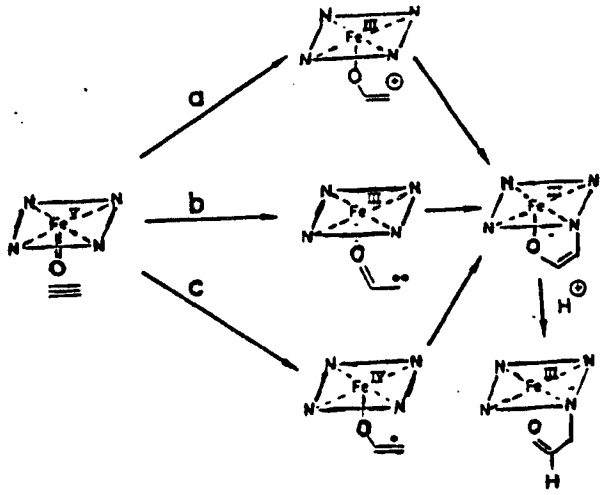
a
b
c
H

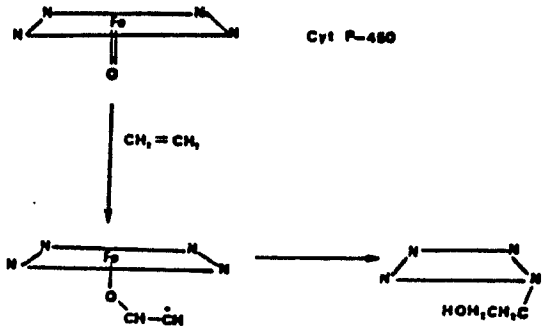
Cyt P-450
CH₂ = CH₂
CH—CH
HOH₂CH₂C

oxygen to the π-bond of the substrate. The formation of green pigments is independent of the electronic distribution in the transition state. This feature of the proposed mechanisms is strongly supported by the structure of the resulting olefin adduct. Different speculative mechanisms are shown in Figure 3.

Ethchlorvynol (1-chloro-3-ethyl-1-penten-4yn-3-ol), introduced in 1955 and still used as a sedative-hypnotic drug, alkylates the prosthetic heme by its oxidatively activated acetylenic function.[12a] The heme biosynthesis it stimulates may explain its deleterious effect in patients with acute porphyrias[12b-e] (When inhibited enzymes from the latter stages of heme biosynthesis can not convert porphyrins into Fe-protoporphyrin (Figure 4), then accumulation of porphyrins make the urine reddish in color; the disorder is known as porphyria). The oxidative metabolism of terminal isolated π-bonds has been exemplified by the activity of AIA administered to dogs[12f] (AIA destroys cytochrome P-450): the metabolism of propanol is altered significantly.

(b) Treatment of rats treated with agents such as griseofulvin (2S-trans-7-chloro-2,4-6-trimethoxy-6-methyl-spiro [benzofuran-2(3H),1'-[2]cyclohexane]-3,4'-dione, isogriseofulvin {(2S-trans)-7-chloro-4,4',6-trimethoxy-6'-methylspiro-[benzofuran-2(3H),1'-[3]cyclohexane]-2'-3-dione}, DDC(3,5-diethoxycarbonyl-1,4-dihydrocollidine) and its 4-ethyl and 4-propyl analogs, DDEP(3,5-diethoxycarbonyl-2,6-dimethyl-4-ethyl-1,4-ethyl-1,4-dihydropyridine), DDPP(3,5-

Figure 4. The inhibition of heme biosynthesis in porphyrias. The green pigments like N-methylprotoporphyrin, N-ethylprotoporphyrin (N-ethyl group on rings A and B) and those derived from griseofulvin and isogriseofulvin are strong inhibitors of ferrochelatase (E.C.4.99.1.1), the enzyme that inserts iron into protoporphyrin IX in the final step of heme biosynthesis (Taken from Frank, B., Angew. Chem. Int. Ed. Eng., 1982, 21, 343-53).

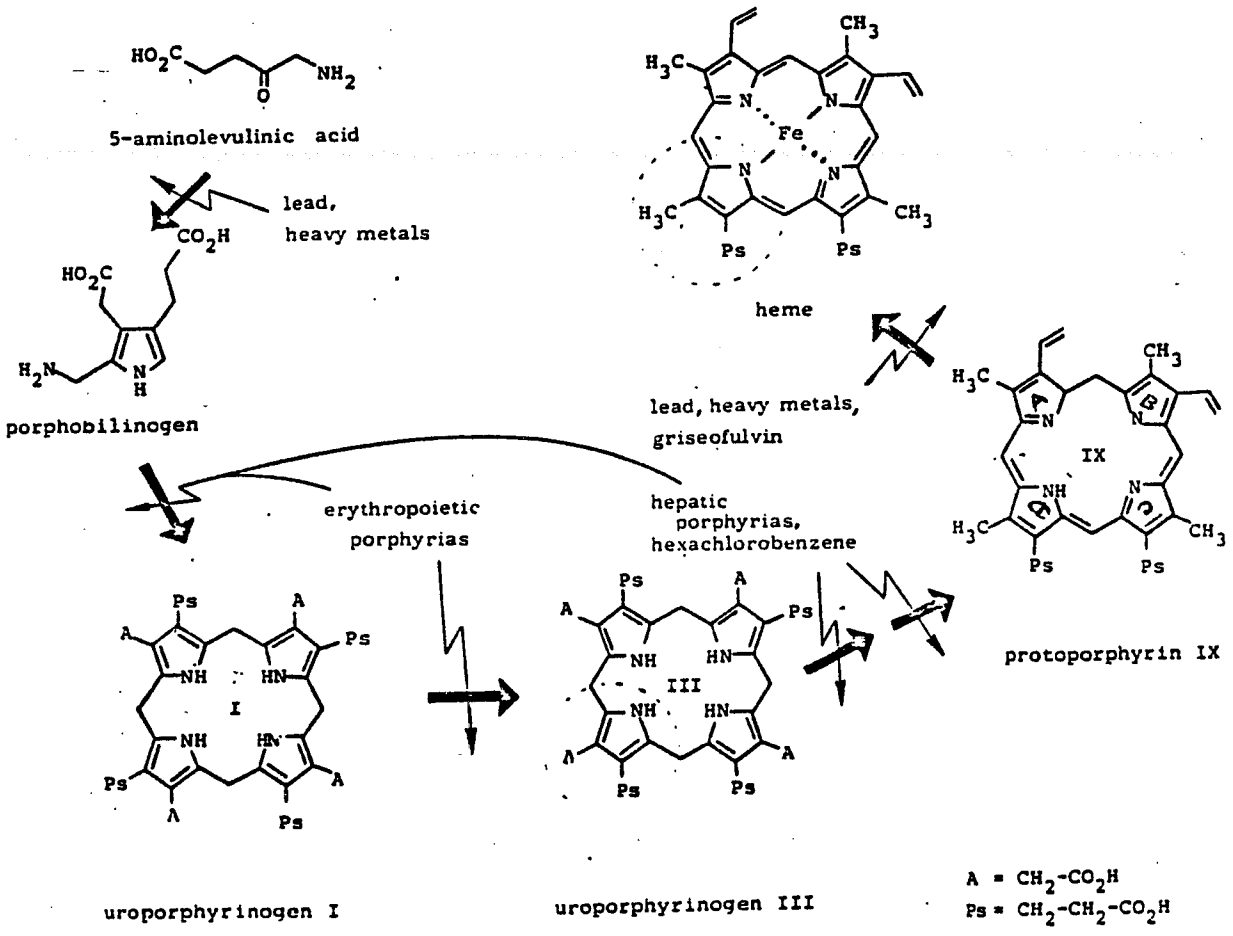
5-aminolevulinic acid
lead,
heavy metals
porphobilinogen
heme
lead, heavy metals,
griseofulvin
erythropoietic
porphyrias
hepatic
porphyrias,
hexachlorobenzene
protoporphyrin IX
uroporphyrinogen I
uroporphyrinogen III
A = CH2-CO2H
Ps = CH2-CH2-CO2H

diethoxycarbonyl-2,6-dimethyl-4-propyl-1,4-dihydropyridine), results in the formation of green pigments. For the cases of DDC, DDEP and DDPP, reaction products have been identified by isotopic labelling. The 4-alkyl group of each of these drugs is transferred to a nitrogen atom of protoporphyrin.[13-17] In this case only a small fragment of the substrate is transferred to the prosthetic heme. Furthermore, although oxygen is required for the destructive event, no oxygenated species becomes bound to the nitrogen atoms (Figure 5). Both endogenous liver heme and exogenous heme can be converted to N-alkylated porphyrins.[13b] It has been deduced by De Matteis and others that alkylation of the cytochrome P-450 is steriospecific and takes place preferentially if not exclusively, from one side of the porphyrin plane.[16]

N-methyl protoporphyrin IX, the corresponding N-ethyl analogs (N-ethyl group on the pyrrole ring A or B) and the green pigments produced by treatment of mice with griseofulvin or iso-griseofulvin are strong inhibitors of ferrochelatase (E.C. 4.99.1.1), the enzyme that inserts an iron atom into protoporphyrin IX in the final step of heme biosynthesis[18-20] (Figure 4). The N-methylmesoporphyrin is an inhibitor of the synthesis of heme in Euglenna gracilis but not of chlorophyll.[21]

N-aryl porphyrins are formed by a different route <u>in vivo</u> than N-alkylporphyrins. Green pigment formation in erythrocytes of animals treated with phenylhydrazine was described by Hoppe-Seyler in 1885.[22] Phenylhydrazine-

Figure 5. The 'R' group of the dihydropyridine (at the top and bottom) can be CH_3, C_2H_5 or C_3H_7. Here it has been shown for R = CH_3 only. Different possible mechanisms in the formation of N-methylprotoporphyrin from the reaction of 3,5-diethoxycarbonyl-1,4-dihydro-2,4,6-trimethylpyridine (DDC) with lever heme: The mechanism (1) has been confirmed by Ortiz de Montellano et al.(J. Biol. Chem.,1981,256, 6708-13) and De Matteis et.al.(FEBS Lett.,1981,129, 328-31). Aromatization of the pyridine ring through the removal of 'R' group as a carbocation is the most probable route of oxidation of 4-alkyldihydropyridines(bottom, taken from Marks, G.S.; Zelt, D.T. and Cole, S.P., Can. J. Physiol. Pharmacol., 1982, 60, 1017-26).

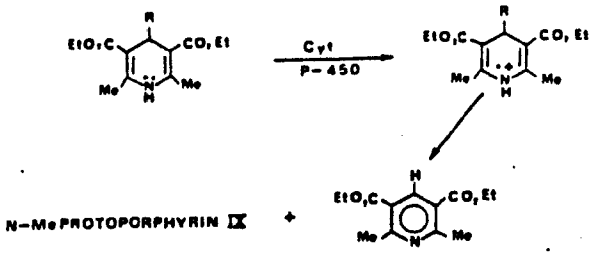
Cyt
P-450
N-Me PROTOPORPHYRIN IX

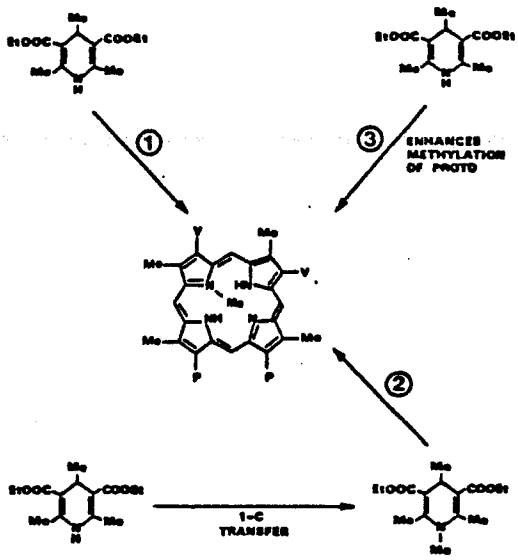
ENHANCES METHYLATION OF PROTO
1-C TRANSFER

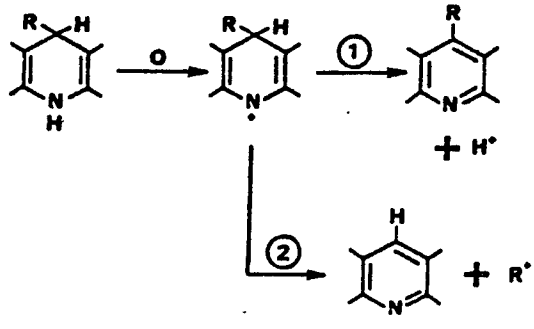
O
+ H•
+ R•

mediated hemolysis is similar in many respects to the hemolysis observed in hereditary Heinz body anemias (Heinz-bodies are named for R. Heinz, who described them in 1890). The inactivation of hemoglobin by phenylhydrazine in vivo accelerates its precipitation in the form of Heinz bodies[23,24] whereas inactivated myoglobin does not precipitate from solution.[25] When such inactivated hemeproteins are denatured aerobically in the presence of acid, N-phenyl protoporphyrins IX are formed.[25]

Studies[26-30] with model systems as well as with natural systems indicate that the inactivation of hemeproteins by phenyl hydrazine or its analogs proceeds by way of an intermediate, in which there is a σ-bound aryl moiety attached to the prosthetic iron atom. A mechanism for formation of N-phenyl porphyrin[25] is shown in Figure 6. The formation of free radicals is supported by EPR experiments. The N-alkylporphyrin like N-ethylprotoporphyrin IX has also been obtained similarly by treatment of ethylhydrazine.

Another reason for studying N-alkylporphyrin complexes is the possibility that they may be useful in cancer chemotherapy. $Cu(N\text{-}CH_3TPPS_4)^{3-}$, [N-methyl-5,10,15,20-tetrakis(p-sulfophenylporphinato]-copper(II) (synthesized in our laboratory), shows reproducible activity in the P388 lymphocitic leukemia test system. In addition, porphyrins have an affinity for neoplastic tissue.[31] Thus there is an interest in an investigation of the cytotoxic effect of porphyrin complexes with different alkyl groups present on one of the

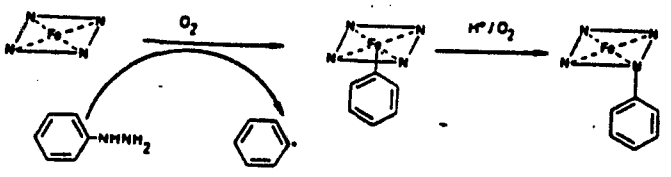

Figure 6. A heme moiety is shown here schematically as well as the proposed structure for the σ-bound intermediate and the mechanism for the N-arylation of prosthetic heme(taken from Augusto, O.; Kunze, K.L. and Ortiz de Montellano, P.R., J. Biol. Chem.,1982, 257, 6231-41).

porphyrin nitrogen atoms. The cytotoxicity of alkylating reagents suggests the possibility that $Cu(N\text{-}CH\text{-}TPPS_4)^{3-}$ is acting as an alkylating reagent in leukemia. The possibility of developing better therapeutic agents is an incentive for finding leaving groups better than the methyl group.

The ability to choose the proper alkyl group and metal ion in the rapid formation of the corresponding non-N-alkylated metalloporphyrins may be useful in the synthesis of radiolabelled metalloporphyrins.[32,33] The complex formation with N-alkyl porphyrins followed by dealkylation with a suitable nucleophile to synthesize the non-N-alkylated metalloporphyrin can be achieved very easily (N-alkyl porphyrins form complexes much more rapidly than corresponding non-N-alkylated porphyrins[34,35]). An example is the synthesis of Palladium-109 hematoporphyrin from N-methyl hematoporphyrin. This compound is being tested as an agent for specific lymphatic ablation to prevent the rejection of transplanted organs.[32,33] The previously used method for the synthesis of palladiumporphyrin involves direct incorporation of a palladium salt into the free base porphyrin in glacial acetic acid and sodium acetate. After refluxing, cooling and precipitation, the product obtained contains 15% of the initial activity. As a result, a large amount of initial ^{109}Pd activity would be required to prevent the rejection of transplanted tissues in human subjects. The ^{109}Pd ($t_{1/2}$=13.43h, principal β at 1.028Mev) presumably prevents homograft rejection in dogs and rats due to its beta emission. The demethylation of other N-methyl porphy-

rin complexes of metal ions, like Tc and In, are slow. So, one would not be encouraged to synthesize the corresponding radio-labelled metalloporphyrins by the demethylation process. But leaving groups better than methyl group can speed up the dealkylation reaction. This possibility provided another incentive for studying the kinetics of dealkylation reactions involving different alkyl substituents on the nitrogen atom.

In subsequent chapters, I will describe how the solvents, nucleophiles, ring substituents on the porphyrin ring system, metal ions, and the alkyl group affects the kinetics and mechanism of the dealkylation reactions. I will attempt to correlate these results to the possible mechanisms of decomposition of the intermediates formed in the destruction of cytochrome P-450 by drugs. These studies *in vitro* are designed to assess the nature of the dealkylation reactions *in vivo*, and to provide information for designing methods for the rapid synthesis of radio-labelled metallo-non-N-alkylporphyrins.

Another major concern of this dissertation involves the thermodynamic properties of N-alkyl or N-arylporphyrins and their metallo-derivatives. One property reported herein is the reduction potentials of the metal atom in a variety of complexes. Porphyrin ligands have a tendency to stabilize the higher oxidation state of transition metal ions,[36] whereas the lower oxidation state is typically stabilized in N-alkylporphyrin complexes. The potentials of different

metallo-N-alkylporphyrins can give us an idea of the driving forces involved in the formation of green pigments from cytochrome P-450 and hemeproteins. Questions of interest are: How do these potentials compare to those for σ-bound alkyl or aryl complexes? Do they depend upon the alkyl or aryl substituents on the nitrogen atom? How do the axial ligands affect the potentials of a redox system? These questions can be answered very well by cyclic voltammetry.

X-ray photoelectron spectroscopy (XPS or ESCA) has not been used to a large extent in the study of molecules of biological interest. It is a well established tool in measuring the charge distribution in molecular systems. The N 1s binding energies are the most sensitive probe for drawing the outline of the charge distribution in porphyrins. XPS has been used to determine the presence of two distinctly different, non-equivalent nitrogen types in the porphyrin free base[37-41] which can be compared with the single, equivalent nitrogen peak found in metalloporphyrins. Lavallee et al.[42] have shown that the differences in core binding energies can be correlated to the distances between the metal atom and the nitrogen atoms of metallo-N-alkylporphyrins. In this project, I have explored the effect of different alkyl or aryl substituents on the nitrogen 1s binding energies. A previous report[42] of XPS data for Mn(N-CH_3TPP)Cl indicates a relatively strong interaction with the methylated nitrogen atom while in the case of Zn(N-CH_3TPP)Cl very little interaction is evident. I have extended the previous work to Mn(II) complexes of different N-alkyl por-

phyrins to see whether such strong interaction is influenced by different alkyl groups or not.

The visible absorption spectra of N-phenyl porphyrins and their metal complexes show a pronounced bathochromic (red) shift in comparison to the N-alkyl analogs. NMR spectroscopy also reveals such differences for the free ligands and their complexes. An additional feature of interest is the difference in basicities of N-phenyl and N-alkyl porphyrins (for the free bases).In this thesis, I will discuss the molecular parameters of an N-phenylporphyrin complex, Zn(N-PhTPP)Cl and compare them with the analogous N-methyl complex.[43]

Lastly, I have obtained EPR spectra of the Cu(II) complexes of N-alkylporphyrins to see the kind of differences that can exist in a distorted coordination site compared to the almost planar coordination site of non-N-alkylated porphyrins.[44-46]

CHAPTER 2

EFFECT OF SOLVENTS, NUCLEOPHILES, AND RING SUBSTITUENTS ON THE RATE OF DEMETHYLATION REACTIONS OF N-METHYLPORPHYRIN COMPLEXES

Introduction: The identification of N-alkylporphyrins as the green pigments which are formed in the destruction of cytochrome P-450 has aroused great interest in the field of N-alkylporphyrin chemistry. The dealkylation of metallo-N-alkylporphyrins can be described by this simple equation:

$$MN\text{-}RP^{+} + Nu \longrightarrow MP + Nu\text{-}R^{+}$$

where 'M' is the metal atom, 'R' is the alkyl group bound to one of the nitrogen atoms, 'P' is the porphyrin, (can be a synthetic or natural) and 'Nu' is the nucleophile. There is no dealkylation by the attack of a nucleophile on the alkyl group bound to the nitrogen in the absence of metal ion. A metal ion, however, assists in removing the alkyl group. Strain is relieved with the formation of planar (or more nearly planar) metalloporphyrin and the movement of metal into the plane of porphyrin is the driving force in the dealkylation reaction (Figure 7). Structures of free base N-alkylporphyrin,[8] metallo-N-alkylporphyrins,[47a-c] metallo-non-N-alkylporphyrins or simply metalloporphyrins,[47d-e] determined by x-ray crystallography, are consistent with the above hypothesis. Shears and Hambright first reported the demethylation of an N-alkylporphyrin complex: chloro-N-methyletioporphinatozinc(II) is demethylated when it is refluxed in pyridine for three days.[48] Lavallee subsequently reported the kinetics of demethylation of N-methyl-5,10,15,20-tetraphenylporphyrin complexes of Cu(II), Ni(II), Zn(II), Mn(II) with dialkylamines in acetonitrile.[49,50] Although studies have been done with different metal ions, the effect of solvent, nucleophiles, and

Figure 7. The demethylation reaction of an N-methyl porphyrin complex of M(II) (M = Pd, Cu, Ni, Zn and Mn) by a nucleophile. On removal of the methyl group by the nucleophile with the assistance of metal ion, the latter moves very close to the plane of the porphyrin ring (in the case of Pd(II),Ni(II) and Cu(II) the final product, metallo-non-N-alkylporphyrin, is almost planar). The same picture holds in the dealkylation reactions of other N-substituted porphyrin complexes of Cu(II)(see text of chapter 3).

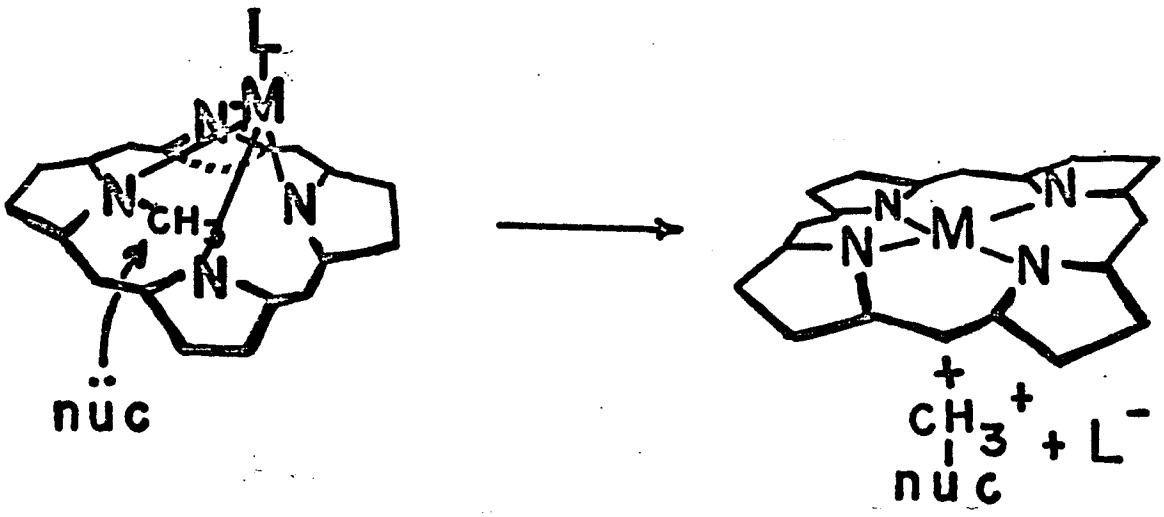
L
M
N
N
CH2
N
N
nüc
N
N
M
N
N
CH3
nüc
+
+ L⁻

especially the effect of porphyrin ring substituents have not been addressed to a great extent.

Since the N-alkylporphyrins are formed by inactivation of cytochrome P-450 only with certain substrates; it can be of interest to know the kinetic factors which may pertain to the decomposition of possible intermediates. Substituents on porphyrin ring affect the basicity of porphyrins to a large extent. It is interesting to know how dealkylation rates are affected by large differences in pK_a values for free base N-methyltetrakis(p-sulfophenyl)porphyrin and non-meso-substituted N-methylporphyrins such as N-methyldeuteroporphyrin (Figure 8). These two free base N-substituted porphyrins have pK_3 values for monoprotonation of >13 while in the case of N-methyltetraphenylporphyrin it is 4 (in DMF)[55]. The effect of the basicity differences and that of the solvent and nucleophile *in vitro*, will help to asses dealkylation reactions *in vivo*.

Experimental: H_2TPP(5,10,15,20,-tetraphenylporphyrin, the starting material for the synthesis of N-CH_3HTPP, was prepared by the method of Adler et al.[51] Lavallee and Gebala reported the synthesis of N-methyl-5,10,15,20-tetraphenylporphyrin (N-CH_3HTPP) in 1974.[52] The recent method widely used in our laboratory is slightly different from the best of the three methods reported in ref. 52. A dilute solution of fluoromethylsulfonate (1.78 mL of CH_3SO_3F in about 300 mL of CH_2Cl_2) or methyltrifluoromethanesulfonate (both from Aldrich, the latter methylating agent is less

Figure 8. The upper diagram shows the structures of N-methyl-5,10,15,20-tetraphenylporphyrin and N-methyl-5,10,15,20-tetrakis(p-sulfophenyl)porphyrin ($X = -SO_3^-$).

The bottom one is the structure of N-methyldeutero-porphyrin IX dimethyl ester.

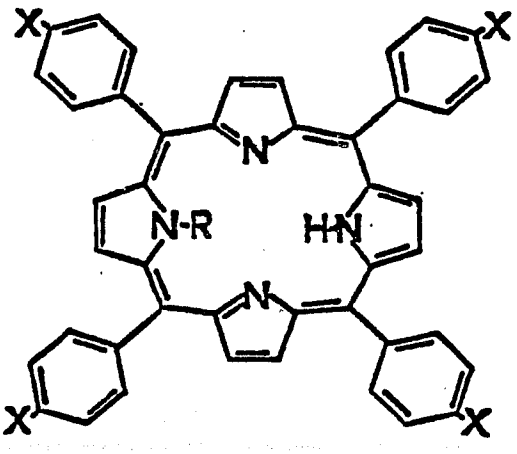
X
X
N
N-R
HN
N
X
X

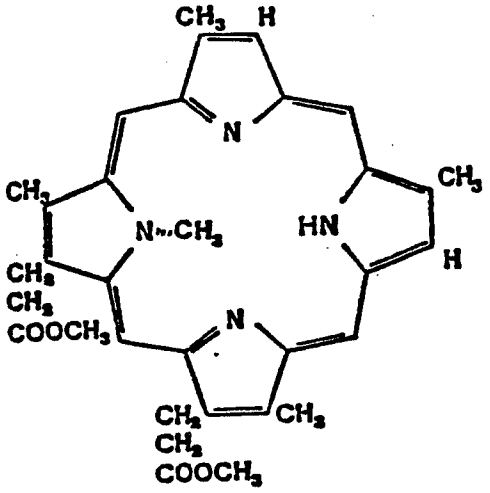
CH3
H
N
CH3
CH3
N
CH3
HN
H
CH2
CH2
COOCH3
N
CH2
CH2
COOCH3
CH3

dangerous than the former one and is as readily available commercially as fluoromethylsulfonate) in dichloromethane was added dropwise to a refluxing dilute solution of H_2TPP in dichloromethane (13.5 gms of H_2TPP in 1.5 L of CH_2Cl_2 for several hours. A dilute solution is used to avoid formation of too much N,N'-dimethyl-TPP. Slow addition as well as concentration of the reactants retard the second step. (As shown below, scheme 1)

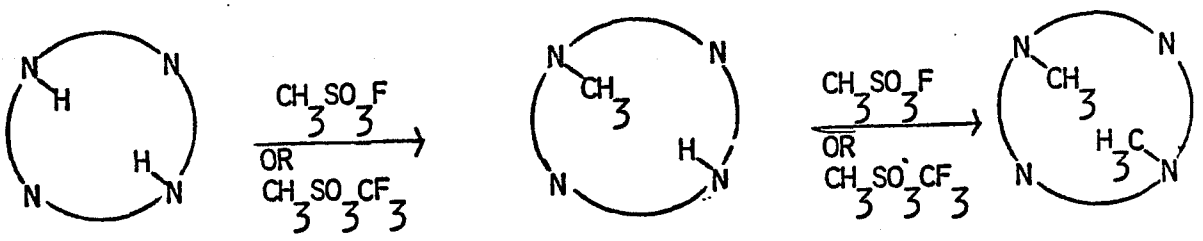

SCHEME 1

The solution was refluxed for about 2 days. The green solution was then neutralized with 1M NH_3 solution, chromatographed on Al_2O_3 using CH_2Cl_2 as eluent. A few mL of CH_3CN was added to the eluent to elute the green band of N-CH_3HTPP. The color of the solution of the N-CH_3HTPP is different on the column from that in solution presumably due to an interaction between Al_2O_3 and N-CH_3HTPP. It was then recrystallized from CH_2Cl_2/CH_3CN. N-CH_3HTPPS$_4$, ((N-methyltetrakis(p-sulfophenyl)porphyrin)[53] and N-CH_3HDP[54] (N-methyldeuteroporphyrin IX dimethylester) were synthesized by the literature methods developed in this laboratory. The elemental analysis of N-CH_3HTPPS$_4$ was not satisfactory. Due to the positive charge on the metal center and negatively

charged periphery, it is possible that the ligand can associate in different geometries that will have different numbers of counterions and waters of crystallization.[55] The sample used for obtaining extinction coefficients gave an analysis of the formulation $C_{45}H_{30}N_4S_4O_{12}Na_3Cl$. A single spot with a R_f, value of 0.71 with $CHCl_3$/MeOH(4:5) as eluent ascertained the purity of the sample; N-CH_3HTPPS$_4$. The interpretation of the 300 MHz proton NMR spectrum indicated a single series of peaks attributable to a para-sulfonated N-methyltetraphenylporphyrin. The proton NMR spectrum taken in 300 MHz spectrometer in the aromatic region is shown in Fig. 9, δ (ppm), 8.984, S, for the pyrrole ring protons opposite to the one bearing methyl group; 8.743, d, J = 4.5Hz adjacent pyrrole ring to the one bearing the methyl group, 8.524, d, J = 4.5Hz adjacent pyrrole ring to the one bearing methyl group, 8.278, d, J = 7.8Hz, for the para substituted meso-phenyl protons, 8.195 d, J = 7.8Hz for the para substituted meso-phenyl protons, S, 7.569, S, for the pyrrole ring protons bearing the methyl group. -4.00, S, for the protons of the methyl group attached to the nitrogen atom (not shown in Figure 9). The high field shift of the protons of the methyl group is due to the high shielding by the porphyrin ring (see chapter 5). The doublet pattern of meso-phenyl ring protons proves that sulfonation occurs in the para position and all the meso-phenyl groups are sulfonated. N-CH_3HTPPS$_4$, $4Na^+$ was not soluble in CH_3CN, so it was converted into tetra-N-butylammonium salt of N-

Figure 9. The 300 MHZ ^{1}H NMR spectrum of a solution of N-methyl-5,10,15,20-tetrakis(p-sulfophenyl)porphyrin [N-CH_3HTPPS$_4$($4Na^+$), the top structure of Fig. 8] in DMSO-d_6.

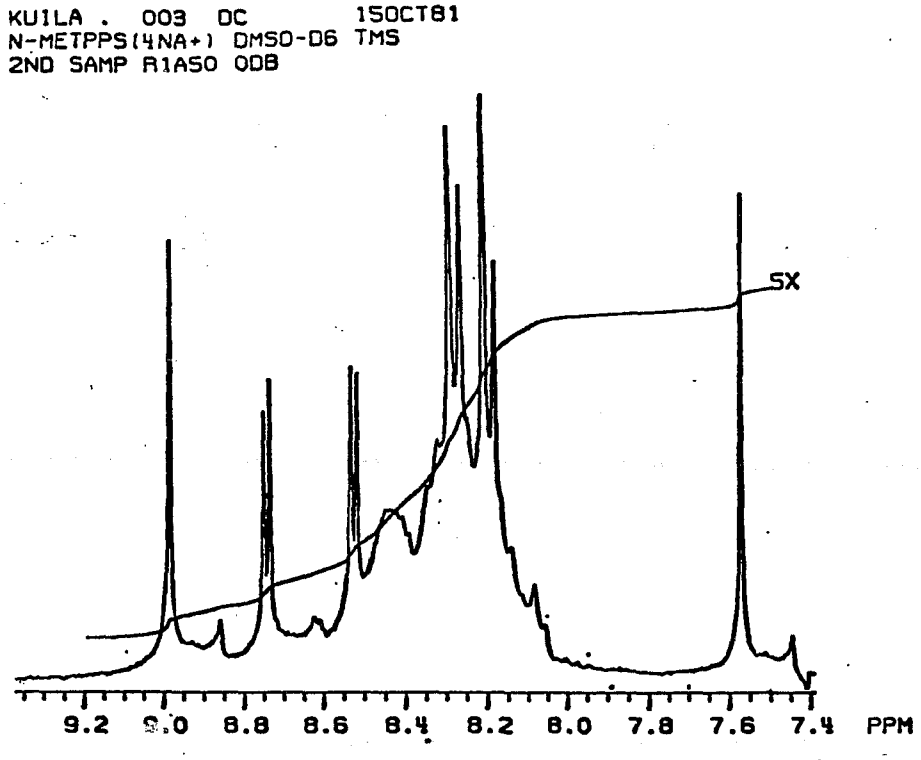
KU1LA . 003 DC 15OCT81
N-METPPS(4NA+) DMSO-D6 TMS
2ND SAMP R1A5O 0DB
5X
9.2
9.0
8.8
8.6
8.4
8.2
8.0
7.8
7.6
7.4
PPM

CH_3HTPPS_4. NBu_4OH was passed through a column of cations exchange in acidic form (AG^R 50W-X4 minus 400 mesh hydrogen form, BIO-RAD LABORATORIES). Then the column was washed with water until the pH of the solution coming of the column was neutral. A solution of $N\text{-}CH_3HTPPS_4(Na^+)_4$ was then passed through the column containing NBu_4^+ ions. The eluted solution was evaporated to dryness.

The $Cu(CF_3SO_3)_2.6H_2O$ was prepared by adding dilute trifluoromethane sulfonic and (CF_3SO_3H, H_2O) to cupric carbonate. It was recrystallized twice from methanol, washed with diethyl ether, and then dried in a vacuum oven and stored in a desicator over P_2O_5. Solvents and dialkylamines were purified by a published procedure.[56] Pyrrole (b. p. 131°C) for preparing H_2TPP was dried over CaH_2 and then distilled under reduced pressure. Benzaldehyde and propionic acid (both from Aldrich) were used as such without further purification. Acetonitrile was kept over molecular sieves for few days; stirred with CaH_2 followed by addition of 0.5 - 1% P_2O_5; fractionally distilled and kept over molecular sieves. Use of too much of P_2O_5 should be avoided due to the formation of brownish-yellow polymer. Dichloromethane was washed with conc. H_2SO_4, water, dried with $CaCl_2$ (anhydrous), distilled over P_2O_5 and kept over molecular sieves. Diethyl amine was distilled over BaO. On standing over molecular sieves it became yellowish in color. Di-n-butylamine was kept over KOH pellets for a day or so. It was then filtered off and distilled after addition of CaH_2. Efforts to dry it with $LiAlH_4$ (as mentioned in ref. 56) were

futile apparently due to a reaction between the two. $LiAlH_4$ can react with amines by the following equations[57]

$$3\ LiAlH_4 + 4Me_3N \longrightarrow Li_3AlH_6 + 2AlH_3(NMe_3)_2$$

$$LiAlH_4 + RNH_2 \longrightarrow LiAl(NHR)_4$$

$LiAlH_4$, a covalently bonded species in solution, can undergo reactions of the above type. On the other hand, ionic $NaAlH_4$ can form solvated species in tetramethylenediamine ($NaTMEDAlH_4$) without undergoing the reactions mentioned above. Tetraethylammonium chloride (Eastman) and tetrabutylammonium perchlorate were recrystallized from ethanol and dried *in vacuo*. Copper complexes of the N-methyl-porphyrins were prepared *in situ* by mixing solutions of a Cu(II) salt in slight excess and the N-methylporphyrin in the presence of noncoordinating base such as 2,6-lutidine or 2,2,6,6-tetramethylpiperidine. The visible absorption spectra exhibited were typical of N-methyl porphyrin complexes.[54a,58] A protonated N-methylporphyrin can give rise to the similar spectrum of metallo-N-methylporphyrins. The lack of change in the spectra of Cu(II) complexes by the addition of a noncoordinating base like 2,6-di-*tert*-butylpyridine or 2,2,6,6-tetramethylpiperidine, indicated that it was a complex, not a protonated species. The spectrum of the isolated trifluoromethanesulfonate salt of (N-methyl-tetraphenylporphinato)copper(II) was different from the one observed by Stinson and Hambright for the corresponding chloride salt.[59] (see chapter 4) The 2,2,6,6-tetra-methylpiperidine, 2,6-lutidine (of Aldrich), and pyridine (Fisher spectral

grade) were used without further purification. The 2,6-di-tert-butylpyridine was refluxed with BaO and distilled from it.

Kinetics Experiments: Absorbance data were obtained with Beckman DU-8, Cary 14 and Varian 635-D spectrophotometers with self-contained solid-state temperature control and Lauda B-2 and Fisher Model 90 circulating constant-temperature baths, respectively. The statistics programs available with the PROPHET[60] computing system were used to analyze the data (see appendix). In all reactions, nucleophiles were used in pseudo-first-order excess.

The stock solutions for kinetics were prepared as follows: Solutions of $Cu(CF_3SO_3)_2 \cdot 6H_2O$ (2.5 mL, 1.11×10^{-3}M in CH_3CN) and $NCH_3HTPPS_4(NBu_4)$[tetra-n-butylammonium salt of N-methyl-tetrakis(p-sulfophenyl)porphyrin] (2.5 mL, 1.03×10^{-3}M in CH_3CN) were mixed with 0.02 mL of 2.6-lutidine and diluted to 50.0 mL in a volumetric flask. Isosbestic points were observed at 518 and 553 nm respectively. Kinetic data were recorded at 596.0 nm. Lavallee[49] had shown that demethylation of $Cu(N\text{-}CH_3TPP)^+$ by di-n-butylamine was independent of the wavelength. Stock solutions of $Cu(N\text{-}CH_3DP)^+$ were prepared by combining 0.64 mL of 8.4×10^{-5}M N-CH_3HDP in CH_3CN, 0.64 mL of 1.4×10^{-4}M, $Cu(CF_3SO_3)_2 \cdot 6H_2O$ in CH_3CN and 1 mL of a solution of 2,2,6,6-tetramethylpiperidine (0.02 mL of tetramethylpiperidine diluted to 25 mL with CH_3CN) and diluting to 10.0 mL with CH_3CN. Isosbestic points were noticed at 380 and 400 nm. Kinetics data were obtained at 393 nm. Isosbestic points at 518 and 550 nm

were observed in the reactions of the trifluoromethanesulfonate salt of $Cu(N\text{-}CH_3TPP)^+$ with di-n-butylamine and a bathochromic shift with a color change from brown to green (from peaks at 540, 588 and 650 nm to peaks at 580, 610 and 664 nm) was observed upon addition of di-n-butylamine and tetraethylammonium chloride to the trifluoromethanesulfonate salt of $Cu(N\text{-}CH_3TPP)^+$ in dichloromethane. The bathochromic shift could be attributed to the axial ligation of amine (see Fig. 10). Kinetics were done at 538.1 nm.

Results: Fig. 8 shows the structures of $N\text{-}CH_3HDP$ IX dimethyl ester, $N\text{-}CH_3HTPP$ and $N\text{-}CH_3HTPPS_4$. The observed pseudo-first-order rate constants for the reactions of copper(II) complexes of N-methyltetraphenylporphyrin ($CU(N\text{-}CH_3TPP)^+$), N-methyltetrakis(p-sulfophenyl)porphyrin ($Cu(N\text{-}CH_3TPPS_4)^{3-}$), and N-methyldeuteroporphyrin IX dimethyl ester ($Cu(N\text{-}CH_3DP)^+$ with di-n-butylamine in acetonitrile are presented in Tables I-III. The non-linear behaviour of the observed pseudo-first-order rate constant with respect to the concentration of di-n-butylamine are shown in Figures 11 and 12 for $Cu(N\text{-}CH_3TPPS_4)^{3-}$ and $Cu(N\text{-}CH_3DP)^+$. Similar behaviour for $Cu(N\text{-}CH_3TPP)^+$ has been reported by Lavallee (Fig. 2 of ref. 49).

Data for the reaction of $Cu(N\text{-}CH_3TPPS_4)^{3-}$ with diethylamine in aqueous solution is given in Table IV. The plot of the observed rate constant vs. the concentration of diethylamine (Fig. 13) at 45.1°C shows it to be first order with respect to amine. Data for the reactions of Cu(N-

Figure 10. Spectra of (N-methyl-5,10,15,20-tetraphenylporphinato)copper(II) cation in CH_2Cl_2; 1) before the addition of di-n-butylamine (the dashed line), 2) just after addition (1) and 3) after completion of the dealkylation reaction (5). The final spectrum (5) corresponds to that of (5,10,15,20-tetraphenylporphinato)copper(II).

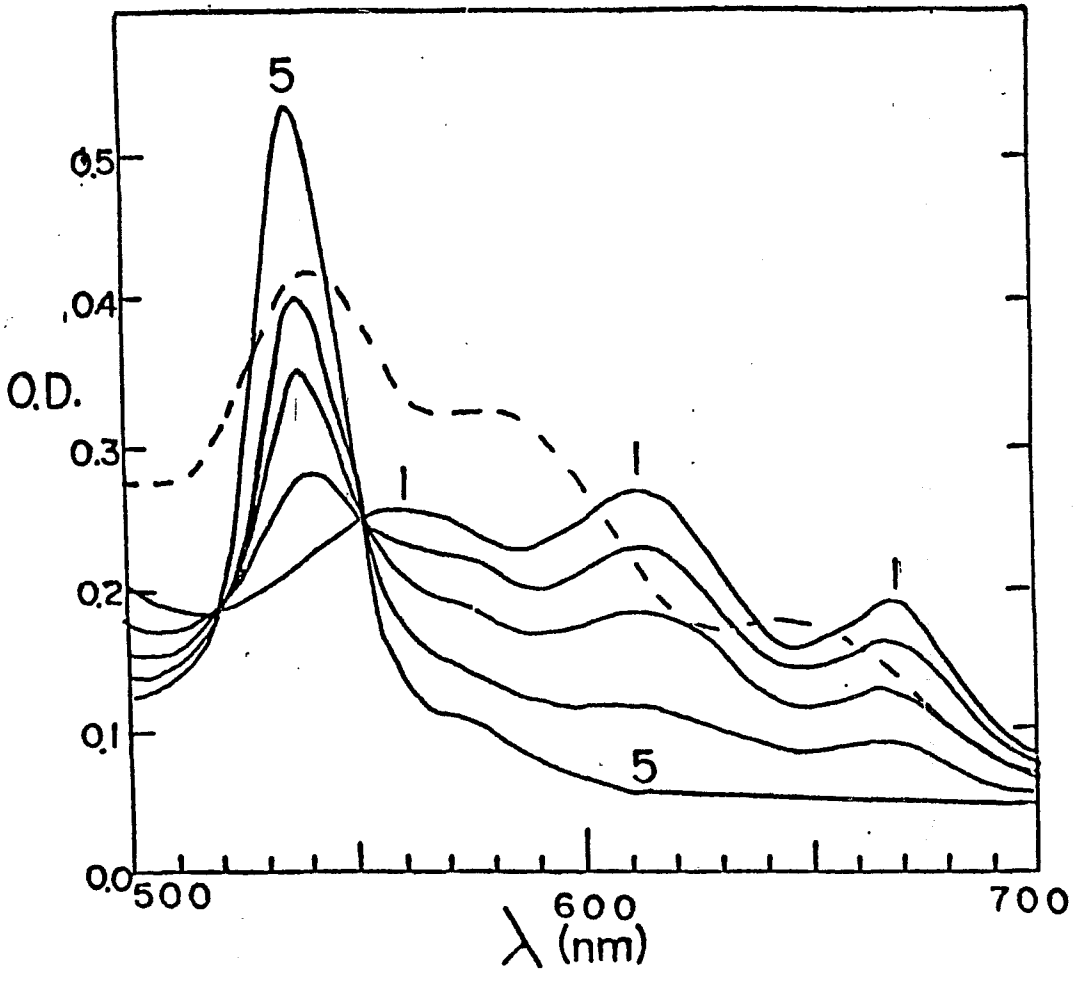
5
0.5
.04
O.D.
0.3
0.2
0.1
0.0
500
600
700
λ (nm)
1
1
5

Table I. First-Order Rate Constants for the Reaction of (N-methyl-5,10,15,20-tetraphenylporphinato)copper(II) Cation with Di-n-butylamine in Acetonitrile at 45^0C[a,b].

[Amine], M	10^3k, s^{-1}	[Amine], M	10^3k, s^{-1}
0.0073	0.088 ± 0.001	0.112	1.64 ± 0.04
0.0182	0.302 ± 0.012	0.145	2.11 ± 0.03
0.0362	0.630 ± 0.007	0.216	2.46 ± 0.07
0.0530	0.808 ± 0.027	0.433	3.96 ± 0.04
0.0725	1.20 ± 0.020	0.868	5.92 ± 0.20
0.108	1.36 ± 0.06	1.30	7.42 ± 0.43

a. Additional data obtained at 25^0C and 65^0C are presented in reference 49.

b. In this and subsequent tables in this chapter, the error limits are averaged deviations for two to six independent determinations of each rate constant. Typically the data for each kinetic run fit a first-order function for at least 4 half-lives with agreement between each calculated and observed absorbance value better than ± 1%.

Table II. First-order Rate Constants for the Reaction of (N-methyl-5,10,15,20-tetrakis(p-sulfophenyl)porphinato)copper-(II) Anion with Di-n-butylamine in Acetonitrile.

Temp., °C	[Amine], M	$10^3 k$, s^{-1}
25.3	0.070	0.251 ± 0.010
25.3	0.14	0.430 ± 0.001
25.3	0.28	0.744 ± 0.002
25.3	0.56	1.14 ± 0.02
44.5	0.14	2.08 ± 0.07
44.5	0.28	3.64 ± 0.16
44.5	0.56	5.82 ± 0.33
63.8	0.14	7.35 ± 0.09
63.8	0.28	11. 4 ± 0.4

Table III. First-Order Rate Constants for the Reaction of (N-methyldeuteroporphyrin IX dimethyl ester)copper(II) Cation with Di-n-butylamine in Acetonitrile.

Temp., °C	[Amine], M	$10^3 k$, s^{-1}
25.4	0.125	0.151 ± 0.003
25.4	0.250	0.233 ± 0.008
25.4	0.500	0.327 ± 0.008
44.2	0.125	0.718 ± 0.009
44.2	0.250	1.19 ± 0.002
44.2	0.500	1.84 ± 0.05
63.0	0.0625	1.63 ± 0.06
63.0	0.125	2.84 ± 0.01
63.0	0.500	7.93 ± 0.08

Figure 11. Plot of the observed pseudo-first-order rate constant for the reaction of the [N-methyl-5,10,15,20-tetrakis(p-sulfophenyl)porphinato]copper(II) anion with di-n-butylamine in acetonitrile at 44.5 ^{o}C vs. the concentration of di-n-butylamine.

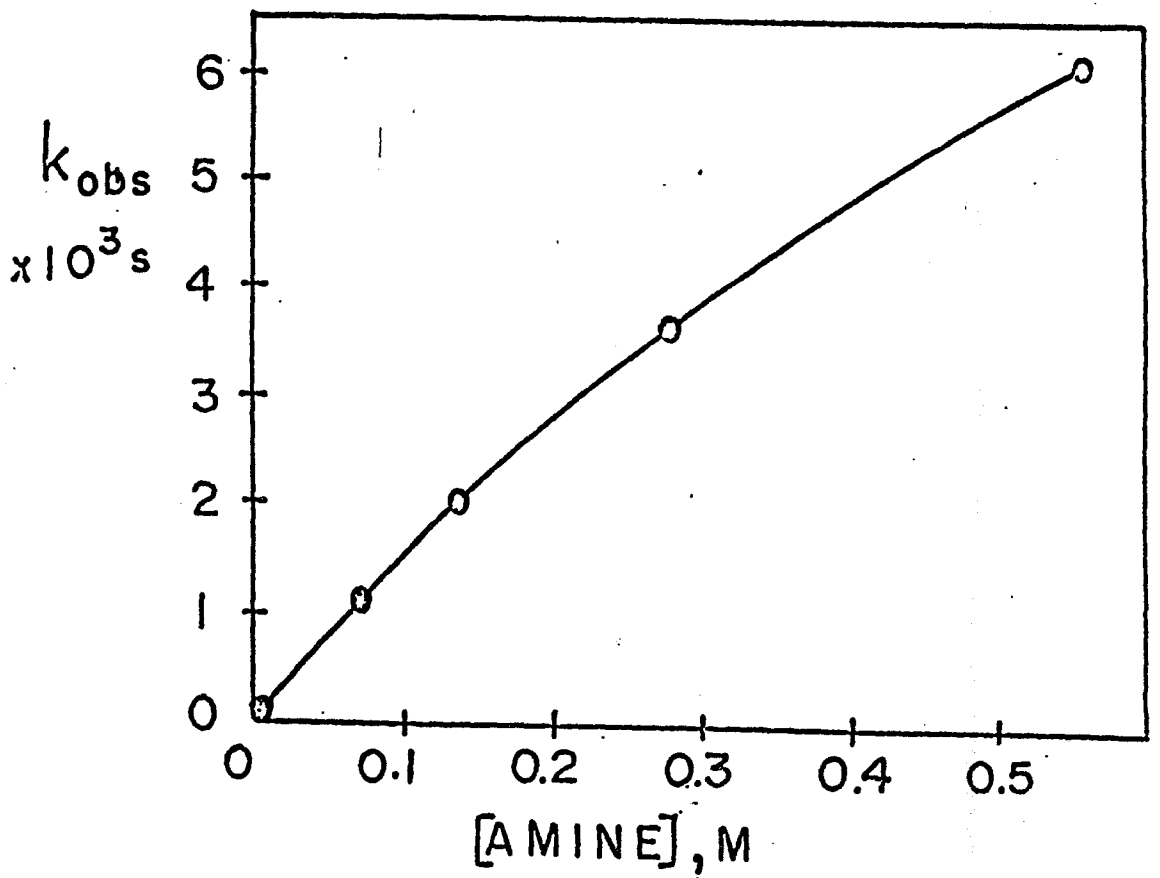
k_{obs}
$\times 10^3 s$
6
5
4
3
2
1
0
0
0.1
0.2
0.3
0.4
0.5
[AMINE], M

Figure 12. Plot of the observed pseudo-first-order rate constant for the reaction of (N-methyldeuteroporphyrin IX dimethyl ester)copper(II) with di-n-butylamine in acetonitrile at 44.2 ^{o}C vs. the concentration of di-n-butylamine.

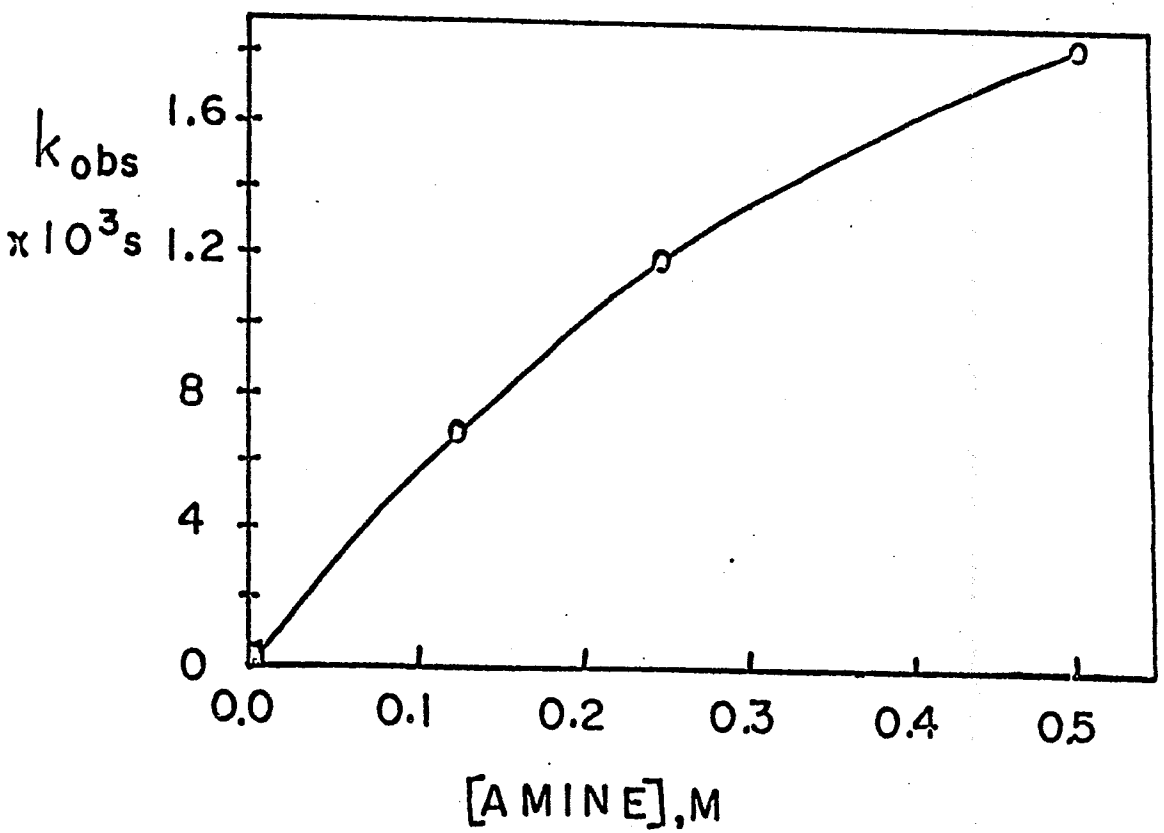
k_{obs}
$\times 10^3 s$
1.6
1.2
8
4
0
0.0
0.1
0.2
0.3
0.4
0.5
[AMINE], M

Table IV. First-Order Rate Constants for the Reaction of (N-Methyl-5,10,15,20-tetrakis(p-sulfophenyl)porphinato)-copper(II) Anion with Diethylamine in Aqueous Solution.

temp, ^{o}C	[amine], M[a]	$10^{3}k$, s^{-1}
25.4	0.242	0.0101
25.4	0.488	0.0219
25.4	0.735	0.0332
37.0	0.488	0.102 ± 0.001
45.1	0.242	0.123 ± 0.001
45.1	0.488	0.273 ± 0.004
45.1	0.735	0.361 ± 0.004
45.1	0.982	0.540 ± 0.008

a. Concentration determined on the basis of the dissociation constant of diethylammonium ion (3.2×10^{-11}). No dealkylation is observed in aqueous solutions containing high concentration of OH^- but no amine. There, OH^- was not considered as a competing nucleophile in these reactions. The solutions were unbuffered.

Figure 13. Plot of the observed pseudo-first-order rate constant for the reaction of [N-methyl-5,10,15,20-tetrakis(p-sulfophenyl)porphinato]copper(II) with diethylamine in aqueous solution at 45.1 °C vs. the concentration of diethylamine.

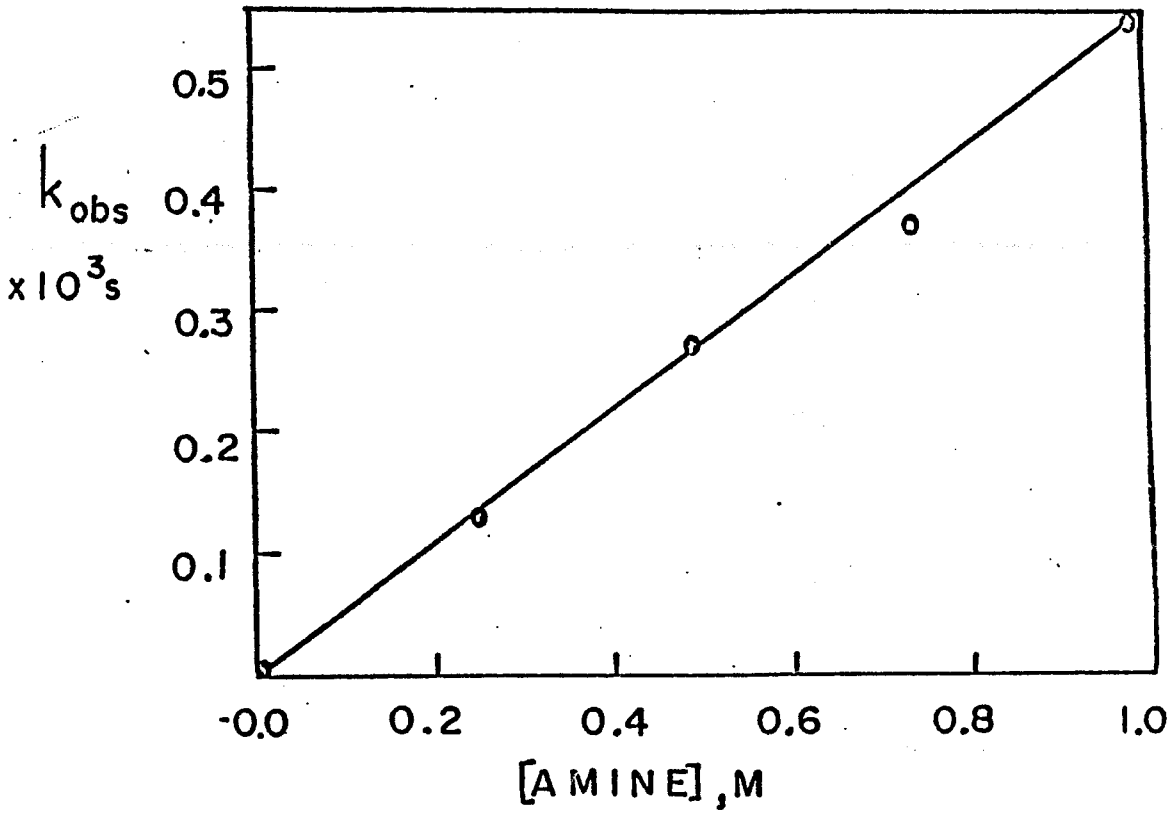
0.5
k_{obs} 0.4
$\times 10^{3}$s
0.3
0.2
0.1
-0.0
0.2
0.4
0.6
0.8
1.0
[AMINE], M

$CH_3TPP)^+$ with di-n-butylamine and tetraethylammonium chloride in CH_2Cl_2 are compiled in Tables V and VI. The observed rate constant vs. the concentration of di-n-butylamine in dichloromethane for the reaction of $Cu(N\text{-}CH_3TPP)^+$ with di-n-butylamine is plotted in Figure 14.

The low boiling point of dichloromethane and the relative slowness of the reactions prevented us from doing the reactions over a wide temperature range.

The values of k_1(path 1), k_2 and Keq (path 2 shown clearly in the scheme 1, in the discussion) are summarized in Table VII. As k_2 has to be decoded from the coupled value of k_2 and Keq (see the rate equation given in discussion section), a wide range of values have been obtained on statistical analysis. All the activation parameters are presented in Table VIII. The linear portions of non-linear plots (giving k_1, in Figures 11 and 12 and Fig. 2 of ref. 49) have been considered for the comparison of activation parameters.

Discussion The demethylation of metallo-N-methylporphyrin complexes by nucleophiles involves the removal of methyl group with the assistance of metal ion in consideration. (There is no reaction in the absence of a metal ion). Different trends are observed for the reactions of different metalloN-methylporphyrins with di-n-butylamine in acetonitrile. The demethylations with Cu(II)[49] or Ni(II)[50] are not first-order with respect to di-n-butylamine at relatively high concentrations of the amine, whereas demethylation with

Table V. First-Order Rate Constants for the Reaction of (N-Methyl-5,10,15,20-tetraphenylporphinato)copper(II) Cation with Di-n-butylamine in Dichloromethane.

temp., °C	[amine], M	10^3k, s^{-1}	temp., °C	[amine], M	10^3k, s^{-1}
25.2	0.00125	0.0390 ± 0.0011	30.0	0.0625	0.0986 ± 0.0036
25.2	0.00625	0.0400 ± 0.0012	30.0	0.0125	0.122 ± 0.001
25.1	0.0188	0.0476 ± 0.0010	30.0	0.250	0.150 ± 0.001
25.1	0.0313	0.0504 ± 0.0006	30.0	0.500	0.241 ± 0.002
25.2	0. 0625	0.0514 ± 0.0002	30.0	1.00	0.394 ± 0.014
25.2	0.125	0.0748 ± 0.0009	35.0	0.00125	0.0429± 0.0006
25.1	0.250	0.0852 ± 0.0004	35.0	0.00625	0.111 ± 0.003
25.2	0.500	0.153 ± 0.005	35.0	0.0312	0.142 ± 0.003
25.2	1.00	0.264 ± 0.005	35.0	0.0625	0.150 ± 0.001
30.0	0.00313	0.0530 ± 0.0080	35.0	0.125	0.186 ± 0.001
30.0	0.00625	0.0681 ± 0.0050	35.0	0.250	0.209 ± 0.008
30.0	0.0188	0.0731 ± 0.0040	35.0	0.500	0.285 ± 0.001
30.0	0.0313	0.0848 ± 0.0008	35.0	1.00	0.429 ± 0.017

Table VI. First-Order Rate Constants for the Reaction of (N-methyl-5,10,15,20-tetraphenylporphinato)copper(II) Cation with Tetraethylammonium Chloride in Dichloromethane.

temp, °C	$[Et_4NCl]$, M	10^3k, s^{-1}
25.1	0.00919	0.0560 ± 0.0003
25.1	0.0122	0.0520 ± 0.0005
25.1	0.122	0.0462 ± 0.0010
30.0	0.00331	0.0992 ± 0.0050
30.0	0.00496	0.0955 ± 0.0010
30.0	0.0331	0.0855 ± 0.0040
30.0	0.165	0.0717 ± 0.0020
30.0	0.331	0.0646 ± 0.0030
35.0	0.00142	0.161 ± 0.008

Figure 14. Plot of the observed pseudo-first-order rate constant for the reaction of (N-methyl-5,10,15,20-tetraphenylporphinato)copper(II) with di-n-butylamine in dichloromethane at 30.0 ^{o}C vs. the concentration of di-n-butylamine.

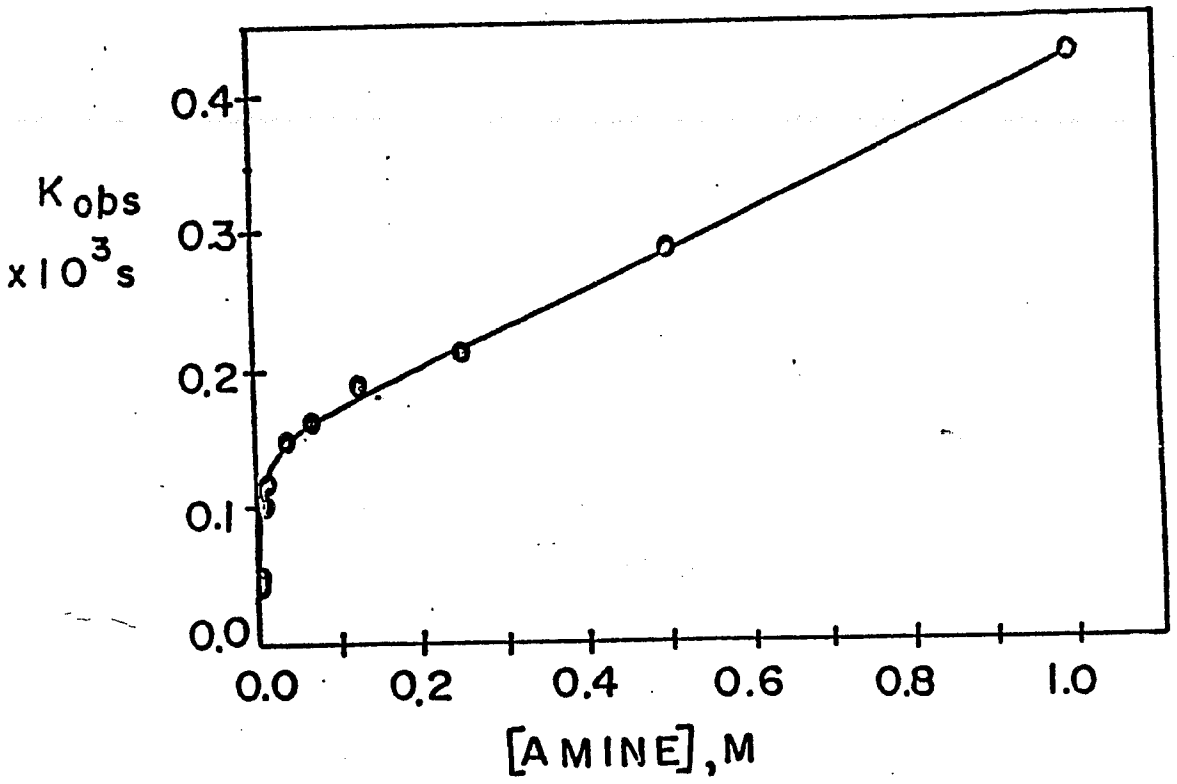
K_{obs}
$\times 10^3 s$
0.4
0.3
0.2
0.1
0.0
0.0
0.2
0.4
0.6
0.8
1.0
[AMINE], M

Table VII. Values of k_1, k_2 and K_{eq} for Several Demethylation Reactions of (N-Methyl-5,10,15,20-tetraphenylporphinato)copper(II) Complexes by Di-n-butylamine[a].

complex	solvent	T, °C	$10^3 k_1$, M^{-1} s^{-1}	K_{eq}	$10^3 k_2 K_{eq}$, $M^{-1} s^{-1}$	$10^3 k_2$[b], M^{-1} s^{-1}
$Cu(N\text{-}CH_3TPP)^+$	CH_3CN	25	2.94 ± 0.05	2.5 ± 0.2	0.75 ± 0.14	0.30
		45	18.0 ± 0.10	3.0 ± 0.5	7.0 ± 2.4	2.3
		65	151 ± 6	17 ± 2	210 ± 30	12
$Cu(N\text{-}CH_3TPPS_4)^{3-}$	CH_3CN	25.3	3.72 ± 0.13	1.5 ± 0.5	0.038 ± 0.84	0.025
		44.5	17.3 ± 0.04	1.8 ± 0.5	8.7 ± 5.2	4.8
		63.8	84.8 ± 1.4	6.0 ± 0.5	88 ± 18	15
$CU(N\text{-}CH_3DP)^+$	CH_3CN	25.4	1.44 ± 0.17	1.6 ± 0.2	-5.6 ± 0.8	-3.5[c]
		44.2	7.30 ± 0.08	3.0 ± 0.5	3.8 ± 0.2	1.3
		63.0	29.3 ± 0.7	4.3 ± 0.6	41 ± 8	9.5
$Cu(N\text{-}CH_3TPP)^+$[d]	CH_2Cl_2	25.1	86 ± 98	2000 ± 2300	440 ± 520	220
		30.0	79 ± 18	1000 ± 300	330 ± 80	330
		35.0	60 ± 10	400 ± 80	110 ± 20	270

a. Values are calculated using the equation $k_{obsd} = (k_1 A + k_2 K_{eq} A^2)/(1 + K_{eq} A)$ where A is di-n-butylamine. Standard deviations are obtained from the nonlinear least squares statistical program of the PROPHET system.
b. Since the values of k_2 is coupled to that of K_{eq}, a wide range of values allow reasonable fits to be obtained. c. Clearly physically unreasonable, but the best-fit values obtained. d. The sharp increase in the rate at very low nucleophile concentration, the volatility of CH_2Cl_2, and the slow rates at low nucleophile concentration make it difficult to obtain sufficient data for better determination of the parameters.

Table VIII. Activation Parameters for Demethylation of Copper(II) Complexes of N-Methylporphyrins.

complex	nucleophile	solvent	$\Delta H^{\ddagger}$, kcal/mol	$\Delta S^{\ddagger}$, eu	$\Delta G^{\ddagger}_{298}$, kcal/mol
$Cu(N\text{-}CH_3TPP)^+$	$(n\text{-}C_4H_9)_2NH$	CH_3CN	16.9 ± 1.0[a]	-13.1 ± 2.9	20.8 ± 1.9
$Cu(N\text{-}CH_3DP)^+$	$(n\text{-}C_4H_9)_2NH$	CH_3CN	15.3 ± 0.3[a]	-20.2 ± 0.9	21.3 ± 0.6
$Cu(N\text{-}CH_3TPPS_4)^{3-}$	$(n\text{-}C_4H_9)_2NH$	CH_3CN	15.6 ± 0.7[a]	-17.6 ± 2.2	20.8 ± 1.3
$Cu(N\text{-}CH_3TPPS_4)^{3-}$	$(C_2H_5)_2NH$	H_2O	23.6 ± 0.2	0.5 ± 0.6	23.4 ± 0.4
$Cu(N\text{-}CH_3TPP)^+$	$N(C_2H_5)_4Cl$	CH_2Cl_2	19.7 ± 0.4	-11.9 ± 1.3	23.2 ± 0.8
$Cu(N\text{-}CH_3TPP)Cl$	Cl^-	$CHCl_3$	24.4 ± 0.5[b]	+3.7 ± 1.1	23.3 ± 0.8

a. In those cases in which the dependence of the observed rate constant in nucleophile concentration is nonlinear, the data from the initial portion of the plot (attributed to the path involving solvent as axial ligand; see text) have been used to determine activation parameters.

b. Reference 59.

Mn(II) and Zn(II) complexes is first order in amine concentration even at high concentration. The proposed mechanism shown in the scheme below seems to be consistent with all the above facts.

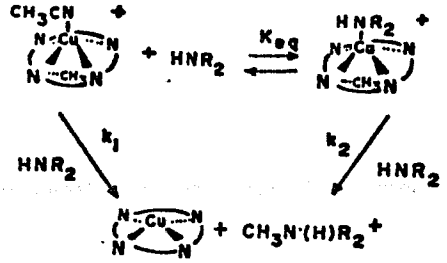

Scheme 2

The rate law consistent with the scheme 2 is:

$$\frac{d[M(TPP)]}{dt} = \frac{k_1 + k_2 K_{eq}[HNR_2]}{1 + K_{eq}[HNR_2]} [HNR_2] \quad [M-(N-CH_3TPP)^+]$$

where M = Cu(II) or Ni(II) and to the equation

$$\frac{d[M(TPP)]}{dt} = k[HNR_2] \; [M(N-CH_3TPP)^+]$$

where M = Mn(II) or Zn(II)

Figures 11 and 12 show the deviation from linearity at higher concentrations of amine in the reaction $Cu(-N-CH_3TPPS_4)^{3-}$ and $Cu(-N-CH_3DP)^+$ with di-n-butylamine in acetonitrile. At low concentrations of amine (<Ø.1M) there is a simple bimolecular reaction (k_1 path in the scheme 2). At higher concentrations of the nucleophile the amine can com-

pete well with the solvent and the amine coordinated metalloporphyrin can then react to form final product, CuTPP, by the reaction with another molecule of di-n-butylamine. However, the possibility of equal rates along either reaction path at low concentration of amine giving rise to the first order behaviour cannot be ruled out. Despite the complex nature of its kinetics, Cu(II) has been chosen because it reacts much faster than any of the other metal ions mentioned above. The non-linear behaviour is also observed for the reaction of $Cu(N\text{-}CH_3TPP)^+$ with di-n-butylamine in dichloromethane (Figure 14). The rates of the reaction of $Cu(N\text{-}CH_3TPP)^+$ with tetraethylammonium chloride are affected very little by the change in concentration of the chloride in dichloromethane. On the other hand, the rate of the reaction of $Cu(N\text{-}CH_3TPPS_4)^{3-}$ with diethylamine in aq. solution is linear with the concentration of amine.

Effect of Porphyrin Ring Substituents: The inactivation of cytochrome P-450 by different drugs or olefinic substrates is a suicidal process and the green pigments formed are all N-alkylprotoporphyrins (shown in Fig. 3 and 5). The N-alkyltetraphenylporphyrins are synthetic, not naturally occurring, porphyrins. We chose N-methyldeuteroporphyrin IX dimethylester to look at the effect of the absence of phenyl groups at the meso-positions on the demethylation reaction. Deuteroporphyrin differs from protoporphyrin in the substituents at 2 and 4 positions. The vinyl groups at the 2 and 4 positions are sensitive to light

and heat and lead to the formation of biliverdin-IX. By replacing vinyl groups by H atoms one obtains the more stable deuteroporphyrin. The naturally occurring N-alkylporphyrins, and the N-methyltetrakis(p-sulfophenyl)-porphyrin are very basic compared to N-CH_3HTPP. But the results in Tables I, II and III show that the great change in thermodynamic properties has no appreciable effect on the kinetics of demethylation reactions of $Cu(N\text{-}CH_3TPP)^+$, $Cu(N\text{-}CH_3DP)^+$ and $Cu(N\text{-}CH_3TPPS_4)^{3-}$ in CH_3CN by di-n-butylamine. Very similar activation parameters also suggest a similar transition state in all three cases. These results seem to suggest that the rates obtained for the dealkylation reaction of an easily available particular synthetic N-methylporphyrin complex may be used to predict the rates for costly naturally occurring porphyrins without meso substituents.

Effect of Solvents: Results in Tables I-III and V and Figures 11, 12 and 14 indicate that solvents like dichloromethane and acetonitrile have a feature in common as shown in scheme 2. Di-n-butylamine displaces coordinated dichloromethane more readily than acetonitrile because the former is a poorer solvent than the latter in coordinating to Copper-(II). The very steep rise in k_{obs} at very low concentration of amine (<Ø.ØØ3M) for the reaction of $Cu(N\text{-}CH_3TPP)^+$ in CH_2Cl_2 with di-n-butylamine shown in Figure 14 supports this contention. (There is no demethylation of $Cu(N\text{-}CH_3TPP)^+$ in the absence of di-n-butylamine. The absorbance changes very little on heating at 35°C for several days). The predominant path with di-n-butylamine in CH_2Cl_2 is the k_2 path

(scheme 2) whereas reactions with tetraethylammonium chloride differ significantly from that with amine in CH_2Cl_2. It is more likely that Cl^- can form an ion-pair very easily with $Cu(N\text{-}CH_3TPP)^+$ (unlike di-n-butylamine, Cl^- has a negative charge). The ion-pair formation with the complex is so favorable that the k_1 path is not observed where we have simple bimolecular reaction between the substrate and the nucleophile as in the case of di-n-butylamine. At the same time, it does not seem as another molecule of chloride ion acts as a nucleophile as in the case of amine. This conclusion can be rationalized by the fact that large excess chloride ion does not increase the reaction rate. (In the case of di-n-butylamine one can clearly see the increase in rate with an increase in concentration of of amine Fig. 14). Also there is a change in the visible spectra and cyclic voltammetry of $Cu(N\text{-}CH_3TPP)^+$ and $Cu(N\text{-}CH_3TPP)Cl$. Excess chloride does not change the visible spectra and the metal redox potential of $Cu(N\text{-}CH_3TPP)Cl$ (Chapter 4). The reactions of $Cu(N\text{-}CH_3TPPS_4)^{3-}$ with diethylamine in aqueous solution are qualitatively as well as quantitatively different from those in the poorly solvating media acetonitrile and dichloromethane. The large decrease in rate (about 100 fold) in H_20 ($Cu(N\text{-}CH_3TPPS_4)^{3-}$ in H_20. $[(C_2H_5)_2NH] = 0.488$ M, Temp. = 25.4°C $k_{obsd} = 2.19x10^{-5}$ sec $^{-1}$, $Cu(N\text{-}CH_3TPPS_4)^{3-}$ in CH_3CN . $[(n\text{-}C_4H\text{-}_9)_2NH] = 0.56$ M Temp. = 25.3°C $k_{obsd} = 1.14x10^{-3}$ sec $^{-1}$) is in accordance with greater stabilization of the reactants which increases the activation ener-

gy in water. Moreover, the observed rate constants for the reaction of $Cu(N\text{-}CH_3TPPS_4)^{3-}$ with diethylamine are linear with the increase in concentration of diethylamine. (Hydroxide ion does not seem to act as a nucleophile at room temperature and the dealkylation is relatively slow even at higher temperature so that OH^- does not affect the rates of demethylation.)[55] Since water can bind more strongly to Cu then acetonitrile it does not seem to be displaced by a dialkylamine. The possibility of equal rates by two paths (as shown in scheme 2) cannot be ruled out completely.

Effect of Nucleophiles: In the previous reports[49] it has been shown that di-n-butylamine and diethylamine have the same nucleophilicity ($Cu(N\text{-}CH_3TPP)^+$ in CH_3CN, [di-n-butylamine] = 0.433 M, k_{obs} = (3.96 ± 0.04)x$10^{-3}s^{-1}$ [diethylamine]= 0.436M, k_{obs} = (3.42 ± 0.01)x$10^{-3}s^{-1}$.) and the product analysis and stoichiometry indicates a 1:1 conversion of nucleophiles to methylated nucleophiles. It also showed pyridine to be a much poorer nucleophile than the dialkylamines.

Chloride ion seems to be a slightly stronger nucleophile than pyridine and pyridine is a much poorer nucleophile than di-n-butylamine (in the reactions of $Cu(N\text{-}CH_3TPPS_4)^{3-}$ in acetonitrile [Et_4NCl] = 0.5M, k_{obsd}=(6.9 ± 0.1)x$10^{-4}s^{-1}$ at 55.0°C and [pyridine] = 2.38 M, k_{obsd} = (6.9 ± 0.1)x $10^{-5}s^{-1}$ at 54.6°C). The nucleophilicity of pyridine is less than that of di-n-butylamine in the reactions of $Cu(N\text{-}CH_3TPP)^+$ in dichloromethane ([pyridine = 2.02M, k_{obsd} = (1.9 ± 0.1) x10^{-5} s^{-1} at 35.5°C). Chloride ion seems to be

ineffective in the demethylation of $Cu(N\text{-}CH_3TPPS_4)^{3-}$ in aqueous solution (limited experiments have been done in this case).

The reaction of $Cu(N\text{-}CH_3TPP)^+$ with chloride ion is not bimolecular as found in the reaction of the former with di-n-butylamine. The demethylation reaction of $Cu(N\text{-}CH_3TPP)^+$ by Cl^- in CH_2Cl_2 is consistent with the results of Stinson and Hambright concerning the spontaneous demethylation of Cu(N-CH_3- TPP)Cl in chloroform[59]. We have added tetraethylammonium chloride to trifluoromethanesulfonate salt of $Cu(N\text{-}CH_3TPP)^+$ where $CF_3SO_3^-$ is very labile and can be replaced by Cl^- very easily. The reactions in dichloromethane are slightly slower than in chloroform[59] ($5.6\times10^{-5}s^{-1}$ at 25.1°C in CH_2Cl_2, $1.54\times10^{-4}s^{-1}$ at 25.5°C in $CHCl_3$). This difference can be attributed to the difference in polarity of the solvents. We have seen that the reaction of $Cu(N\text{-}CH_3TPP)^+$ with di-n-butylamine in acetonitrile is faster than in dichloromethane ($k_{obs} = 5.2\times10^{-4}s^{-1}$ for [di-n-butylamine] = 0.48M in CH_3CN, 25°C, $1.5\times10^{-4}s^{-1}$ for [di-n-butylamine] = 0.50M in CH_2Cl_2, 25°C). The non coordinating ion, tetrabutylammonium perchlorate (0.50M), has very little effect on the reaction rates (at 30.0°C, $(9.9\pm0.1)\times10^{-5}s^{-1}$ compared with $(7.8 \pm 0.2)\times10^{-5}s^{-1}$ in the presence of excess perchlorate). The fact that the rate of demethylation by chloride does not depend upon the concentration of chloride in our case and the spontaneous demethylation of $Cu(N\text{-}CH_3TPP)Cl$ results in the formation of CH_3Cl and CuTPP[59] by a first-

order mechanism suggests that Cl^- has to be on the same side as the methyl group attached to the nitrogen atom. But all the crystal structures of M(N-CH_3TPP)Cl (where M = Zn(II), Co(II), Mn(II), Fe(II)) indicate that chloride ion is bound to the opposite side of metal ion. It is then reasonable to think that Cl^- is present as an outer-sphere ion, (Cu-N-CH_3TPP)$^+Cl^-$, the reactivity of which is less than the inner-sphere ion form. Stinson and Hambright also have attributed the slowness of the demethylation of Cu(N-CH_3TPP)Cl in methanol to the stability of this outer-sphere adduct.[59] The outer-sphere Cl^- can then attack the methyl group and prevent one from seeing the second order behaviour expected for the attack of free Cl^- on the methyl group of solvated Cu(N-CH_3TPP)$^+$. It is very interesting that at the same time it has to be a rather tight ion-pair to give the demethylation rate independent of the total porphyrin concentration from ca. 10^{-4} to 10^{-6}M.[59]

Conclusion: From the results above and those presented in ref. 49 and 50 we can conclude that the dealkylation rates are influenced by the metal ions and nucleophiles to a greater degree than the porphyrin ring substituents. Solvents as well as nucleophiles have profound effect on the dealkylation rates and its mechanism. Synthetic metallo-N-alkylporphyrins can be used to predict the dealkylation rates of metallo-N-alkylporphyrins without meso substituents, i.e. naturally occurring porphyrins.

CHAPTER 3

EFFECT OF ALKYL AND ARYL GROUPS ON THE KINETICS OF DEALKYLATION REACTIONS OF METALLO-N-ALKYL(OR ARYL)-PORPHYRINS

INTRODUCTION

The disruption of heme biosynthetic pathway by drugs like 3,5-diethoxycarbonyl-1-4-dihydro-2,4,6-trimethylpyridine (DDC) and its 4-ethyl analog, 3,5-diethoxycarbonyl-2,6-dimethyl-4-ethyl-1,4-dihydropyridine (DDEP), leads to the formation of green pigments, N-alkylporphyrins, by transfer of the 4-alkyl substituent onto one of the pyrrole nitrogen atoms. A different mechanism operates in the destruction of cytochrome P-450 by drugs containing an allyl group (for example 2-alkyl-2-isopropylacetamide, AIA). In these cases, a monooxygenated derivative of the drugs gets bound to the nitrogen atom. We have undertaken this work to explore the kinetic factors which are related to the decomposition of the possible intermediates, in the inactivation of cytochrome P-450. It is our interest to investigate factors which are responsible in the dissociation of an alkyl group from an N-alkylporphyrin complex[49,50,55] and those which favor the removal of metal atom.[61] The products obtained in the inactivation of cytochrome P-450 by the above drugs suggest that iron atom removal predominates over dealkylation.

Radioactive palladium-109-hematoporphyrin is being currently used in selective lymphatic ablation to prevent the rejection of transplanted organs.[32,33]. The reactions in which metallo-non-N-alkylporphyrins are formed from the demethylation of metallo-N-methylporphyrins are very slow

with the metal ions which unlike palladium, do not form that relatively planar metalloporphyrins.[50] One of the objectives of this Chapter is to find better leaving alkyl groups that can be helpful in rapid synthesis of the desired radiolabelled metalloporphyrin by the method of dealkylation.

Previous studies with Cu(II) N-methylporphyrin[49,55] complexes have indicated that the demethylation reactions are bimolecular, in which the nucleophiles attack the methyl group presumably through a S_N2 type mechanism involving a transition state with considerable carbocation character. Therefore we have considered different N- alkylporphyrins (alkyl = - C_2H_5, $-CH_2-\langle\bigcirc\rangle-NO2$, $CH_2COOC_2H_5$, C_6H_5, Fig. 15) of Cu(II) to explore the kinetic as well as steric factors involved in the dealkylation process. We have chosen Cu(II) only because the previous studies have involved Cu(II) complexes and the reactions with Cu(II) have been found to be reasonably fast compared to Ni(II), Zn(II), and Mn(II) (with methyl group on nitrogen).[49,50,55]

Figure 15. The structures of N-substituted-5,10,15,20-tetraphenylporphyrin and N-phenylprotoporphyrin IX dimethyl ester(R = $-CH_3$, $-C_2H_5$, $-C_6H_5$, $-p-CH_2C_6H_4NO_2$ and $-CH_2CO_2C_2H_5$ and R' = $-C_6H_5$).

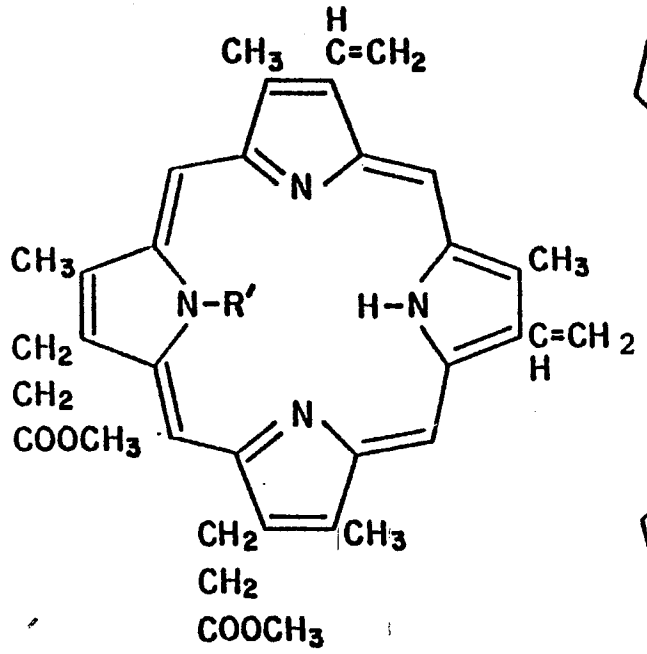
H
CH3 C=CH2
N
CH3
N-R'
H-N
CH3
C=CH2
H
CH2
CH2
COOCH3
N
CH2 CH3
CH2
COOCH3

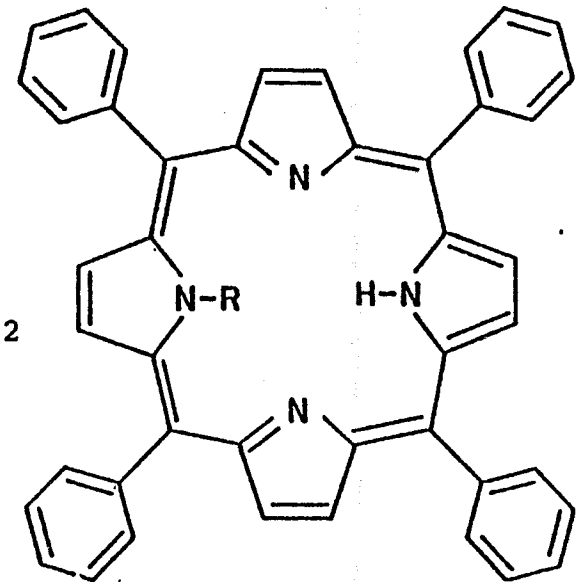
N
N-R
H-N
N

SYNTHESIS

Syntheses of N-ethyl-tetra-5,10,15,20-phenylporphyrin (N-C_2H_5HTPP):

Method A: A Slight excess over a stoichiometric amount of dilute solution of ethylfluorosulfonate in methylene chloride was slowly added drop-by-drop to a refluxing solution of tetraphenylporphyrin (H_2TPP prepared by the method of Adler, et al.[51] was used without further purification of small amount of chlorin present in the sample) and refluxed for 2 days. The resulting green solution was neutralized with NH_3 and dried over Na_2SO_4. The only band (UV-VIS) at 675 nm of the mixture indicated the presence of N-C_2H_5HTPP. The rest of the peaks were from TPP (due to the high extinction coefficients and greater percentage of the latter). TLC indicated the presence of unreacted H_2TPP and more highly alkylated products as well as N-C_2H_5HTPP. Using CH_2Cl_2/EtOAC (5:1) as eluent, the middle spot matched that of an authentic sample of N-C_2H_5HTPP. The mixture was purified on silica gel (Merck type 400-230 mesh) using flash chromatography.[62] The H_2TPP was removed with CH_2Cl_2 and the slow increase of polarity of the eluent with EtOAC yielded N-C_2H_5HTPP. Purity of the sample was checked by TLC and by NMR and UV-VIS spectroscopy. Yield = 14-15% ^{1}H NMR ($CDCl_3$, 200 MHz) δ, -4.43 (7.2H); 1.635(t,3H), 7.5(s, 2H; the pyrrole ring bearing the ethyl group), 7.77 to 8.38 (m, 20H, meso-phenyl groups) 8.49(d, 2H, pyrrole ring adjacent to the alkylated ring), 8.7 (d, 2H pyrrole ring adjacent to the

alkylated ring), 8.81 (s, 2H pyrrole ring opposite to the one bearing the ethyl group).

Method B: Few modifications of the method developed by Callot et al.[63] were used.

i) Syntheses of N,N'-bridged TPP: In a typical experiment, a mixture of H_2TPP (2.0 gm), benzyltriethylammonium chloride (BTEA) (200 mg; Aldrich), NaOH 2.0 gm). H_2O (2 mL), absolute ethanol (2.0 mL), and $CHCl_3$ (120 mL, freshly distilled over P_2O_5) were stirred vigorously with a magnetic stirbar under N_2 or Ar for 2-3 hours. 20 gms of Na_2SO_4 (anhydrous) were added and the mixture was filtered through a frit. The solid left on the frit was extracted with CH_2Cl_2; and the extracts were combined with the filtrate and evaporated to about 30 mL. It was then filtered through glass wool plugged in a disposable pipette or funnel to remove some of H_2TPP and was then purified by flash chromatography with ~20% EtOAc in CH_2Cl_2 as eluent as described in method A. Flash chromatography seems to be a very good technique in the purification of N,N'-bridged TPP. The bridged porphyrin seemed to decompose on standing which was prevented by keeping it in the freezer. Yield 30-35%.

ii) Syntheses of NC_2H_5HTPP: A solution of N,N' bridged TPP (50mg) and ethyl iodide (2 mL) in dry CH_2Cl_2 (8 mL) was stirred at room temperature for 72 h. TLC indicated the completion of the reaction. The solvent was evaporated and the crude iodide was dissolved in CH_2Cl_2. Then TSOH.H_2O (0.1 gm) was added and the green solution was

stirred for 4 h at room temperature (Fig. 16). It was then washed with aqueous Na_2CO_3 or $NaHCO_3$, dried, filtered and purified by flash chromatography to eliminate H_2TPP. Yield 70%. Overall yield:21%.

In all flash chromatographic purifications, silica gel 40-63 mu (400-230 mesh), 60 (E. merck No. 9385) were used (available from MCB).

Syntheses of N-p-nitrobenzyl-5-10-15-20-tetraphenylporphyrin (N-p-CH_2-$C_6H_4NO_2$HTPP): The N-$CH_2C_6H_4NO_2$HTPP was synthesized by the method of Callot et al.[63] (Figure 16). It was purified by flash chromatography and recrystallized with CH_2Cl_2/CH_3CN. A single spot on TLC and UV-VIS spectroscopy ascertained the purity of the sample. ^1H NMR ($CDCL_3$, 200 MHz), δ , N-CH_2 -3.44(s), 4.650 (d, J=8.8Hz). 7.409 (d, J = 8.8Hz), (benzyl group attached to the nitrogen atom), 7.587 (s, 2 pyrrolic H, the pyrrolic ring bearing the p-nitrobenzyl group), 7.771 (m, 12H, meta and para protons of meso-phenyl proton groups), 8.100 (m, 4H ortho protons of meso-phenyl groups), 8.185(s, 2H, o-H), 8.296 (s, 2H, o-H), 8.505 (d, 2H, J = 4.6Hz, pyrrole ring adjacent to the benzylated ring, 8.614 (d,2H, J = 4.6Hz, pyrrole ring adjacent to the benzylated ring), 8.87 (S, 2H, pyrrole ring opposite to the one bearing the p-nitrobenzyl group).

Synthesis of N-ethylacetato-5-10-15-20-tetraphenylporphyrin(N-$CH_2CO_2C_2H_2$TPP)

Method A: The method of Henry Callot[69] was followed in this case. In the original procedure, ethyldiazopropionate was used in the synthesis of N-CH(-CH_3)$CO_2C_2H_5$HTPP. Ethyl

Figure 16. The synthetic scheme for N-RHTPP (R = $-C_2H_5$ and $-p-CH_2C_6H_4NO_2$) is shown at the top.

Lower. The syntheses of $N-C_6H_5HTPP$ is presented schematically.

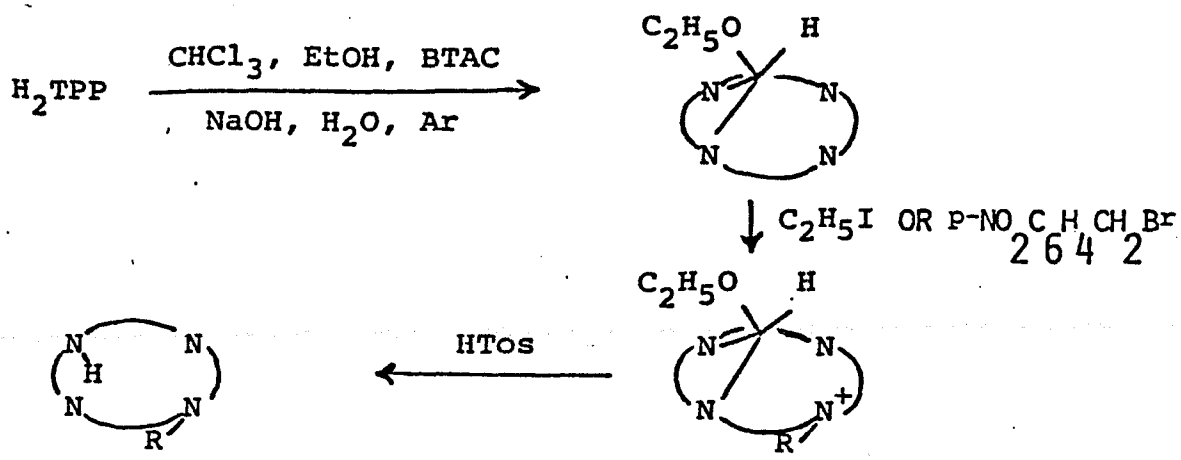
H2TPP
CHCl3, EtOH, BTAC
NaOH, H2O, Ar
C2H5O
H
C2H5I OR p-NO2C6H4CH2Br
HTos

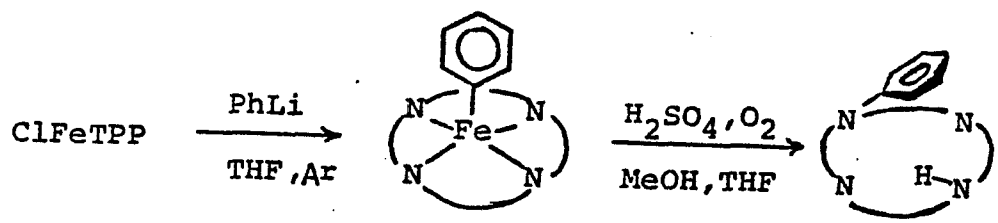
ClFeTPP
PhLi
THF, Ar
Fe
H2SO4, O2
MeOH, THF

diazoacetate (Aldrich) instead of ethyl diazopropionate was added to the refluxing solution of ZnTPP(150mg), xylene (5mL) and H_2O (0.05mL) and the refluxing was continued for 20 minutes after the addition. The solution was cooled, treated with HCl to remove the metal. Yields from different attempts were not satisfactory (less than 15%).

Method B: Thermal decomposition of ethyldiazoacetate (N_2CHCO_2Et) in the presence of ZnTPP was carried out as mentioned in the literature.[65] N_2CHCO_2Et (3mL) was added drop-by-drop to the refluxing solution of ZnTPP (1.005 gm) in xylene (25mL) for 1 hr and stirred vigorously. It was refluxed for 15 minutes more and the xylene was removed. The crude product was dried using a vacuum pump (80°C, 10^{-2} torr) to eliminate ethyl fumarate. The residue was chromatographed on silica gel (200 gm) with benzene as eluent. Traces of cyclopropanic compounds and 222 mg. of product were removed. A mixture of $CHCl_3$ and CH_3CO_2Et(96:4) eluted the traces of cyclopropanic products and a mixture of green products. The fractions eluted by a mixture of polar solvents, ($CH_3CO_2C_2H_5$, CH_3OH) were combined with the previous fractions. After the removal of solvents, it was dissolved in CH_2Cl_2 and 0.5mL of conc. HCl was added and allowed to stand for 5 minutes. It was then treated with aqueous saturated ammonium carbonate and washed with water (3x) and dried over Na_2SO_4, filtered and the solvent was evaporated off. The residue was chromatographed over Al_2O_3 (140 gm). CH_2Cl_2 elutes the traces of H_2TPP and the cyclopropanic

products followed by violet N-CH_2CO_2EtHTPP; then finally the unidentified products. The yield was quite good. (300 mg. 30%)

Method C: The best method for the synthesis of N-CH_2CO_2EtHTPP involved heating of ZnTPP (500 mg.) and ethyl diazoacetate (1.5mL) in chlorobenzene (10mL) at 100°C for 24 hrs in an oil bath.[66] Concentrated HCl(3 mL) and and CH_2Cl_2 (100 mL) were added to the mixture and stirred for 5 minutes followed by neutralization with solid ammonium carbonate. The washed dichloromethane layer was evaporated to dryness and passed through Al_2O_3 Column (Al_2O_3 was dried in an oven at 100°C). A mixture of toluene and hexane (50:50) eluted H_2TPP. The polarity of the eluent was increased gradually with the addition of toluene, then ethylacetate. When there was no more H_2TPP left in the column, CH_2Cl_2 was used to elute N-CH_2CO_2EtHTPP. The spectrum of the crude product before demetallation with acid showed it to be ZnN-$CH_2CO_2C_2H_5$HTPP (which was further proved by the removal of the metal). Yield: 295 mg.,58% It was recrystallized with CH_2Cl_2/CH_3CN. The proposed reaction scheme for the formation of N-$CH_2CO_2C_2H_5$HTPP is as follows:

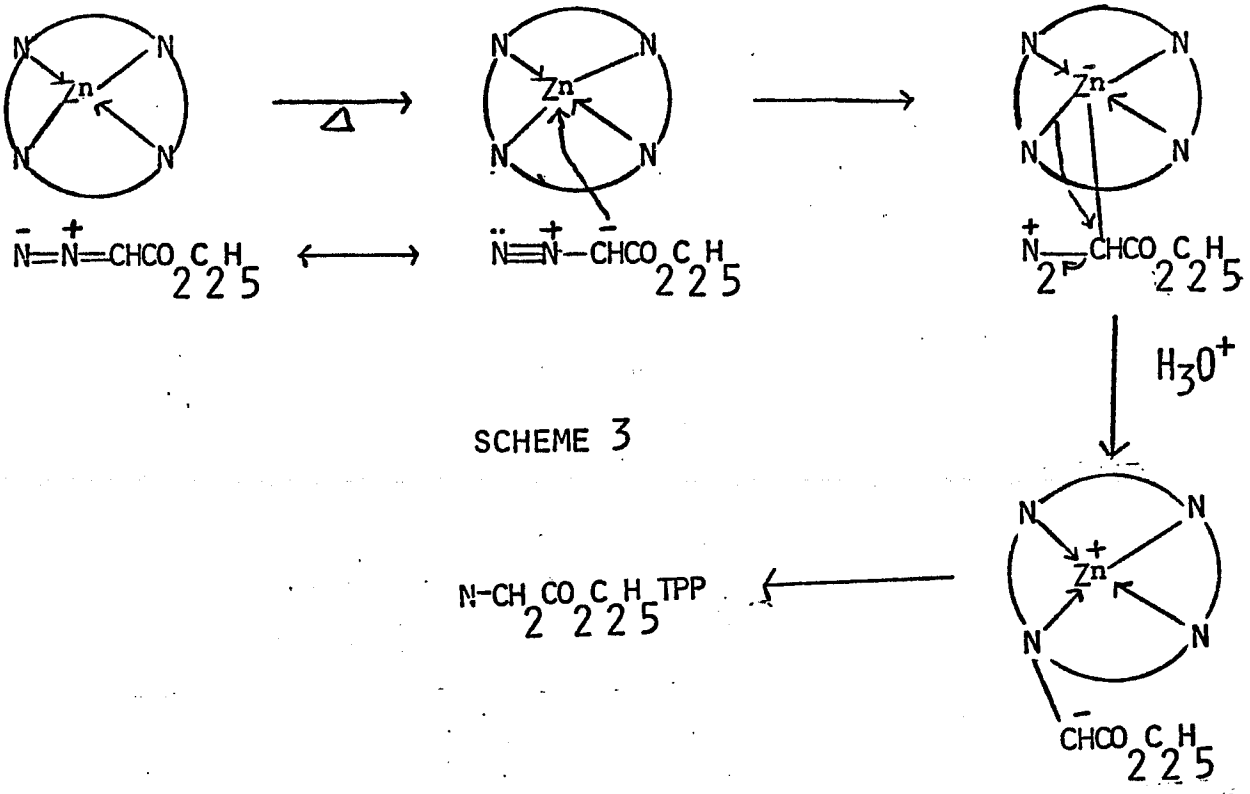

SCHEME 3

Synthesis of N-phenyl-5-10-15-20-tetraphenylporphyrin.

The N-PhHTPP was synthesized by an adaptation of the method of Ortiz de Montellano et al.,[26] Pyhenyllithium(Alfa) rather than phenylmagnesium bromide was used to form the iron-phenyl complex, PhFeTPP;which was used without further purification. The Fe(TPP)Cl was prepared by the method of Fleisher et al.[67] and recrystallized from CH_2Cl_2/CH_3CN or obtained from Strem Chemicals. In a typical preparation, 400 mg. of Fe(TPP)Cl was taken in a 100 mL. R.B. flask and dried with a flame under vacuum and Ar. 80 mL. of dry THF (freshly distilled under Ar over metallic potassium) was transferred to the flask containing Fe(TPP)Cl in an atmosphere of Ar using a needle lock syringe (Available from

Popper & Sons., Inc., New Hyde Park, N.Y. 11040). The solution became red just after the addition of 0.25 mL. of phenyllithium (2.1M in pentane) and 20-25 mg. of BHT (2,6-di-tert-butyl-4methylphenol) were added. (The yield for the formation of PhFeTPP is lowered drastically if the reaction mixture is not strictly dry). The visible spectrum of the red solution (PhFeTPP) has peaks at 613 nm(sh), 531 nm, 429 nm(sh), 417 nm and 396 nm(sh). 120 mL of THF containing 25-40 mg. of BHT and 200 mL. of CH_3OH containing 5% H_2SO_4 were added to the mixture and the mixture was stirred overnight. The mixture was then washed with H_2O, extracted with CH_2Cl_2 and the CH_2Cl_2 layer was washed with $NaHCO_3$ solution, dried over Na_2SO_4 and the product purified by flash chromatography, Yield: 30-35%. (Figure 16) It was recrystallized from CH_2Cl_2/heptane. The NMR spectrum matches literature values.[26]

The N-phenylprotoporphynatozinc(II) was generously supplied by the group of Ortiz de Montellano of the University of California, San Francisco. The synthesis of this material and its free base have been reported in the literature.[68,25]

Synthesis of the Copper(II) Complexes. In a typical synthesis of N-ethyl-5-10-15-20-tetraphenylporphinatocopper(II) trifluoromethanesulfonate, 45 mg. of N-C_2H_5HTPP and three fold excess of $Cu(CF_3SO_3)_2.6H_2O$ (preparation of $Cu(CF_3SO_3)_2.6H_2O$ has been mentioned in Chapter 2) were dissolved in dry CH_3CN.(N-C_2H_5HTPP, free base, is slightly sol-

uble in CH_3CN). About 0.2 mL of 2,2,6,6-tetramethylpiperidine was added to the mixture and stirred for an hour. The formation of the complex was quantitative on the basis of the visible spectrum. It was then filtered and evaporated using a rotary flash evaporator. The excess of Cu-salt was removed by washing the complex with water. The product was then extracted with dichloromethane and dried over Na_2SO_4. The visible spectrum in the soret region showed a small amount of CuTPP (~5%). The mixture of $Cu(N\text{-}C_2H_5TPP)^+ CF_3SO_3^-$ containing CuTPP was then purified by flash chromatography with ~2-3% methanol in CH_2Cl_2 as eluent. The less polar CuTPP, red colored, came off the column first. The pure complex of $Cu(N\text{-}C_2H_5TPP)^+ CF_3SO_3^-$ was recovered using a flash rotary evaporator. It was then kept in a standard freezer to avoid its decomposition into CuTPP. Yield: 57%. Though the formation of $Cu(N\text{-}C_2H_5TPP)^+ CF_3SO_3^-$ was quantitative, purification as well as formation of CuTPP lowered its yield. The uv-vis spectrum in CH_3CN, with extinction coefficients in $M^{-1}\ cm^{-1}$ in parentheses, is: 657 nm ($1.2X10^5$). 590nm ($7.0X10^3$), 547nm($9.0x10^3$), 441nm($1.2x10^5$), 434($1.1x10^5$). Analysis (performed in Analystische Laboratorien: Postfack 1249-5250 Engelskricken, West Germany) calculated for $CuC_{47}H_{33}N_4SO_3F_3$: C 66.02%; H, 3.86%; N 6.55% Found. C, 66.05%; H, 4.12%; N, 6.16%.

The N-phenyltetra-5,10,15,20-phenylporphinatocopper(II) trifluoromethanesulfonate, $Cu(N\text{-}PhTPP)^+CF_3SO_3^-$, complex was similarly synthesized and purified by flash chromatography. The complex is extremely stable in the solid

state or in solution. The uv-vis spectrum in CH_3CN, with extinction coefficients in $M^{-1}cm^{-1}$ in parenthesis is 675 nm($5.5x10^3$), 609 nm($9.8x10^3$), 556 nm($10.2x10^3$), 455 nm($1.3x10^5$), 440 nm(sh, $1.1x10^5$). Analysis (done in Analystiche Laboratorien) calculated for $CuC_{51}H_{33}N_4S0_3F_3$. C, 67.89%; H,3.69%; N 6.2%. Found: C, 67.88%; H, 4.18%;N 5.89%.

The p-nitrobenzyl-5,10,15,20-tetraphenylporphinatocopper(II) complex was readily debenzylated to form CuTPP so that isolation of pure complex was not achieved. The pure material obtained using flash chromatography had fleeting existence in solution. However, the complexes prepared <u>in situ</u> by the addition of a 2-3 fold excess of $Cu(CF_3S0_3).6H_20$ to a solution of $NCH_2-C_6H_4N0_2TPP$ in dry CH_3CN with non-coordinating base, 2,2,6,6-tetramethylpiperidine (about 0.10 mL of a 0.02 M solution in CH_3CN was added to 20 mL of the reaction mixture) were consistent with quantitative formation and were stable for months when kept in freezer. The uv-vis spectrum: 659 nm($7.3x10^3$), 599 nm($1.09x10^3$), 547 nm($1.38x10^3$) and 441 nm($1.73x10^5$).

EXPERIMENTAL

Purification of solvents and amine have been mentioned in the previous chapter (i.e. chapter 2).

<u>Kinetics Experiments.</u> The instruments used for kinetics experiments have been mentioned in chapter 2. Data analysis were performed similarly[60] (see appendix). In all reactions mentioned here di-n-butylamine was present in pseudo-first-

order excess.

The stock solution of N-ethyl-5,10,15,20-tetraphenylporphinatocopper(II) trifluoromethanesulfonate was prepared by mixing N-C_2H_5HTPP and 2-3 fold excess $Cu(CF_3SØ_3)_2.6H_2Ø$ in dry CH_3CN with few drops of diluted 2,2,6,6-tetramethylpiperidine (Ø.ØØ5M in CH_3CN). The visible spectrum of stock solution matched with that of analyzed solid Cu(N-C_2H_5TPP)$^+CF_3S\bar{Ø}_3$ dissolved in CH_3CN. The stock solution was stable for several months in the light at room temperature without formation of any CuTPP. The kinetics of dealkylation reactions of Cu(N-C_2H_5TPP)$^+$ $CF_3SO_3^-$ prepared in acetonitrile with excess Cu(II) were similar to that with the analyzed sample of Cu(N-C_2H_5TPP)$^+CF_3SO_3^-$ under similar conditions (At 25.Ø°C, [di-n-butylamine]= Ø.5ØØM, k_{obs}= (Ø.719 ± Ø.Ø15) x 10^{-14} sec^{-1} with excess copper (II) and k_{obs} = (Ø.578 ± Ø.ØØ8) x $10^{-4}sec^{-1}$ for the analyzed sample.

In a typical experiment, the stock solution of Cu(N-$CH_2CO_2C_2H_5$TPP)$^+CF_3SO_3^-$ was prepared by mixing a 1.6-2 fold excess of $Cu(CF_3SØ_3)_2.6H_2Ø$ with N-$CH_2CØ_2C_2H_5$HTPP in CH_3CN(25 mL) with Ø.75 mL of Ø.ØØ5M 2,2,6,6-tetramethylpiperidine (non-coordinating base) in CH_3CN (added dropwise) Stock solutions were stable for several months. Stock solution of Cu(N-C_6H_5TPP)$^+$ were prepared by mixing $Cu(CF_3SO_3)_2.6H_2Ø$ in excess (2-3 fold) to N-C_6H_5HTPP in CH_3CN with the addition of approximately Ø.1Ø mL of Ø.Ø55 M 2,2,6,6-tetramethylpiperidine ion CH_3CN. The visible absorption spectrum matched that recorded with the analyzed solid of Cu(N-

PhTPP)$^{+}CF_3SO_3^{-}$ dissolved in CH_3CN. Stock solutions were stable for months at room temperature. The CuN-C_6H_5 protoporphyrin complexes were prepared similarly <u>in situ</u> by mixing a copper salt with N-phenyl-protoporphyrin IX in CH_3CN in the presence of noncoordinating base, 2,2,6,6-tetramethylpiperidine.

Stock solutions of Cu(N-p-$CH_2C_6H_4NØ_2$TPP)$^{+}$ prepared similarly (in the synthesis part of this chapter) were stable for months when kept in the freezer. However, on exposure to light at room temperature they formed an, as yet unidentified species which was not CuTPP. This decomposition was not observed with other synthetic N-alkylporphyrins. In some cases we obtained spectra with isosbestic points at 621 nm and 658 nm with new peaks at 643 nm and 602 nm(sh) as shown in Figure 17. This new species was stable for several days at room temperature. Addition of di-n-butylamine resulted in the formation of CuTPP. The time scale (as indicated in the overlays) of the formation of this species was too slow to interfere with debenzylation of kinetics done with added di-n-butylamine in pseudo-first-order excess. In most cases, a new species appeared with the formation of CuTPP (not shown here).

The products from the reaction of Cu(N-C_2H_5TPP)$^{+}CF_3SO_3^{-}$ with di-n-butylamine were analyzed as described in reference 49. A two-fold excess of di-n-butylamine was added to a solution of Cu(N-C_2H_5TPP)$^{+}$(6.5×10^{-3}M) and the solution was kept at 30-45°C for 2.5 days until the formation of CuTPP (checked by visible absorption spectroscopy) was complete.

Figure 17. Upper. Absorbance changes for (N-p-nitrobenzyl-5,10,15,20-tetraphenylporphinato)copper(II) in acetonitrile at 25 ^{o}C. The overlay interval was 90 minutes.

Lower. The reaction of (N-p-nitrobenzyl-5,10,15,20-tetraphenylporphinato)copper(II) with di-n-butylamine in acetonitrile does not show the presence of the species giving the spectrum shown above. The overlay interval was approximately 2 minutes.

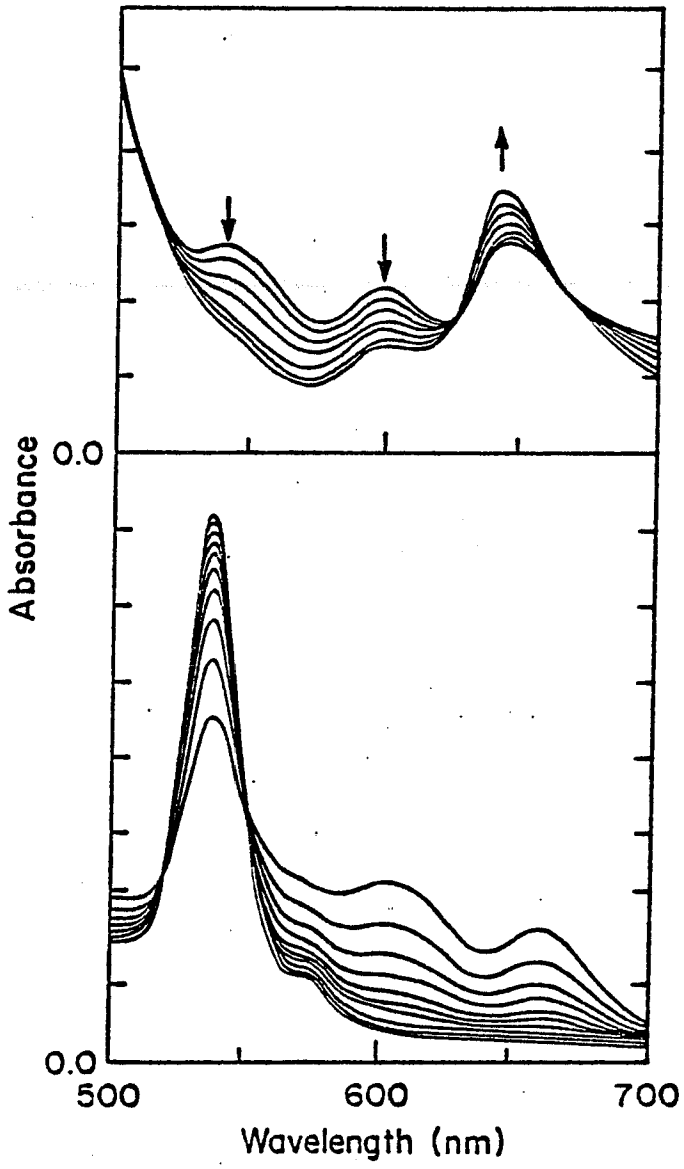
Absorbance
0.0
0.0
500
600
700
Wavelength (nm)

Solid NaOH was added to male the solution alkaline abd gc analysis was performed using an HP model 5700A instrument and a 1% SP-1000 column (Supelco). The chromatogram shows peaks attributable to di-n-butylamine and di-n-butylethytlamine and the assignments were confirmed using authentic samples under similar conditions. The analysis for the products from the reaction of (N-p-nitrobenzyl-5,10,15,20-tetraphenylporphinato)copper(II) trifluoromethanesulfonate with di-n-butylamine was not done in the same way because of the lower volatility of di-n-butyl-p-nitrobenzylamine. A sample of di-n-butyl-p-nitrobenzylamine was prepared by the reaction of p-nitrobenzylbromide with di-n-butylamine and the nmr spectrum of the sample was recorded. The products from the reaction of $Cu(N\text{-}p\text{-}C_6H_4NO_2TPP)^+$ with di-n-butylamine (a two-fold excess) gave an nmr spectrum of di-n-butylamine and di-n-butyl-p-nitrobenzylamine. In addition, the R_f values of the products matched those of authentic samples of di-n-bvutylamine and di-n-butyl-p-nitrobenzylamine. In all the dealkylation reactions considered here, the final spectrum of the product was that of CuTPP.

RESULTS: Fig. 15 shows the structures of N-alkyltetraphenylporphyrin and N-arylprotoporphyrin IX dimethyl ester used in the text. The synthesis of $N\text{-}C_2H_5HTPP$ by using $FSO_3C_2H_5$ is probably the first report on synthesis of $N\text{-}C_2H_5HTPP$. The direct ethylation of H_2TPP with C_2H_5I under normal condition or in a pressurized vessel does not seem to work. The report on the synthesis of N-ethylprotoporphy-

rin[69] by mixing ethylfluorosulfonate and protoporphyrin(IX) dimethyl ester proceeds due to the big difference in pk_as of protoporphyrin and N-substituted protoporphyrin (>10). In the case of synthetic porphyrins like H_2TPP, the respective pk_a values are very close, so that the formation of N,N'-dialkylTPP predominates. The last method for the synthesis of $N\text{-}CH_2C\emptyset_2C_2H_5HTPP$ is relatively easy and straightforward as far as the work-up is concerned. The two step synthesis without purification of the intermediate, $Fe(C_6H_5)TPP$, essentially gives the same yield (overall) as reported in ref. 26. Flash chromatography proves to be a very good technique over column chromatography, which has been used in the purification of N-substituted porphyrins and metallo-N-substituted porphyrins. Indeed N,N' bridge-TPP can be purified readily without its further decomposition to H_2TPP. The efficiency of this method lies between HPLC and ordinary column chromatography. Copper(II) complexes of N-alkylporphyrins can be easily made in CH_3CN by mixing the metal ion and the ligand in the presence of few drops of noncoordinating base, like 2,2,6,6-tetramethylpiperidine. As this report is concerned about the dealkylation reactions, the kinetics and mechanism of metallation will not be discussed here. The reports on this reaction can be found elsewhere.[70-72,34,35,41] Saito *et al.* have claimed that N-phenylprotoporphyrin (IX) dimethyl ester does not form a Cu-complex in $CHCl_3$.[73] But in our case, when $Cu(CF_3S\emptyset_3)_2.6H_2O$ and N-ph-protoporphyrin are mixed in CH_3CN in the presence of 0.25 mL of 0.005 M 2,2,6,6-tetramethylpiperidine in

CH_3CN, the spectrum changes from etiotype to two banded spectrum, which is consistent with the spectrum of Cu(N-CH_3DP(IX)DME)$^+$ reported earlier.[54a] Analysis of Cu(N-PhTPP)$^+CF_3SO_3$ further supports the formation of the Cu(II) complex of N-phenylprotoporphyrin IX dimethyl ester, which has been prepared in the same way as the former.

The Cu(N-p-$CH_2C_6H_4N\emptyset_2$TPP)$^+$ complex behaves differently from all other Cu(II) complexes of N-alkylporphyrins on standing at room temperature in the presence of light. Although the stock solutions are stable for months when kept in the freezer, in most cases an unidentified product is produced with the formation of CuTPP in the presence of light at room temperature. In some cases, isosbestic points are observed at 621 and 658 nm. A green colored compound without formation of CuTPP is being formed with the peaks at 602 and 643 nm. However, whatever the new species are, they all react very fast with di-n-butylamine to form CuTPP. The isosbestic points observed for the debenzylation of Cu(N-p-$CH_2C_6H_4N\emptyset_2$TPP)$^+$ by di-n-butylamine (520 and 552 nm respectively, Fig. 17) are different from the slowly formed green solution (upper one of Fig. 17). The time scale for the two overlays in Fig. 17 (90 minutes compared to 2 minutes for the bottom one) suggests that the formation of green product does not interfere with the debenzylation process.

A beautiful overlay for the reaction of Cu(N-C_2H_5TPP)$^+$ with di-n-butylamine in acetonitrile is shown in Fig. 18.

Figure 18. Absorbance changes for the reaction of (N-ethyl-5,10,15,20-tetraphenylporphinato)copper(II) with di-n-butylamine in acetonitrile at 49.2 °C. The interval time was approximately 2 minutes.

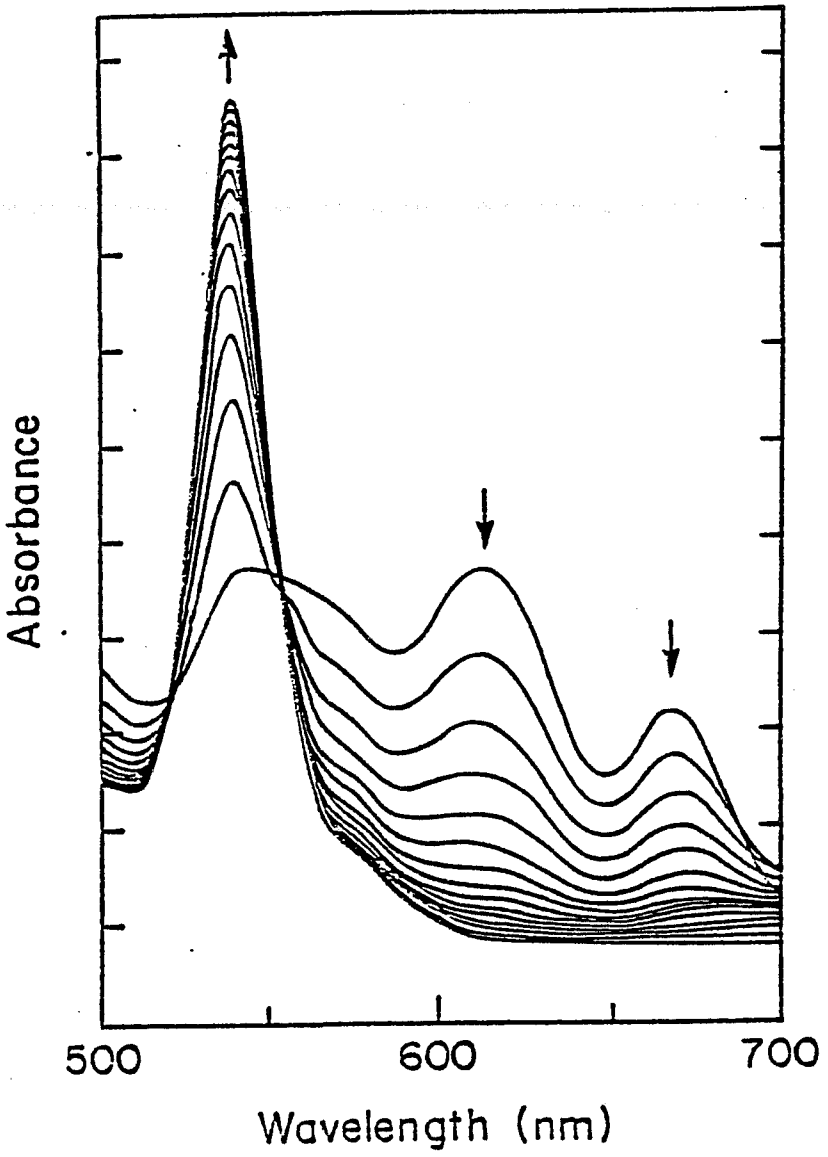
Absorbance
500
600
700
Wavelength (nm)

Isosbestic points are observed at 526 nm and 553 nm respectively. Kinetics data obtained at 536 nm are listed in Table X. These rates constants are much smaller than that of the dealkylation reaction of N-methyl-tetraphenylporphinatocopper(II).[49] The former reactions as well as the later are not simply first-order as is evident from Fig. 19. A plot of k_{obsd}(observed rate constants) vs. [Amine] for the reaction of $Cu(N\text{-}p\text{-}CH_2C_6H_4N\emptyset_2TPP)^+$ with di-n-butylamine is shown in Figure 2Ø. Table IX contains the observed rate constants at three temperatures at different concentrations of amine. The values of k_1, k_2 and k_{eq} discussed latter (with the rate law we propose) for different reactions are presented in Table XI and the activation parameters are listed in Table XII.

DISCUSSION: Different mechanisms have been proposed (discussed in Ch. 1) in the transfer of the alkylating moiety to the nitrogen of prosthetic heme. The bond between carbon and nitrogen is stable enough that the iron atom is removed. With the concomitant release of iron, free base or protonated N-alkyl protoporphyrin (N-alkyl protoporphyrins are highly basic and have $pK_3 > 8$) is being formed. N-methyl, or N-ethyl (the ethyl group bound to nitrogen of pyrrole ring A or B, Fig. 4 of Chapter 1, p.11 protoporphyrins and the green pigments isolated from the treatment of mice with griseofulvin or isogriseofulvin are strong inhibitors of ferrochelatase that catalyzes insertion of the iron atom into protoporphyrin.[18-2Ø] Similarly, N-phenyl-protoporphyrin is produced on acidic treatment of inactivated

TABLE X. First-order rate constants for the reaction of N-ethyl-5,10,15,20-tetraphenylporphinatocopper (II) Cation with Di-n-butylamine in Acetonitrile.

Temp, °C	[Amine], M	$kx10^4$, s^{-1}
49.2	1.000	9.52 ± 0.02
49.2	0.500	6.39 ± 0.10
49.2	0.250	4.10 ± 0.05
49.2	0.125	2.42 ± 0.02
49.2	0.0625	1.40 ± 0.02
49.2	0.03125	0.69 ± 0.03
37.2	1.000	3.79 ± 0.03
37.2	0.500	2.35 ± 0.01
37.2	0.250	1.60 ± 0.07
37.2	0.125	0.91 ± 0.01
37.2	0.0625	0.454 ± 0.001
37.2	0.03125	0.250 ± .001
25.0	1.000	1.11 ± 0.01
25.0	0.500	0.719 ± 0.015
25.0	0.250	0.420 ± 0.001
25.0	0.125	0.268 ± 0.014

Figure 19. Plot of the observed pseudo-first-order rate constant for the deethylation of (N-ethyl-5,10,15,20-tetraphenylporphinato)copper(II) by di-n-butylamine in acetonitrile at 49.2°C as a function of the amine concentration.

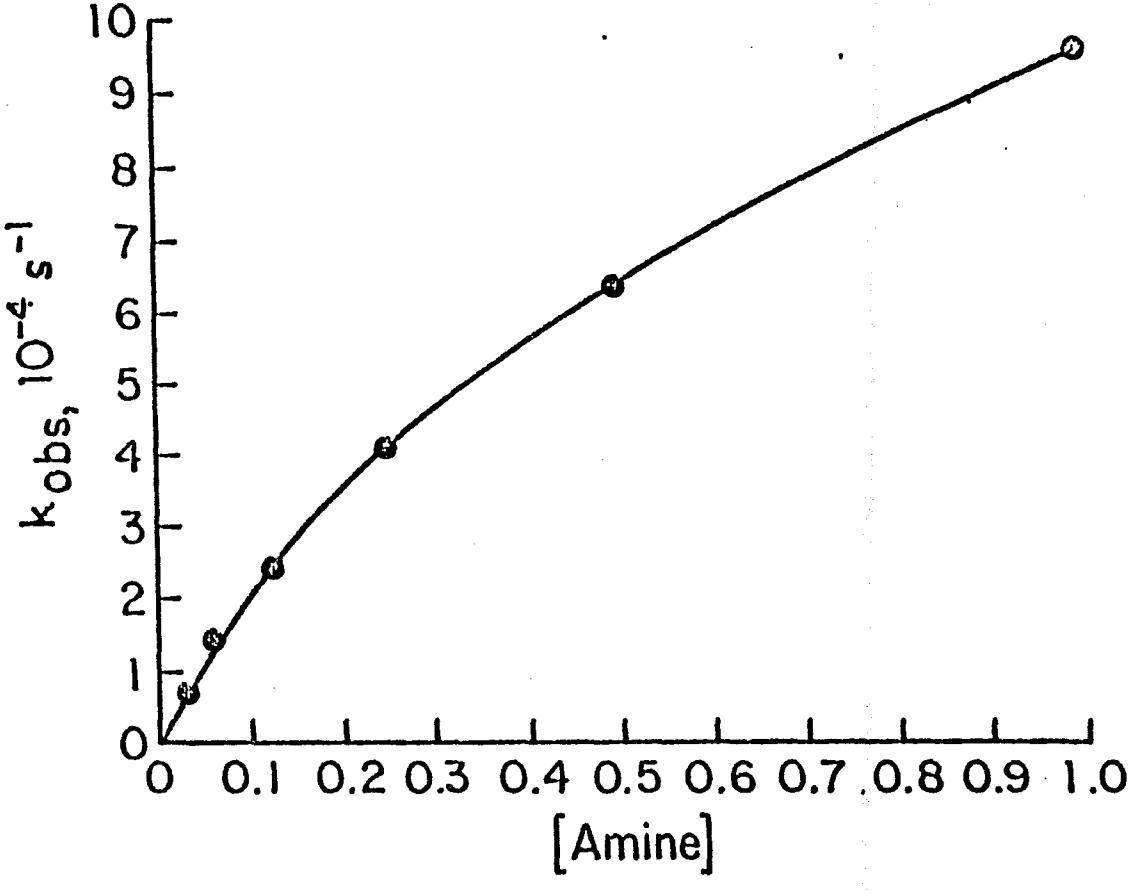
k_{obs}, 10^{-4} s^{-1}
10
9
8
7
6
5
4
3
2
1
0
0 0.1 0.2 0.3 0.4 0.5 0.6 0.7 0.8 0.9 1.0
[Amine]

TABLE IX. First-order Rate constants for the reaction of N-p-nitrobenzyl-5,10,15,20-tetraphenylporphinato-copper(II) cation with Di-n-butylamine in Acetonitrile.

Temp, °C	[Amine], M	$k \times 10^3$, s^{-1} [a]
25.0	0.0125	2.33 ± 0.02
25.0	0.025	3.90 ± 0.05
25.0	0.050	6.37 ± 0.03
14.3	0.0125	0.982 ± 0.003
14.3	0.025	1.58 ± 0.01
14.3	0.050	2.62 ± 0.20
14.3	0.100	4.05 ± 0.14
6.8	0.0125	0.449 ± 0.002
6.8	0.050	1.03 ± 0.01
6.8	0.100	1.42 ± 0.01

a. Averages with average deviation of 2-3 runs are reported. Each individual run gave a fit to first-order kinetics with a correlation coefficient better than 0.998 and the average $|OD_{obs} - OD_{calc}|$ is 0.003 or less. Similar fits were obtained for results given in Table X.

Figure 20. Plot of the observed pseudo-first-order rate constant for the debenzylation of (N-p-nitrobenzyl-5,10,15,20-tetraphenylporphinato)copper(II) by di-n-butylamine in acetonitrile at 14.3 ^{o}C as a function of the amine concentration.

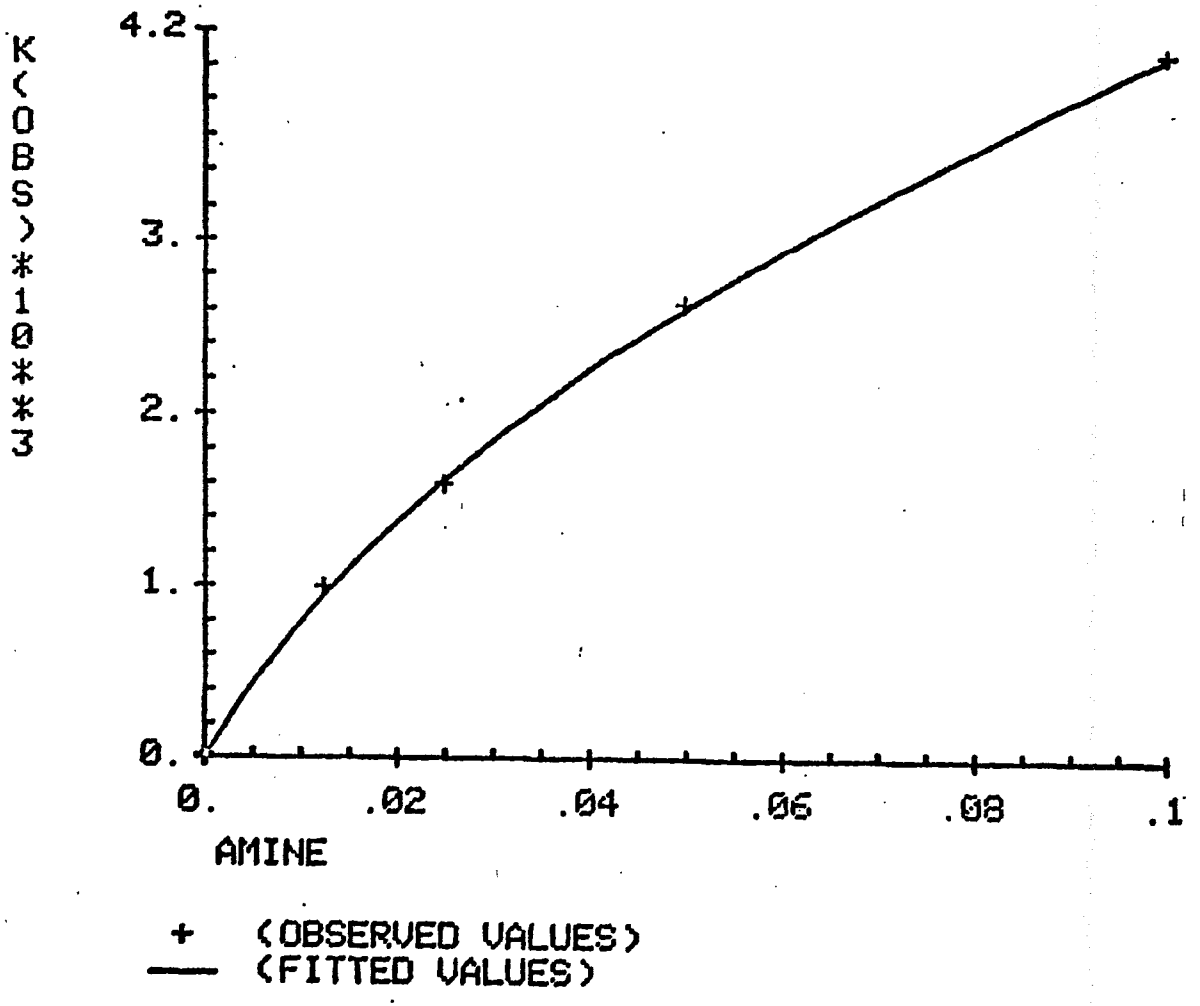
K(OBS)*10***3
4.2
3.
2.
1.
0.
0.
.02
.04
.06
.08
.1
AMINE
+ (OBSERVED VALUES)
(FITTED VALUES)

TABLE XI. Values of Kinetics Parameters of Dealkylation Reactions of N-methyl-, N-ethyl- and N-p-nitrobenzyl-5,10,15,20-tetraphenylporphinatocopper(II) by Di-n-butylamine in Acetonitrile.[a]

Complex	Solvent	T °C	$k_1 \times 10^3$ $M^{-1}s^{-1}$	K_{eq}	$k_2K_{eq} \times 10^3$ $M^{-1}s^{-1}$	$k_2 \times 10^3$ $M^{-1}s^{-1}$
$Cu(N\text{-}CH_3TPP)^+$ [b]	CH_3CN	25.0	2.94 ± 0.05	2.5 ± 0.2	0.75 ± 0.14	0.30
		45.0	18.0 ± 0.10	3.0 ± 0.5	7.0 ± 2.4	2.3
		65.0	151 ± 6	17 ± 2	210 ± 30	12
$Cu(N\text{-}C_2H_5TPP)^+$	CH_3CN	25.0	0.227 ± 0.004	1.6 ± 0.2	0.058 ± 0.015	0.037
		37.0	0.89 ± 0.05	3.2 ± 0.7	0.70 ± 0.21	0.22
		49.2	2.48 ± 0.05	2.7 ± 0.2	1.01 ± 0.02	0.38
$Cu(N\text{-}CH_2C_6H_4NO_2\text{-}TPP)^+$	CH_3CN	25.0	271 ± 12	58 ± 11	4600 ± 1100	79
		14.3	97.6 ± 3.5	31 ± 4	680 ± 140	22
		6.8	50.6 ± 0.4	38 ± 1	177 ± 9	467

a. Observed rate constants have been fit using the non-linear least square program of the PROPHET system using the equation $k_{obs} = (k_1[A] + k_2K_{eq}[A]^2)/(1 + K_{eq}[A])$.

b. Data from ref. 55

TABLE XII. Activation Parameters for Dealkylation of Copper (II) Complexes of N-ethyl-5,10,15,20-tetra-phenyl-porphyrin and N-p-nitrobenzyl-5,10,15,20-tetraphenylporphyrin by Di-n-butylamine in Acetonitrile.

	Path 1[a]			Path 2[b]		
Complex	$\Delta H^{\neq}$ Kcal/mole	$\Delta S^{\neq}$ e.u.	$\Delta G^{\neq}$, 298°K Kcal/mole	$\Delta H^{\neq}$ Kcal/mole	$\Delta S^{\neq}$ e.u.	$\Delta G^{\neq}$, 298°K Kcal/mole
CuN-CH_2-NO_2TPP$^+$	14.8 ± 1.0	-11.6 ± 3.4	18.3 ± 2.0	24.9 ± 2.6	20.3 ± 9.0	18.9 ± 5.3
CuN-CH_3TPP$^+$[c]	19.0 ± 1.6	-6.4 ± 5.1	20.9 ± 3.1	17.8 ± 04	-14.7 ± 1.4	22.2 ± 0.9
CuN-C_2H_5TPP$^+$	18.2 ± 1.0	-13.9 ± 3.3	22.4 ± 2.0	17.9 ± 5.0	-18.5 ± 16.4	23.4 ± 9.9

a. The predominant path at low concentration of di-n-butylamine
b. " " " high " " "
c. data from reference 55.

hemoglobin, myoglobin or rather hemoproteins in the presence of O_2.[25]

In this report, we have considered the stability of N-alkylporphyrin complexes (presumably the intermediate that decomposes eventually to the green pigment, N-alkylporphyrin, in vivo with different alkyl substituents. Free base, N-alkylporphyrins are quite stable except under drastic conditions (e.g., Smith et al.,[74] have reported, recently, thermal dealkylation of N-methyl, N-ethyl and N-1-propyl mesoporphyrin IX dimethyl ester during electron impact mass spectrometry with varying source temperature from 180-240°C. Also a significant amount of the parent porphyrin, i.e., mesoporphyrin IX dimethyl ester is produced from thermal dealkylation of N-methyl mesoporphyrin IX dimethylester under N_2(within 5 min.) at 200°C. All the N-alkylporphyrins considered in this Chapter are unaffected by nucleophiles like di-n-butylamine in CH_3CN. The spectra of free base N-p-$CH_2C_6H_4NO_2$TPP in CH_3CN (as we will see later in this part, benzyl is the best leaving group) are unchanged on long standing at room temperature when [di-n-butylamine] ~2M was employed. However, metallo-N-alkylporphyrins can be dealkylated readily. Two types of mechanisms have been invoked, a) an oxidative addition mechanism[75,27,28] where the alkyl group migrates to the metal center accompanied with the oxidation of metal; b) a bimolecular reaction involving metal-ion assisted nucleophilic removal of the alkyl group[49,50,55,76] where the leaving group is the less polar

metallo-non-N-alkyl-porphyrin. (This is similar to OTS^- or X^- in a typical S_N2 or S_N1 reaction.) The discussion here concerns reactions of the latter type.

In the previous chapter, we have seen that the dealkylation reactions depend upon several factors: the nucleophile, the reaction medium, and the substituents on the porphyrin ring.[55] The dependence of rates on the metal ions have been also investigated[50,76] and the dealkylation rates are governed by the stability of the final product or rather the porphyrin complexes of the metal ion in consideration. All the data are consistent with a bimolecular nucleophilic displacement mechanism and suggest that the activated complex is very similar to the product (Hammond's postulate). We have found that the dealkylation rates are influenced very little by the porphyrin ring substituents and the rates obtained with naturally occurring N-alkyl porphyrins are similar to those obtained with synthetic N-alkylporphyrins[55] and so then the latter can be used in predicting the rates of dealkylation of the former. We have chosen different alkyl groups: ethyl($-C_2H_5$), -p-nitrobenzyl ($-p-CH_2-C_6H_4NO_2$), -ethylacetato($-CH_2CO_2C_2H_5$), and phenyl ($-C_6H_5$) to compare their dealkylation rates with that of methyl(CH_3) and to investigate both steric effects, of importance with respect to nucleophilic attack, and electronic effects, i.e., the stability of incipient carbocation formed in the activated complex. At the onset of doing kinetics, we have prepared the Cu(II) complexes simply because Cu(II) has been used to analyze the factors above.

As mentioned in the chapter 2, the demethylation of Cu(N-CH_3TPP)$^+$ by amine in acetonitrile proceeds by a competitive two-path mechanism.[49,55] We have proposed that at low concentration of amine, there is a simple bimolecular reaction (k_1 path) whereas with the increase in concentration of amine the latter can compete with the solvent, CH_3CN, for axial coordination and can then go to the final product as shown in the scheme below:

$$\text{S-Cu(N-RTPP)} + \text{Nu} \longrightarrow \text{CuTPP} + \text{S} + \text{RNu}^+$$

(1st. order with respect to concentration of amine)

$$\text{S-Cu(N-RTPP)}^+ + \text{Nu} \rightleftharpoons \text{Nu-CuN-RTPP}^+ + \text{S}$$

$$\text{Nu-Cu(N-RTPP)}^+ + \text{Nu} \longrightarrow \text{CuTPP} + \text{RNu}^+ + \text{Nu}$$

(2nd. order with respect to concentration of amine)

The rate law consistent with the scheme is:

$$\frac{d[\text{CuTPP}]}{dt} = \left\{\frac{k_1 + k_2K_{eq}[\text{Nu}]}{1 + K_{eq}[\text{Nu}]}\right\}[\text{Nu}]\ [\text{Cu(N-RTPP)}^+]$$

where 'S' signifies the solvent and 'Nu' is the nucleophile. The plot of k_{obs} vs. [Amine] for the reactions of N-ethyltetraphenylporphinatoCu(II) trifluoromethanesulfonate and N-p-nitrobenzyltetraphenylporphinatoCu(II) trifluoromethanesulfonate (Fig. 19 and 20) are consistent with this above rate law. The activation parameters for these reactions (Table XII) also support a common mechanism, since they show compensation effect, with less favorable activation enthalpies being compensated by more favorable activation

entropies (not a linear compensation).

The dealkylation reactions with $Cu(N\text{-}CH_2CO_2C_2H_5TPP)^+$ are very similar to those with $Cu(\text{-}N\text{-}C_2H_5TPP)^+$. An apparent side reaction in the former system has not however allowed us to complete the kinetic data to be presented in this section. An infrared spectrum of the final product of the reaction mixture for the reaction of $Cu(\text{-}N\text{-}CH_2CO_2C_2H_5TPP)^+$ with di-n-butylamine shows the disappearance of the carbonyl peak due to the ester group and instead a peak for an amide appears. From the overlays at different temperatures and the infrared spectra it is hard to determine whether amide formation takes place before dealkylation or both occur simultaneously. Further work will be necessary to clarify the processes occurring in this system.

The dephenylation of the Cu(II) complex of N-phenyl-protoporphyrin IX dimethyl ester at 45° with [di-n-butyl-(amine)] 1M is extremely slow compared to its decomposition to some unknown product. Though the decomposition of the complex by heat and light prevented us from seeing any changes in the region of 700-500 nm, a peak in the soret region at 412 nm, which may be due to CuPP(IX)DME, forms very slowly. Decomposition to some unknown product, ambiguity in the final product from the reaction of Cu(N-PhPP IX DME)$^+$ with di-n-butylamine and the very small effect of porphyrin ring substituents on the demethylation reactions (chapter 2) prompted us to look ardently at the dearylation of $Cu(N\text{-}phTPP)^+CF_3SO_3^-$ (which is extremely stable due to the

absence of vinyl groups on pyrrole rings and the phenyl group's presence at the meso positions) by di-n-butylamine in CH_3CN. The reaction is extremely slow; too slow, in fact, to assign a proper value for comparison ($t_{1/2}$ of over a week at 45°C with [di-n-butylamine] = 2M). Besides, the overlaid spectra show that the reaction proceeds through an intermediate. Upon addition of few drops of acid, the intermediate gives the original spectrum obtained just after the addition of amine to $Cu(N\text{-}PhTPP)^+CF_3SO_3^-$. $Cu(N\text{-}PhTPP)^+CF_3SO_3^-$ can be demetallated with acid, HCl, to form protonated N-PhHTPP but the final product obtained after heating the solution of $Cu(N\text{-}PHTPP)^+CF_3SO_3^-$ first at 45°C for more than a month and then at 64°C gave a red solution (the color changes from brown to green in addition of amine then very slowly becomes red) and the characteristic spectrum of CuTPP. The rate constants for the dealkylation reactions of Copper(II) N-alkyl and N-aryl porphyrin complexes with p-nitrobenzyl, methyl and phenyl substituent are clearly dictated by the ability to form a carbocation in each case. The relative rates (in units of M^{-1} s^{-1} for k_1 path at 25°C) are 100: 1: $<10^{-4}$ and the relative rates for a series of metallo-N-methyltetraphenylporphyrin complexes with Cu(II), Ni(II), Zn(II) and Mn(II) at 70°C: $1:0.4:2\times10^{-2}$: $<10^{-4}$ indicating the relative importance of the stability of the final product and hence the resemblance of the activated complex to the reaction products. Since an incipient carbocation should be more stabilized by an ethyl group than a methyl group (due to the higher inductive effect of the

former) and be destabilized by a group like the ethylacetoxy moiety (due to the inductive effect of an ester group), the retardation of the dealkylation rate by ethyl and ethylacetoxy groups can be attributed to their greater steric hindrance. The effect (a factor of about 10 at 25°C) is not that pronounced in comparison to the effect of other substituents. We have previously found very small difference in the demethylation of $Cu(N\text{-}CH_3TPP)^+$ with nucleophiles of different size. ([diethylamine] = 0.436M, Temp. = 45°C k_{obs} = (3.42 ± 0.01)x10^{-3}; di-n-butylamine] = 0.433M, temp. k_{obs} = (3.96 ± 0.04) x 10^{-3} s^{-1}).[49]

Great stabilization of the positive charge by the nitrogen bound alkyl substituent can cause rapid dealkylation of a metallo-N-alkylporphyrin. Preliminary results from the debenzylation of N-p-nitrobenzyltetrakis(p-sulfophenyl)porphinatocopper(II) in water in the absence of any nucleophile suggest that possibility <u>in vivo.</u> (But debenzylation of $Cu(N\text{-}p\text{-}CH_2C_6H_4NO_2TPP)^+$ occurs only in the presence of a good nucleophile). We have previously reported that Fe(II) is not as effective as Cu(II) in facilitating dealkylation. One may think Fe(III) would be more effective than Fe(II) in the above process, but the oxidation of Fe(II) to Fe(III) is difficult, since the potential of $Fe^{3+/2+}$ increases by 0.7 volt on N-alkylation (Chapter 4). Therefore, direct dealkylation of an N-alkylated iron protoporphyrin remains a burning question. Heme biosynthesis can, however,be still maintained in the case where the

alkyl group can migrate to the metal center with its concomitant oxidation.

CONCLUSION: The practical applications of the N-alkylporphyrins and their complexes are very broad. The two step synthesis of non-N-alkylated metalloporphyrin can be useful in making radio-pharmaceuticals. The rapid formation of Pd-109-hematoporphyrin by the two step synthesis is currently being investigated in selective lymphatic ablation to prevent the rejection of transplanted organs. The sluggishness of the demethylation of other N-methyl porphyrin complexes has limited the two step synthesis of appropriate non-N-alkylated complexes but may now be possible using benzyl or similar substituents. On the contrary, sterically hindered N-alkyl or N-phenyl species may be used as electrochemical catalysts where long-term stability is needed.

The fact that $Cu(N\text{-}CH_3TPPS_4)^{3-}$ has reproducible activity in P-388 lymphocytic leukemia prompted us to examine the transfer of methyl group to DNA bases *in vitro*. Dr. Douglas Miller and I attempted this reaction using different media under a variety of conditions (such as temperature, pH etc) with Calf-thymus DNA, guanine, and guanozine and we observed no detectable amount of methylated guanine or guanosine when an HPLC system with a refractive index detector was utilized.[77] The formation of 7-methyl guanine or guanosine is fastest among all DNA and RNA bases in any methylation reaction.[78] Therefore we tried to concentrate mainly on the reactions of guanine and guanosine. We noticed that $Cu(N\text{-}CH_3TPPS_4)^{3-}$ gets demethylated to the same

extent with or without any nucleophile like guanine or guanosine. In this series of experiments demethylation of $Cu(N\text{-}CH_3TPPS_4)^{3-}$ only takes place at elevated temperatures (over 80°C) with or without added nucleophiles. But we still are attempting to find if there are any alkylated bases present in the system. It is possible that these reaction are slow because it has been found that pyridine reacts much more slowly than amines in removing the methyl group of $Cu(N\text{-}CH_3TPP)^{+4}$[9] (ch-2). In addition, the demethylation reactions are 100 times slower in water than in acetonitrile with amines as nucleophiles (ch-2).[55] $Cu(N\text{-}CH_3TPPS_4)^{3-}$ is stable in water at room temperature even in the presence of NaOH. NaOH does not act as a nucleophile presumably due to its high degree of solvation at room temperature.[55] Preliminary results suggest that the rate of debenzylation of $Cu(N\text{-}CH_2\text{-}p\text{-}C_6H_4NO_2TPPS_4)^{3-}$ in water at room temperature is the same with and without DNA. Further research is necessary to ascertain the integrity of Cu-N-alkyl complexes <u>in vitro</u> as well as <u>in vivo</u>.

CHAPTER 4

CYCLIC VOLTAMMETRY OF M(II)[M=Fe(II), Mn(II) AND Cu(II)] N-ALKYL AND N-ARYL 5,10,15,20-TETRAPHENYLPORPHYRIN COMPLEXES: THE EFFECT OF COORDINATION GEOMETRY ON THE REDOX PROPERTIES OF THESE SYSTEMS.

INTRODUCTION

Different techniques: potentiometry, polarography; spectroelectrochemistry , cyclic voltammetry, are used in the electrochemistry of porphyrins. Earlier work on potentiometry has been summarized in the reviews by Falk[79] and Clark[80]. In theory it is possible to get the same half-wave potential by using any of these methods mentioned above. But complexity arises due to the competition between the charge transfer process and the equilibrium in the solution maintained by diffusion. So due to a quasireversible or irreversible charge transfer (use of the term charge transfer is favoured over electron transfer because the latter is only one of the steps the change transfer process), $E_{1/2}$ may not be equal to E^{o} and it is not easy to know if the measured half-wave potential is close to the thermodynamically significant standard potential.

A reversible charge transfer process is the one in which charge transfer is fast compared to the rate of diffusion of the oxidant or reductant to the electrode surface. Cyclic voltammetry is widely used for measuring the reversible redox potentials of metalloporphyrins. There are greater advantages of this technique over earlier techniques of potentiometry and polarography: a) The potential of a redox couple can be easily determined from the voltammogram

(plot of current vs. voltage) b) The species oxidized or reduced at an electrode in the forward scan is reduced or oxidized in the reverse scan and thus the chemical stability of the species present in the bulk solution is ascertained. c) Moreover, in the case of coupled chemical reactions, a variation of the potential sweep rate (scan rate) and the measurement of the new current voltage curve might help one to determine the coupled chemical reactions and the mechanism involved in the charge transfer process.[81]

There have been a few reports on the cyclic voltammetry of metallo-N-alkylporphyrins.[82-84] Most of the papers on the cyclic voltammetry of porphyrins deal with metallo-non-N-alkylporphyrins. The formation of green pigments, N-alkyl or N-aryl porphyrins, in vivo as well as in vitro (chapter 1), through σ-alkyl (or σ-aryl) and carbene[85-86] inserted iron complexes has created interest concerning the redox potentials of iron N-alkyl or N-aryl porphyrins (ie, before the removal of iron atom). This information may help us to elucidate the mechanism for the production of these pigments.

Until now, there has been no report on the reduction of Cu(II) porphyrins to its Cu(I) analog. So the potentials of Cu(II)/Cu(I) of N-RTPP along with the effect of axial ligands have been investigated in this chapter to know a) how it differs from the potentials of other metallo-N-alkylporphyrins and b) how the geometry of CuTPP deludes one to see such redox processes present in the complexes of $Cu(N\text{-}RTPP)^{+}X^{-}$. We have also extended our work on Mn(N-

RTPP)Cl (with R=-CH_3, C_6H_5, -p-$CH_2C_6H_4NO_2$) to determine how the different R groups on the nitrogen atom affect the potentials of Mn(III)/Mn(II) system and their difference (of >/1.00 volt) from the non-N-alkylated analogs. The manganese complex is of interest in the light of the activity of the manganese porphyrin complexes as catalysts which stimulate the role played by manganese in the photosynthetic liberation of oxygen from water.[87] Uses of non-aqueous system (in the present case) instead of water has been discussed recently.[88] In many instances, it can be argued that the biological medium more closely approximates an aprotic solvent.

EXPERIMENTAL

General: Dichloromethane and acetonitrile were purified as mentioned in the earlier chapters. Spectrograde DMF was used without further purification. The supporting electrolyte tetrabutylammonium perchlorate (TBAP) was recrystallized from ethanol several times. Tetraethylammonium perchlorate (Fisher grade) and tetrabutylammonium perchlorate (Fisher grade) were also used as supporting electrolytes. The latter was not used in other cases due to some problems (mentioned latter). Preparation of $Cu(CF_3SO_3)_2.6H_2O$ and tetraethylammonium chloride have been reported in chapter 2. THF was freshly; distilled under Ar over metallic potassium. Noncoordinating bases like 2,6-lutidine and 2,2,6,6-tetramethylpiperidine (both from Aldrich) were used as such without further purification. In the synthesis of iron complexes ferric chloride(anhydrous), from Aldrich and iron wire (from Mallinckrodt) were used.

Synthesis of N-alkyl and N-phenyl 5,10,15,20-tetraphenylporphyrins: Synthesis and purification of N-ethyltetra-5,10,15,20-phenylporphyrin ($N-C_2H_5HTPP$), N-p-nitrobenzyltetra-5,10,15,20-phenylporphyrin($N-p-CH_2C_6H_4NO_2HTPP$) and N-phenyl-tetra-5,10,15,20-phenylporphyrin have been described in chapter 3. Synthesis of N-methyl-5,10,15,20-tetraphenylporphyrin ($N-CH_3HTPP$) has been mentioned in chapter 2.

Synthesis of Fe(II),Cu(II) and Mn(II) complexes of N-substituted-porphyrins: The synthesis, characterization,

cyclic voltammetry and crystal structure of chloro(N-methyl-15,10,15,20-tetraphenylporphinato)iron(II) has been reported recently.[83] Chloro(N-ethyl-5,10,15,20-tetraphenylporphinato)iron(II) and chloro-N-phenyl-5,10,15,20-tetraphenylporphinato)iron(II) were prepared similarly on a smaller scale than mentioned before. In a typical experiment, 15-25 mg. of N-C_2H_5HTPP or N-PhHTPP were used: THF was deaerated with Ar for 15 minutes. About 15 mg. of anhydrous $FeCl_3$ (0.0924 mole) and excess iron wire were refluxed in a two neck flask, one neck of which had the addition funnel (20 mL) containing the solution of N-C_2H_5HTPP or N-Ph HTPP in THF under argon or nitrogen. The refluxing was done for a long period until an amber color developed. Then the solution of N-C_2H_5HTPP(violet) or N-PhHTPP(green) was added drop by drop. The refluxing was continued for about half an hour after the addition was over. A stoichiometric amount of non-coordinating base, 2,2,6,6-tetramethylpiperidine, was added to the mixture after it was cooled. The mixture was the filtered through Whatman 42 filter paper and evaporated to dryness. Fe(N-C_2H_5TPP)Cl was sufficiently stable to be isolated. Fe(N-PhTPP)Cl was not as stable in the solid form. Fe(N-CH_3TPP)Cl and Fe(N-PhTPP)Cl have been synthesized by others in the same way.[28,29] Visible spectra of Fe(N-CH_3TPP)Cl, Fe(N-C_2H_5TPP)Cl and Fe(N-C_6H_5TPP)Cl are given in Table XIII

Synthesis of Chloro(N-phenyl5,10,15,20-tetraphenylporphinato)manganese(II) Mn(N-PhTPP)Cl: Mn(N-PhTPP)Cl was syn-

Table XIII. Visible Absorption Spectra of N-Alkyl and N-Phenylporphyrin Complexes.

Complexes	Absorption Maxima (in nanometers)	Complexes	Absorption Maxima (in nanometers)
$Fe(N\text{-}CH_3TPP)Cl$[a]	447,459,564,610,662	$Mn(N\text{-}CH_3TPP)Cl$[a]	450, 565,619,668
$Fe(N\text{-}C_2H_5TPP)Cl$[b]	446,457,563,612,662	$Mn(N\text{-}p\text{-}CH_2C_6H_4NO_2TPP)Cl$[d]	450,540,567,621,666 (sh)
$Fe(N\text{-}PhTPP)Cl$[b]	454,465,570,630,681	$Mn(N\text{-}PhTPP)Cl$[d]	457,468,572,638,689
$Cu(N\text{-}CH_3TPP)^+$ [c]	430,442,546,597,656	$Cu(N\text{-}CH_3TPP)Cl$[d]	371,451,564,617,672
$Cu(N\text{-}C_2H_5TPP)^+$ [c]	434,442,546,596,657	$Cu(N\text{-}C_2H_5TPP)Cl$[d]	371,450,568,616,671
$Cu(N\text{-}PhTPP)^+$ [c]	440,455,556,609,675	$Cu(N\text{-}PhTPP)Cl$[d]	378,459,569,627,689

a. In CH_2Cl_2

b. In THF

c. Counter ion $CF_3SO_3^-$ or ClO_4^-

d. In CH_3CN

thesized in the same way as $Mn(N\text{-}CH_3TPP)Cl$.[58] In a typical experiment, 48mg (Ø.Ø7 millimoles) of N-PhHTPP was dissolved in about 1ØmL of dry dichloromethane and mixed with about 7Ømg (Ø.35 millimoles) of $MnCl_2.4H_2Ø$ (from Fisher) dissolved in 1ØmL absolute ethanol (N-Ph HTPP has a green color in solution as a free base. So no color change was noticed, unlike the procedure with $N\text{-}CH_3HTPP$ and $N\text{-}p\text{-}CH_2C_6H_4NO_2HTPP$). Acetonitrile(1Ø-15 mL) was added to the green solution followed by addition of 55mL of 2,6-lutidine to the reaction mixture and was stirred overnight. The visible absorption spectrum slowly changed from that of free base to the complex (Table XIII) and is consistent with the slowness of the formation of the complexes of $Mn(N\text{-}CH_3TPP)Cl$.[34] The residue was washed with water and extracted with dry CH_2Cl_2 (to avoid any trace of acid present in ordinary dichloromethane) and evaporated to dryness. An attempt to purify Mn(N-Ph-TPP)Cl by flash chromatography was partially successful. Buchler has reported that non-N-alkylated class IV metalloporphyrins (Mn(II) belongs to class IV) are demetallated partially or fully on purification by chromatography on alumina or silica gel columns.[89] Elemental analysis performed at Analytische Laboratorien, Engelskrichen, West Germany, was not satisfactory. Calculated for $MnC_5OH_{33}N_4Cl$: C 76.94%; H, 4.27%; N, 7.18%. Found C, 75.65%; H, 4.94%;N 7.Ø6%. The visible spectrum recorded in CH_3CN is shown in Table XIII. The spectrum did not change on addition of excess non-coordinating base 2,6-lutidine to the solution of Mn(N-

PhTPP)Cl. There is a bathochromic shift in the peak positions with other complexes of N-PhTPP (see Table XIII).

Synthesis of Chloro(N-p-nitrobenzyl-5,10,15,20-tetraphenylporphinato)manganese(II) $Mn(N\text{-}p\text{-}CH_2C_6H_4NO_2TPP)Cl$: $Mn(N\text{-}p\text{-}CH_2C_6H_4NO_2TPP)Cl$ was synthesized in the same manner as above. Elemental analysis performed at Engelskrichen, West Germany was not satisfactory. Calculated for $Cl\text{-}MnC_{51}H_{34}N_5O_2$: C, 72.97%, H, 4.09%, N, 8.35, found C, 69.05%, H, 4.73%, N, 7.02%. But the visible absorption spectrum was similar to that of $Mn(N\text{-}CH_3TPP)Cl$ (Table XIII). The spectrum did not change on addition of excess non-coordinating base 2,6-lutidine to prove that it was not that of protonated N-alkylporphyrin(Monoprotonated N-alkylTPP gives a similar spectrum to that of the metal complex).[58]

Synthesis of N-ethyl-5,10,15,20-tetraphenylporphinatocopper(II) trifluoromethanesulfonate and its N-phenyl analog have been described in chapter 3. N-methyl-5,10,15,20-tetraphenylporphinatocopper(II)-trifluoromethanesulfonate was prepared in situ by mixing 15.7mg of $N\text{-}CH_3HTPP$ and 12.3mg of $Cu(CF_3SO_3)2.6H_2O$ in CH_3CN and stirring the solution for about 2 hrs. 2.5mL of a 0.005M solution of 2,2,6,6-tetramethylpiperidine in CH_3CN (total volume) was added drop by drop until the complex formation was completed as indicated by its characteristic spectrum. The total volume at this stage was about 17mL. The visible spectrum is listed in Table XIII. It was converted into its chloride salt by the addition of tetraethylammonium chloride (7/100 fold excess). Similarly, the chloro complexes of $Cu(N\text{-}PhTPP)^+$ and $Cu(N\text{-}C_2H_5TPP)^+$ were

prepared. The visible spectra of the chloro complexes are different from that of their cations as shown in Fig. 21 [for $Cu(N\text{-}CH_3TPP)^+$ and $Cu(N\text{-}CH_3TPP)Cl$ and the peaks are listed in Table XIII. There is no change in the visible spectra of Cu(N-RTPP)Cl complexes upon addition of excess chloride. There is also no change in the cyclic voltammograms of Cu(N-RTPP)Cl complexes when additional chloride is added.

Cyclic Voltammetry: Cyclic voltammetric experiments were done on a bio-analytical systems CV-1A instrument equipped with a three electrode system. A Pt wire electrode and a Pt wire coil were used as the working and auxiliary electrodes respectively. The reference electrodes used were either a commercial aqueous saturated calomel electrode (SCE) or Ag/AgCl electrode with porous vycor acting as the bridge between the reference and the solution of interest. Except in the case of Fe(III)/Fe(II) system, all other potentials have been measured in acetonitrile. Table XIV reproduces potential limits and physical characteristics of the solvents most often used in the electrochemistry of iron porphyrins. Tetraethylammonium perchlorate (TEAP, Fisher grade CV only) 0.1 M in DMF was used as the supporting electrolyte in Fe(III)/Fe(II) systems. The tetrabutylammonium perchlorate (TBAP) from Fisher was acidic enough to displace the Mn(II) from Mn(N-PhTPP)Cl in CH_3CN. Also, the clear solution of TBAP in CH_3CN turned brownish yellow on standing. On the contrary, tetrabutylammonium perchlorate recrystallized several times from ethanol was very satisfactory for use in all

Figure 21. The visible absorption spectra of (N-methyl-5,10,15,20-tetraphenylporphinato)copper(II) cation and (chloro-N-methyl-5,10,15,20-tetraphenylporphinato)-copper(II) in CH_3CN (700-500 nm). The spectra of the chloro complex do not change on addition of excess tetraethylammonium chloride consistent with the results from cyclic voltammetry of Cu(N-CH_3TPP)Cl (Figure 22).

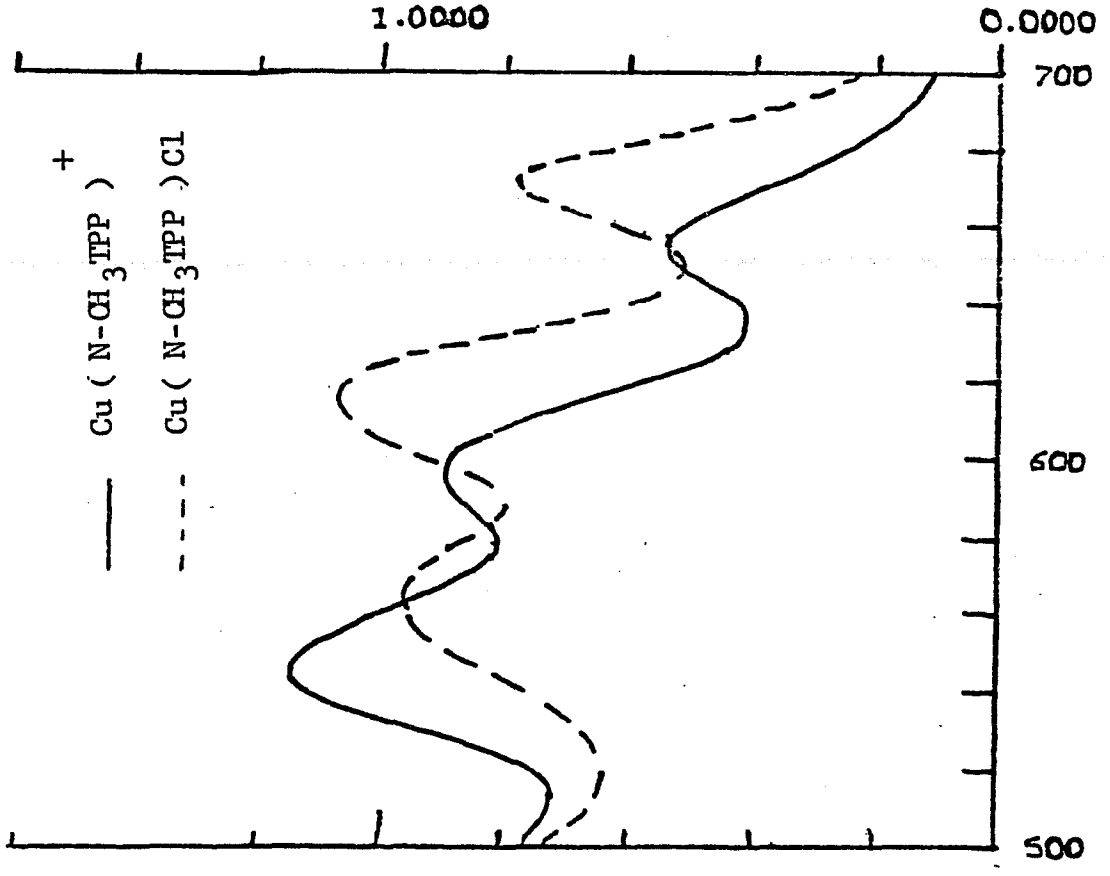
1.0000
0.0000
700
600
500
Cu (N-CH3TPP)+
Cu (N-CH3TPP)Cl

Table XIV. PHYSICAL PROPERTIES AND MAXIMUM POTENTIAL RANGE OF SEVERAL COMMON SOLVENTS USED FOR PORPHYRIN ELECTROCHEMISTRY.[b]

Solvent	(abbreviation)	F.P. (°C)	B.P. (°C)	Cathodic limit[a]		Anodic limit[a]	
				Pt	Hg	Pt	Hg
1,2-dichloroethane	($EtCl_2$)	-35	83.4	-1.9	--	+1.8	--
Methylene chloride	(CH_2Cl_2)	-96.7	40	-1.9	-1.9	+1.8	0.6
Benzonitrile	(BN)	-13.5	191.1	-1.8	--	+1.7	--
Acetonitrile	(AN)	-45.7	81.6	-2.0	-2.8	+1.8	+0.6
Tetrahydrofuran	(THF)	-108.5	65	-3.6	-3.6	+1.8	0.0
Dimethylacetamide	(DMF)	-61	153	-2.5	-3.0	+1.6	+0.5
Dimethylacetamide	(DMA)	-20	165	--	--	+1.3	--
Dimethylsulfoxide	(DMSO)	18.5	189.0	-1.9	-3.0	+0.7	+0.4
Pyridine	(Py)	-41.6	115.5	-1.8	-1.6	+0.8	--

a. Values given are the maximum limits observed in the literature and are reported versus SCE. The observed values may be substantially less, depending on the type of supporting electrolyte and the purity of the solvent.

b. Data taken from Kadish, K.M., "The Electrochemistry of Iron Porphyrin in Nonaqueous Media" in Iron Porphyrins, edited by A.B.P. Lever and Harry B. Gray, Reading (Massachusetts), 1983, Part Two, P-183.

experiments performed in dry CH_3CN. The concentration of supporting electrolyte was either 0.1 or 0.5M. Potential range (V vs. SCE) of several supporting electrolytes in dichloromethane are shown in Table XV. As it is clear from Table XV, salts of I^-, Br^-, or Cl^- may be used for reductions, but their oxidations to I_3^-, Br_3^- and Cl_2 at potentials less than 1.0V may present problems. Indeed, this is the case in CH_3CN where I used excess tetraethylammonium chloride to convert trifluoromethanesulfonate salts of CuN-alkyl or CuN-aryl porphyrins (see in the latter part of this chapter). In addition, these anions can complex with the central metal ion. Kadish[90] has raised the question of concentration of inert electrolyte. Potentials measured with concentrations of 1.0M TBAP are not some that measured with 0.10 or 0.001M. A difference of several hundred millivolts can occur depending upon the reactions concerned.

Due to the higher sensitivity of the cyclic voltammetry techniques, over polarography, one may use a dilute solution[91] (10^{-4}M or less) to obtain a voltammogram. However, a better looking curve results at a concentration of about $5x10^{-3}$M and the potentials can be measured very easily. About 3mg of metalloN-alkylporphyrin was dissolved in 5-6 mL of CH_3CN containing ca. 0.1M (0.5M in the case of ClMnNPh-TPP) TBAP and deaerated for 15 minutes with Ar prior to the measurements. In most cases, a blanket of Ar over the solution was maintained during the experiments.

The current-voltage output was recorded on an ominographic X-Y recorder. The average of cathodic and anodic peak

Table XV. Available Potential Range (V vs. SCE) of Different Supporting Electrolytes in CH_2Cl_2[a].

Supporting Electrolyte	Electrode Material	
	Platinum	Mercury
Tetrabutylammonium perchlorate	1.8 to -1.7	0.8 to -1.9
Tetrabutylammonium chloride	0.86 to -1.9	-0.35 to -1.7
Tetrabutylammonium bromide	0.59 to -1.7	-0.37 to -1.7
Tetrabutylammonium iodide	0.18 to -1.7	-0.45 to -1.7

a. Data taken from C.K. Mann, "Nonaqueous Solvents for Electrochemical Use," in Electroanalytical Chemistry, A.J. Bard (ed.), New York, 1969, Vol. 3, P-123.

potentials, (Epa + Epc)/2, was considered as half-wave potential. All the potentials reported here are measured against SCE or Ag/AgCl electrodes. In the case of Mn(N-CH_3TPP)Cl. It was first dissolved in Ø.2mL (because of its insolubility in CH_3CN) spectrograde benzonitrile and then diluted to 5mL with Ø.1M TBAP in CH_3CN. There is no effect of benzonitrile on the cyclic voltammogram of Mn(N-PhTPP)Cl.

RESULTS: The potentials for the Fe(II) complexes are presented in Table XVI. All the assignments of redox potentials for the metal atoms of N-substituted porphyrin complexes reported here are based upon the cyclic voltammograms of free base N-CH_3HTPP[84] and Zn(N-CH_3TPP)Cl.[82] Except in the case of $Fe^{III/II}$ system, all other potentials have been measured and reported against Ag/AgCl electrode. In the case of iron complexes, the measured potentials have been reported against SCE(Saturated Calomel Electrode), which is +35 mv relative to the Ag/AgCl reference electrode. Visible spectra were taken before and after the cyclic voltammetry experiments to ensure the integrity of the N-alkyl and N-arylporphyrin complexes. The visible absorption spectra are shown in Table XIII. The potentials measured for Cu(II) complexes are given in Table XVII. Elemental analysis results and the visible absorption spectra for the Cu(II) complexes with $CF_3SO_3^-$ (or ClO_4^-) counteranion have been presented in Chapter 3. Fig. 22 shows the cyclic voltammograms of Cu(N-CH_3TPP)$^+$ ClO_4^-, and those after separate additions of $N(C_2H_5)_4Cl$ and PPh_3. The visible absor-

Table XVI . Comparison of the half-wave potentials of chloro(N-alkyl-5,10,15,20-tetraphenylporphinato)iron(II) complexes.[a,b,c]

Complexes	$Fe^{III/II}$	Ligand Oxidation Ox_1	Ligand Reduction Rd_1	Ligand Reduction Rd_2	$\Delta E^{d}_{1/2}$ (Ox-Red)	$\Delta E^{d}_{1/2}$ (Red)
Fe(N-CH_3TPP)Cl[e,f]	0.50	1.52	-0.85	-1.34	2.37	0.49
Fe(N-C_2H_5TPP)Cl	0.51	-	-0.86	-1.09	-	0.23
Fe(N-C_6H_5TPP)Cl	0.54	-	-0.83	-	-	-

a. Solvent DMF or DMF/THF
b. Supporting Electrolyte 0.1 M Tetraethylammonium Perchlorate
c. $E_{1/2}$ (volt) measured against SCE
d. See text.
e. Measured in CH_2Cl_2 with 0.1 M TBAP
f. Taken from Kopelove, A. B,,M.S. Thesis, Colorado State University, 1981, P-38.

Table XVII. Comparison of the half-wave potentials[a,b,c] of $Cu(N\text{-}RTPP)^{+}X^{-}$.

Copper Complexes	Cu(II)/Cu(I)	Ligand Oxidation OX_1	Ligand Oxidation OX_2	Ligand Reduction Rd_1	Ligand Reduction Rd_2	$\Delta E_{1/2}$ (OX-RED)	$\Delta E_{1/2}$ (OX)	$\Delta E_{1/2}$ (RED)
$Cu(N\text{-}CH_3TPP)^{+}ClO_4^{-}$	-0.29	1.29	1.53	-1.15	-1.36	2.44	0.24	0.21
$Cu(N\text{-}CH_3TPP)Cl$	-0.38	-	-	-1.51	-1.70	-	-	0.19
$Cu(N\text{-}CH_3TPP)^{+}ClO_4^{-} + PPh_3$	-0.04	-	-	-	-	-	-	-
$Cu(N\text{-}C_2H_5TPP)^{+}ClO_4^{-}$	-0.25	1.31	1.52	-1.14	-1.41	2.45	0.21	0.27
$Cu(N\text{-}C_2H_5TPP)Cl$	-0.38	-	-	-1.28	-1.50	-	-	0.22
$Cu(N\text{-}PhTPP)^{+}ClO_4^{-}$	-0.32	1.24	1.46	-1.01	-1.27	2.25	0.22	0.26
$Cu(N\text{-}PhTPP)Cl$	-0.415	-	-	-	-1.46	-	-	-

a. Solvent-CH_3CN

b. Supporting Electrolyte- Tetrabutylammonium Perchlorate

c. All the potentials have been measured against Ag/AgCl ,Cl^{-} electrode

Figure 22. Cyclic voltammograms of $Cu(N\text{-}CH_3TPP)^+$ (with no mark, Y-axis = 10 μA) and after separate addition of tetraethylammonium chloride(Y-axis = 10 μA) and triphenylphosphine(Y-axis = 5 μA) in CH_3CN, 0.043 M TBAP. Platinum electrode. There is no change in the voltammogram of $Cu(N\text{-}CH_3TPP)Cl$ after addition of excess chloride.

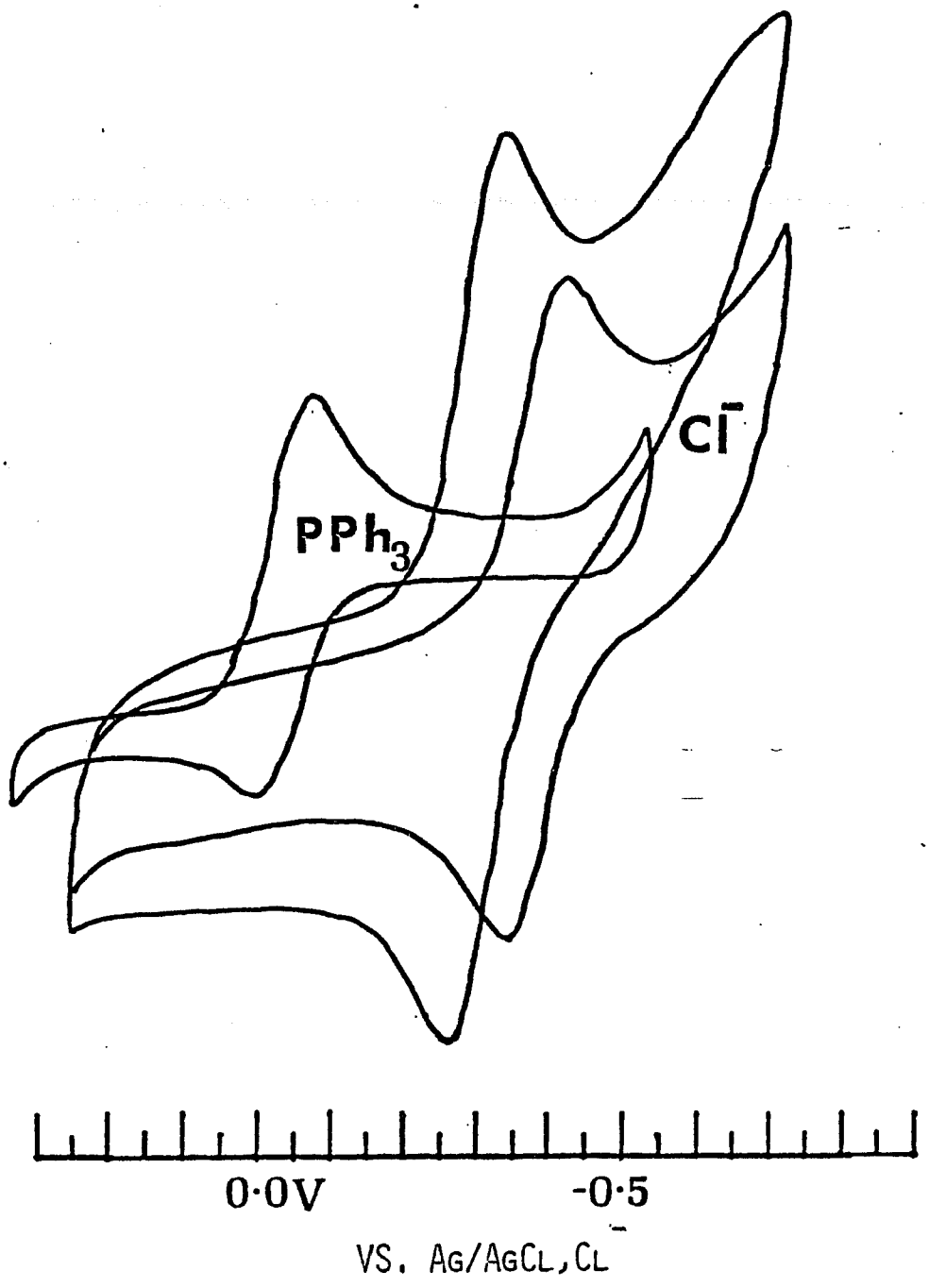
Cl⁻
PPh3
0·0V
-0·5
VS. Ag/AgCl,Cl⁻

ption spectra are presented in Table XIII. The cyclic voltammogram of $Cu(N\text{-}C_2H_5TPP)^+$ has been shown in Fig. 23. The visible absorption spectra for the Cu(II) complexes with $CF_3SO_3^-$ and Cl^- as axial ligands are different for N-Ph and N-ethyl complexes as in $Cu(N\text{-}CH_3TPP)^+$ and $Cu(N\text{-}CH_3TPP)Cl$ on (Fig. 21). The potentials for the Mn(II) complexes are given in Table XVIII. The elemental analysis results obtained for $Mn(N\text{-}CH_3TPP)Cl$ were satisfactory. The $Mn(N\text{-}p\text{-}CH_2C_6H_4NO_2TPP)Cl$ and Mn(N-PhTPP)Cl complexes did not give satisfactory elemental analysis results but the visible absorption spectra are those expected for these complexes (Table XIII). The cyclic voltammograms of the Mn(II) complexes (metal-centered) are shown in Fig. 24.

DISCUSSION The electrochemistry of N-substituted complexes of Fe(II), Mn(II) and Cu(II) is discussed in this chapter. The Fe(II) complexes have direct relevance to biological processes, while the Mn(II) and Cu(II) complexes are of interest with respect to previously reported electrochemistry of N-alkylated and non-N-substituted metalloporphyrins.

The redox processes which occur in the cyclic voltammetry experiment include oxidations and reductions that predominantly involve the porphyrin and those which are predominantly metal-centered. The focus of this chapter is on the metal-centered processes. In making assignments, investigators have noticed that cyclic voltammograms of free ligands and of metal complexes of many different porphyrins exhibit

Figure 23. Cyclic voltammogram of(N-ethyl-5,10,15, 20-tetraphenylporphinato)copper(II) cation in acetonitrile, 0.1 M TBAP. Platinum electrode. The peaks for the reduction of the ligand have not been shown here (See Table XVII).

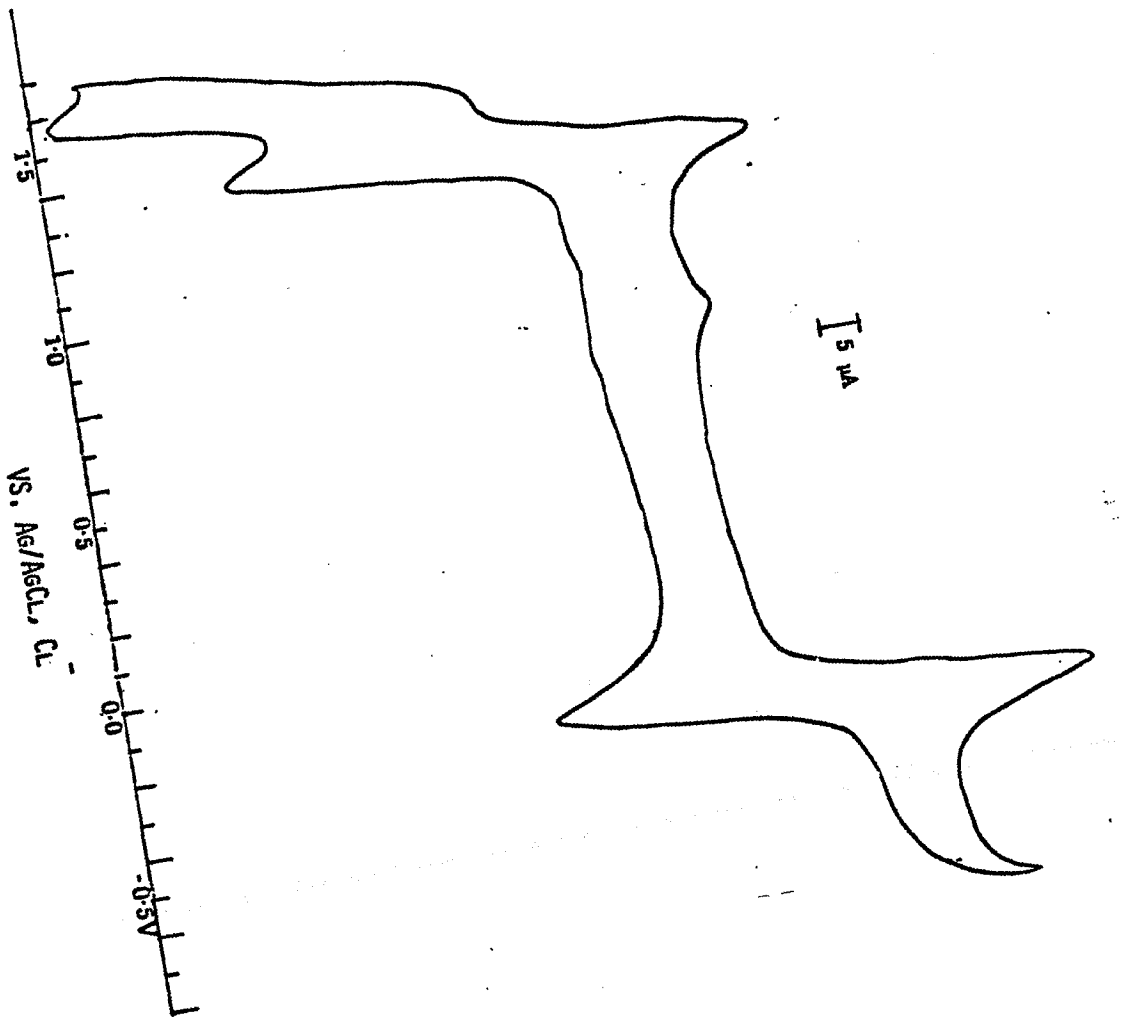
1.5
1.0
0.5
0.0
-0.5
ΔS
VS. Ag/AgCl, Cl⁻
5 mA
I

Table XVIII . Half-wave potentials (V vs. Ag/AgCl) for chloro(N-substitued-5,10,15,20-tetraphenyl-porphinato)manganese(II) complexes.[a,b]

Complex	III/II Mn	Ligand Oxidation OX_1	Ligand Oxidation OX_2	Ligand Reduction Rd_1	Ligand Reduction Rd_2	$\Delta E_{1/2}$ (OX-RED)[d]	$\Delta E_{1/2}$ (OX)[d]	$\Delta E_{1/2}$ (RED)[d]
Mn(N-CH_3TPP)Cl[c]	0.815	1.19	1.40	-1.10	-1.31	2.29	0.21	0.21
Mn(N-PhTPP)Cl	0.82	1.12	1.32	-1.00	-1.28	2.12	0.20	0.28
Mn(N-PhTPP)Cl[c]	0.82	1.15	-	-0.955	-1.20	2.10	-	0.245
Mn(N-p-$CH_2C_6H_4$-NO_2TPP)Cl	0.91	1.24	-	-0.85	-1.14	2.09	-	0.29

a. Solvent-CH_3CN
b. Supporting electrolyte- 0.1 M TBAP except in the case of Mn(N-PhTPP)Cl, where it was 0.5 M in CH_3CN and 0.4 M in CH_3CN/C_6H_5CN.
c. Solvent-CH_3CN/C_6H_5CN
d. See Text.

Figure 24. Cyclic voltammograms of (chloro-N-substituted-5,10,15,20-tetraphenylporphinato)manganese(II) in acetonitrile (For CH_3 and p-$CH_2C_6H_4NO_2$, 0.1 M TBAP, and for C_6H_5, 0.5 M TBAP, Y-axis for p-$CH_2C_6H_4NO_2$ = 5 μA/cm and for CH_3 and C_6H_5, it is 10 μA/cm). Platinum electrodes were used. The unmarked voltammogram corresponds to that of Mn(N-p-$CH_2C_6H_4NO_2$TPP)Cl.

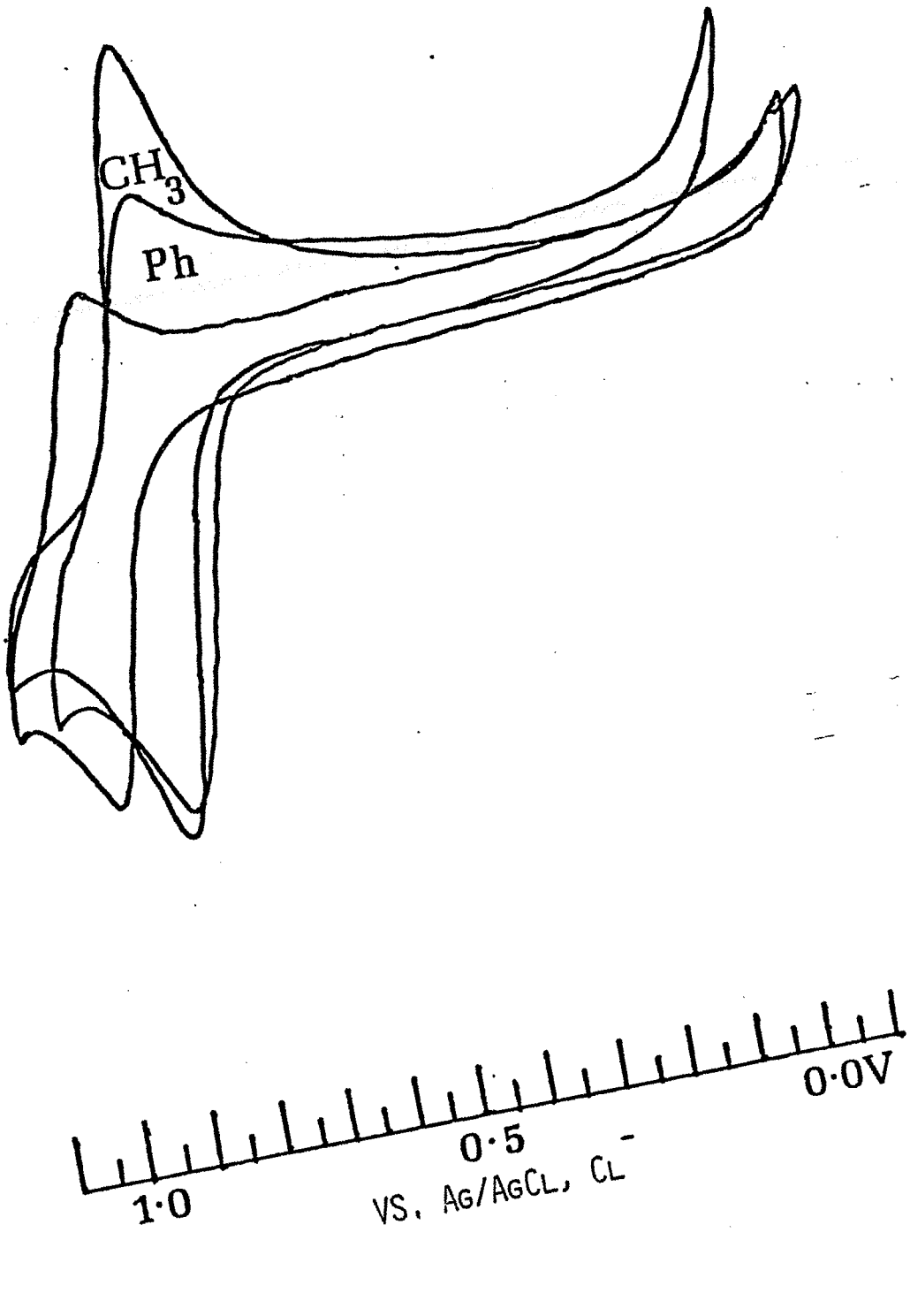
CH3
Ph
1·0
0·5
0·0V
VS. AG/AGCL, CL-

peaks which have similar separations in each voltammogram. The peaks, which are found for free ligands, complexes of redox-inactive metal atoms such as Zn(II), and for complexes of redox-active species such as Fe(III), have been assigned to ligand-centered processes. The separations of these peaks are represented by $\Delta E_{1/2}$ (ox- red), $\Delta E_{1/2}$ (ox) and $\Delta E_{1/2}$ (red). $\Delta E_{1/2}$ (ox -red) is the difference between the first ring oxidation yielding a π-cation radical and the first ring reduction producing a π-anion radical. It is typically 2.25 ± 0.15v.[92-95] $\Delta E_{1/2}$(ox) is the difference between the two ring oxidations, and it is typically 0.29 ± 0.05v.[92] $\Delta E_{1/2}$(red) is the separation between two ring reductions, typically 0.42 ± 0.05v.[92] Complexes of redox-active metal ions show an additional peak which is generally found in the intermediate potential region between the ligand centered peaks. These are assigned to the metal-centered process.

The N-substituted porphyrins and their complexes exhibit similar behavior with respect to ligand-centered processes. The separation of the peaks assigned to the ligand-centered process are in the range of 2.30 ± 0.16v; 0.30 ± 0.11V; and 0.39 ±0.17V respectively.[84] Significant differences, however, are found for the N-substituted metalloporphyrin: the extent of reversibility, the ability to observe particular oxidation states, and the values of the $M^{3+/2+}$ potentials.

Such differences will be discussed in detail later in

this chapter.

Iron: The formation of green pigments (N-alkyl or N-arylporphyrins, chapter 1) in vivo is a complicated process. The removal of iron atom with simultaneous formation of protonated N-alkyl porphyrins (N-alkylprotoporphyrins have a pKa greater than 8) suggests that the sequence involves an iron N-alkylporphyrin. Model studies by Mansuy and his coworkers[28] and Ortiz de Montellano et al.[26] have shown that an alkyl or aryl group can migrate to the nitrogen atom from the metal center, Fe(III), with the reduction to Fe(II) as shown below.

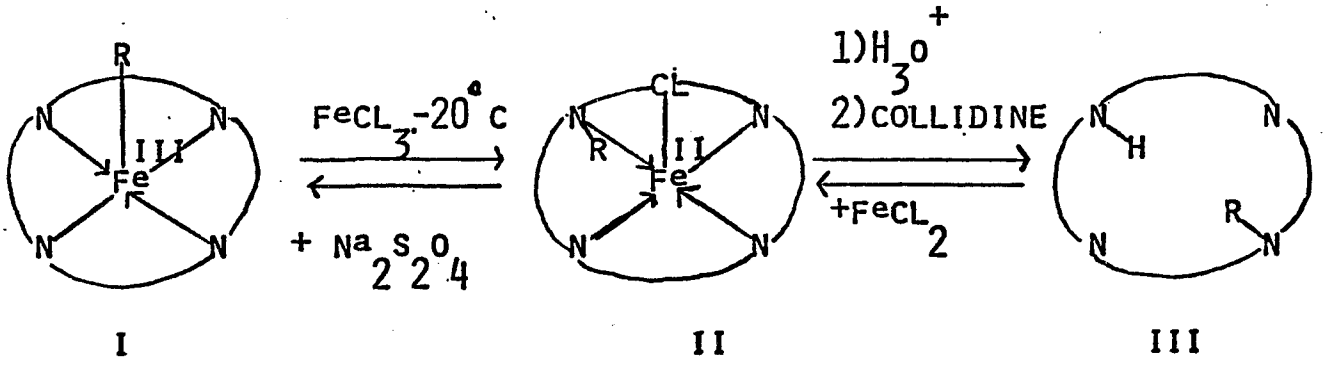

I II III

(SCHEME 4, Adapted from Mansuy, D. et. al., J. Am. Chem. Soc. 1982, 104, 6159-61)

The product of the migration (II) has been identified by its

visible spectrum, which is the same as the complex found by reacting III with Fe(II).[28] Reversible migration of alkyl or aryl groups is also known in other metalloporphyrin systems.[75] Since these model studies indicate that reduction of the Fe(III) atom is a likely feature for the mechanism of formation of N-substituted porphyrins in vivo, the reduction potentials of iron complexes of N-substituted porphyrins are of interest. The potential for only one iron complex of an N-substituted porphyrin, Fe(N-CH_3TPP)Cl,[83] has been determined. Thus the mechanism by which the green pigments are formed and the possible effects of different alkyl or aryl groups have not been previously investigated. For this reason, I have decided to look at the effect of ethyl and aryl groups on the potential of $Fe^{3+/2+}$ system.

In investigating the electrochemistry of N-substituted iron porphyrin complexes, our main concern has been to determine the effect of the N-substituent. Therefore, we have made comparisons in which the axial ligand, porphyrin ring substituents and solvent have been held constant for a series of complexes with different N-substituents.

The $Fe^{III/II}$ potentials for Fe(N-CH_3TPP)Cl,[83] Fe(N-C_2H_5TPP)Cl and Fe(N-PhTPP)Cl are very similar (Table XVI). They are significantly different from the potential of non-N-alkylated iron porphyrin complex presented in Table XIX. To determine the most appropriate non-alkylated complex for a comparison of the effect of the N-substituent, other factors which affect the potential must be eliminated.

Table XIX. Half-wave potential (V vs. SCE) for the Fe(III)/Fe(II) couple of Fe(TPP)X in selected solvents.[a]

Solvent	Donor number	Dielectric constant	$E_{1/2}(X)$ ClO_4^-	Br^-	Cl^-	N_3^-	F^-
$EtCl_2$	0.0	10.7	0.24	-0.19	-0.31	-0.38	-0.47
CH_2Cl_2	0.0	8.9	0.22	-0.21	-0.29	-0.42	-0.50
CH_3NO_2	2.7	35.9	0.10	b	b	b	b
Ø-CN	11.9	25.2	0.20	-0.18	-0.34	-0.39	-0.57
CH_3CN	14.1	37.5	0.11	b	b	b	b
PrCN	16.6	20.3	0.13	-0.15	-0.27	-0.33	-0.45
$(CH_3)_2CO$	17.0	20.7	0.09	-0.16	-0.28	-0.34	-0.43
THF	20.0	7.6	0.17	-0.24	-0.34	-0.38	-0.47[a]
DMF	26.6	38.3	-0.05	-0.05	-0.18	-0.25	-0.40
DMA	27.8	37.8	-0.04	09.05	-0.15	-0.24	-0.36
DMSO	29.8	46.4	-0.09	-0.09	-0.10	c	-0.09(-0.40)[d]
Py	33.1	12.0	0.15	0.17	0.16(-0.25)[d]	0.15(-0.28)[d]	0.16(-0.46)[d]

a. Data taken from Bottomley L.A. and Kadish K.M., Inorg. Chem. 1981, 20 1348
b. Complex was insoluble in solvent system.
c. Reduction consisted of two overlapping processes.
d. Second reduction process

These factors include the axial ligand, ring substituents, solvent and, perhaps, spin state.

In non-N-alkylated porphyrin complexes of iron, the axial ligands and the solvents have a pronounced effect on the redox potential of the metal center, i.e., Fe(III)/Fe(II) (Table XIX). In CH_2Cl_2, reduction of tetraphenylporphinatoion(III) complexes becomes much more difficult (by upto Ø.71 IV) when the counterion is changed from ClO_4^- to F^-. This trend is consistent with the extent of bonding of the ligand. The solvent also has a considerable effect on the $Fe^{III/II}$ potential as shown in Table XIX. In dichloromethane and DMF the $Fe^{III/II}$ potentials of chlorotetraphenylporphinatoiron are -Ø.29 and -Ø.18V (vs. SCE) respectively. The substituents of the porphyrin ring also affect the $Fe^{III/II}$ potential as presented in Table XX.

Thus, the most appropriate choice for comparison is the potential of Fe(TPP)Cl in DMF, which is -Ø.18V vs. SCE. The differences due to N-substitution are Ø.68 V for Fe(N-CH_3TPP)Cl[83] (measured in CH_2Cl_2), Ø.69 V for Fe(N-C_2H_5TPP)Cl and Ø.72 V for Fe(N-PhTPP)Cl. (The $M^{III/II}$ potentials of N-substituted porphyrin complexes are not much affected by a change of solvent). In addition, the voltammograms of these N-alkyl(aryl) complexes are reversible (Fig. 25) unlike that of Fe(TPP)Cl. The high irreversibility found in the voltammograms of Fe(TPP)Cl is due to the dissociation of Cl^- from the reduced species (Fig. 25).[96]

In contrast to the nice peaks observed for the metal centers in Fe(N-RTPP)Cl complexes, the oxidation and reduc-

Table XX. Half-Wave Potentials of Several Mn(III) and Fe(III) Porphyrins[a].

Porphyrin	Mn(III)/Mn(II)[b,d]		Fe(III)/Fe(II)[c,d]
	CH_3CN	DMF	DMF
OEP	-	-	-0.34
Etio	-0.45	-0.40	-0.34
Meso DME	-0.43	-0.40	-
Deutro DME	-0.38	-0.33	-0.30
Hemato DME	-0.37	-0.32	-
Proto DME	-0.35	-0.31	-0.27
TPP	-0.23	-0.22	-0.18
Pheophorbide a MME	-0.23	-0.21	-
$TPP(CN)_4$	-	-	-0.12

a. Potentials are reported as $E_{1/2}$ (V) vs. SCE

b. Taken from Boucher, L.J. and Garber, H.K., Inorg. Chem., 1970, 9, 2644-49.

c. Taken from Kadish, K.M., "The Electrochemistry of Iron Porphyrins in Nonaqueous Media" in "Iron Porphyrins",Part Two, edited by A.B.P., Lever and H.B.,Gray, Reading(Massachusetts), 1983, P-183.

d. Chloride ion as the axial ligand.

Figure 25. Cyclic voltammograms of Fe(N-CH_3TPP)Cl and Fe(TPP)Cl in CH_2Cl_2, 0.1 M TBAP. Platinum electrode(Taken from Kopelove, A.B., M.S. Thesis, Colorado State University, 1981).

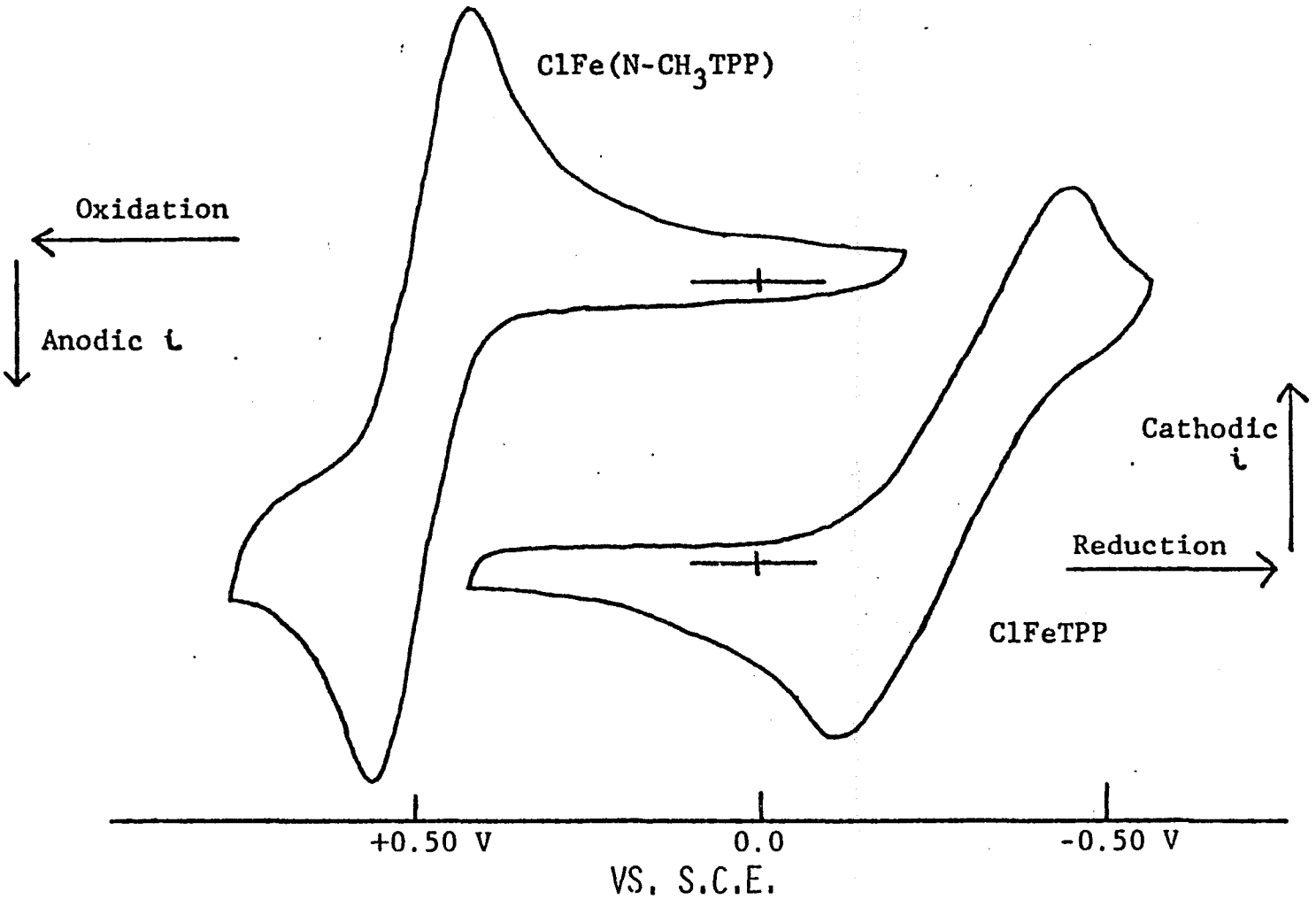
ClFe(N-CH3TPP)
Oxidation
Anodic i
Cathodic i
Reduction
ClFeTPP
+0.50 V
0.0
-0.50 V
VS. S.C.E.

tion of the ligands are not well defined. The $\Delta E_{1/2}$(Ox-red), and $\Delta E_{1/2}$(red) of Fe(N-CH_3TPP)Cl are 2.37V and Ø.49V respectively.[83] The ease of reducing the porphyrin ligands in Fe(N-RTPP)Cl compared to their non-N-alkyl analog indicates that less electron density is supplied to the central metal ion by the porphyrin core. As expected from this hypothesis, it is harder to oxidize the N-alkylated porphyrin ring.

The most obvious explanation for the large change in $Fe^{3+/2+}$ potential is the difference in geometry caused by N-substitution. The crystal structure of Fe(N-CH_3TPP)Cl[83] is very similar to the other N-CH_3TPP complexes (Table XXI). The coordination geometry is a distorted square base pyramid. The magnetic moment of the complex is 5.2 μ_B(by Faraday Method), showing it to be a high spin complex[83] as found for other N-methylporphyrin complexes.[82]

Though the magnetic moment of the Fe(N-CH_3TPP)Cl^+ has not been determined, a recent report of the magnetic susceptibility and ESR parameters of (Fe(N-CH-$_3$OEP)Cl)$^+$ ClO_4^-(OEP = octaethylporphyrin) shows the complex to be high spin[97] (s = 5/2). It is very likely that Fe(N-CH_3TPP)Cl^+ would be high spin, like Fe(N-CH_3OEP)Cl^+ based upon the structural and spin state similarities found among a variety of N-alkylporphyrin complexes. Very similar coordinating geometry and the same spin state have been found for CØ(N-CH_3TPP)Cl[47a] and CØ(N-$CH_2CO_2C_2H_5$OEP)Cl.[98] The geometry of the Fe(N-C_2H_5TPP)Cl and Fe(N-PhTPP)Cl are probably very

Table XXI. Metal Ligand Bond Distances in M(N-CH_3TPP)Cl Complexes[a,b].

	Mn(II)	Fe(II)	Co(II)	Zn(II)
M-Cl	2.295(3)	2.244(1)	2.243(2)	2.232(3)
M-N1	2.368(5)	2.329(2)	2.381(5)	2.530(7)
M-N2	2.155(6)	2.118(2)	2.063(5)	2.089(6)
M-N3	2.156(5)	2.116(2)	2.063(5)	2.081(9)
M-N4	2.118(5)	2.082(2)	2.016(4)	2.018(9)

a. Taken from Anderson, O.P.; Kopelove, A.B. and Lavallee, D.K., Inorg. Chem. 1980, 19, 2101-07.

b. Estimated standard deviations in parentheses.

similar to that found in Fe(N-CH_3TPP)Cl.[83] (The visible absorption spectra of Fe(N-C_2H_5TPP)Cl and Fe(N-CH_3TPP)Cl are very similar. The crystal structures of Zn(N-PhTPP)Cl[99] (chapter 5) and Zn(N-CH_3TPP)Cl are very similar. The crystal structures of N-CH_3TPP complexes of Mn(II), Zn(II), CO(II), Fe(II) are very closely related[83] (Table XXI). The spectra of Zn(N-PhTPP)Cl and Fe(N-PhTPP)Cl resemble each other[98], so the structures of Fe(N-PhTPP)Cl and Fe(N-CH_3TPP)Cl[83] are probably very similar. (See next chapter). The geometry of Fe(N-C_2H_5TPP)Cl^+ and Fe(N-PhTPP)Cl^+ are also probably very similar to that of Fe(N-CH_3TPP)Cl^+.

The crystal structures (Table XXI) reported earlier[47a,b,43,83] and that of Zn(N-PhTPP)Cl[99] reported in this thesis show that the bond between the nitrogen bearing the alkyl and aryl group and the metal ion is long and that the metal atom is out the plane of porphyrin core. X-ray photoelectron spectra also show that the interaction between substituted nitrogen and the metal ion is weak.[42] It appears therefore, that the large reduction in the σ and d-π metal-ligand bonding interaction, caused by N-substitution, leads to a dramatic change in the redox behaviour.[84] This effect is similar for a variety of N-substituents. It is expected, therefore, that any process which leads to the formation of an N-substituted porphyrin complex will make a reduction of Fe(III) to Fe(II) more favorable.

These results can be related to the mechanism for formation of N-alkyl and N-aryl porphyrins through routes of hydrazines, carbenes and 4-substituted di-hydropyridines.

The carbene inserted iron porphyrins produce the N-substituted porphyrins when they are treated with acid.[85,86] Inactivated hemoproteins are produced when Hb, Mb, etc., are treated with ethyl and phenylhydrazines[25] and the corresponding N-ethyl and N-phenylprotoporphyrins are formed when these inactivated hemoprotein are denatured in the presence of oxygen and acid.[29,30,68] The inactivated hemoprotein, obtained from the reaction of Hb with phenylhydrazine, has been established as a σ-phenyl complex[29] (i.e., a phenyl group is bound to the iron atom A of scheme 4). The σ-aryl and σ-alkyl ironporphyrins can be obtained by other routes; through migration of alkyl or aryl group to this metal center[26,28] or interaction of alkyl radicals with iron porphyrins.[100,101] They can also be obtained through two electron reduction of carbene inserted iron porphyrins[102,106] in the presence of acid.[107] The σ-alkyl and σ-aryl complexes can be reasonably postulated where they have not been established.

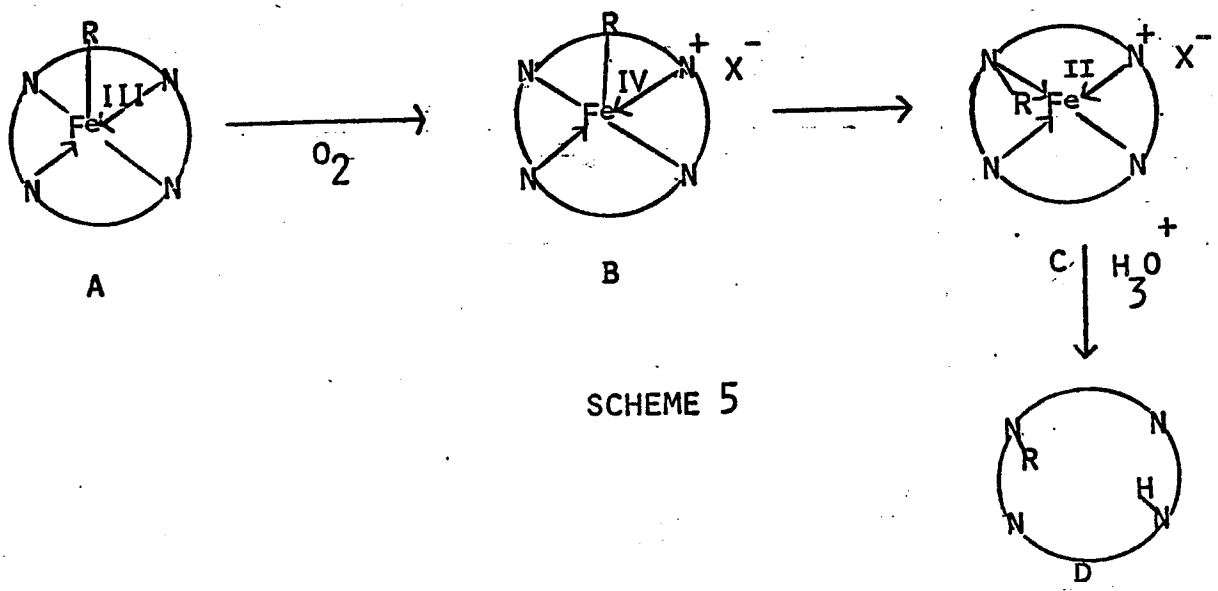

SCHEME 5

The $Fe^{III/II}$ potentials for σ-alkyl and σ-aryl porphyrin complexes are unfavorable (i.e. more negative than -Ø.6V vs. SCE, for example, -Ø.76V for σ-CH_3 and σ-$CH_2C_6H_5$, -Ø.7ØV for σC_6H_5 and σC_2H_4CN). In other words σ-alkyl or σ-aryl intermediate (A) is fairly stable and is formed first in the mentioned cases. The fact that oxygen is necessary[25,26,29] in the formation of N-substituted porphyrin leads us to postulate a Fe(IV) intermediate which then easily rearranges to form the Fe(II) N-alkyl intermediate (scheme 5). The Fe(II) N-alkyl or N-arylporphyrin complexes are more stable in their +2 state (by +Ø.5ØV vs. SCE) A small amount of acid then releases the iron atom, since the iron atom in Fe(II) complexes is readily removed by acids. The N-alkylprotoporphyrin has a pKa greater than 8 and therefore it is very easy for the N-alkylprotoporphyrin to be protonated to form the green pigments. The same mechanism is probably applicable in the formation of green pigments from the reactions of cytochrome P-45Ø with 4-substituted dihydropyridines.

Manganese: The isolation of Mn(II) complexes of N-alkyl and N-aryl 5,1Ø,15,2Ø-tetraphenylporphyrin is easier than the isolation of the Fe(II) complexes. Then Mn(II) complexes are also more stable than the Fe(II) complexes. I have extended the previous work on Mn(N-RTPP)Cl (R = CH_3)[82] to R = C_6H_5 and -$CH_2C_6H_4NO_2$) to determine the effect of the N-substituent on the $Mn^{III/II}$ potential. The manganese complexes are also of interest because some manganese porphyrin complexes are known to simulate the role played by

manganese in the photosynthetic liberation of oxygen from water.[87]

As in the case of iron complexes, for Mn(II) complexes of N-alkyl(aryl)porphyrins the solvent (CH_3CN), axial ligand and the porphyrin ring substituents have been kept the same and the N-substituent has been altered.

The redox potentials of Mn(N-CH_3TPP)Cl and Mn(N-PhTPP)Cl are very similar (Ø.815V) and Ø.82ØV vs. Ag/AgCl respectively) though their visible spectra differ (Table XIII). The $Mn^{III/II}$ potential for Mn(N-CH_2-p-$C_6H_4NO_2$TPP)Cl is Ø.91V against Ag/AgCl reference electrode. As in the case of iron, these metal center redox potentials are greatly different from potentials of non-N-alkylated manganese porphyrin complexes presented in Table XXII In order to compare the effect of N-substituent on the $Mn^{III/II}$ potential, the other factors, like the effect of axial ligands, ring substituents and solvents, must be excluded.

In Mn(TPP)X complexes the $Mn^{III/II}$ potential is affected by the axial ligands (Table XXII). By changing the counter ion from ClO_4^- to N_3^-, the $Mn^{III/II}$ potential changes by 18Ø mV.[1Ø8] The greater stabilization of Mn(III) over Mn(II) by N_3 accounts for this change. The solvents also affect the $Mn^{III/II}$ potential (Table XXII). Another important thing to notice is the change in $Mn^{III/II}$ potential caused by the basicity (by the ring substituents) of the porphyrins. For example, Mn(TPP)Cl and Mn(EP)Cl (EP = etioporphyrin) have half wave potentials at -Ø.23 and -Ø.45V

Table XXII. HALF-WAVE POTENTIALS (V) VS. SCE OF THE Mn(III)/Mn(II) REDOX COUPLE FOR Mn(TPP)X IN SELECTED SOLVENTS[a]

Solvent	Donor number	Dielec Const	Counterion, X					
			ClO_4^-	I^-	SCN^-	Br^-	Cl^-	N_3^-
$MeCl_2$	0.0	8.9	-0.16	-0.24	-0.25	-0.26	-0.29	-0.34
$EtCl_2$	0.0	10.7	-0.17	-0.23	-0.23	-0.25	-0.26	-0.31
PhCN	11.9	25.2	-0.14	-0.16	-0.23	-0.24	-0.27	-0.30
CH_3CN	14.1	37.5	-0.19	-0.19	-0.20	-0.20	-0.23	-0.29
PrCN	16.6	20.3	-0.13	-0.14	-0.17	-0.18	-0.22	-0.26
$(CH_3)_2CO$	17.0	20.7	-0.09	-0.07	-0.07	-0.09	-0.14	-0.17
THF	20.0	7.6	-0.12	-0.12	-0.18	-0.16	-0.23	-0.31
DMF	26.6	38.3	-0.19	-0.19	-0.19	-0.20	-0.20	-0.20
DMA	27.8	37.8	-0.12	-0.12	-0.11	-0.11	-0.11	-0.12
Me_2SO	29.8	46.4	-0.25	-0.25	-0.25	-0.25	-0.25	-0.25
Py	33.1	12.0	-0.23	-0.23	-0.24	-0.23	-0.24	-0.25

a. Taken from Kelly, L.S. and Kadish, K.M., Inorg. Chem. 1982, 21, 3631-39.

vs. SCE respectively (Table XX).

So in order to compare the effect of N-substituent on the $Mn^{III/II}$ potential, our best choice is Mn(TPP)Cl. The half-wave potential for the $Mn^{III/II}$ couple is -0.23 vs. SCE (i.e., -0.195V vs. Ag/AgCl).[108] The differences due to N-alkyl (aryl) groups are 1.01V for Mn(N-CH_3TPP)Cl, 1.06V for Mn(N-PhTPP)Cl and 1.15V for Mn(N-p-CH_2-$C_6H_4NO_2$TPP)Cl. An anodic shift of 90 mv in the case of Mn(N-p-CH_2-$C_6H_4NO_2$TPP)Cl is presumably due to the presence of strong electron withdrawing nitro group at the para position of the benzyl moiety. This shift of 90 mv is comparable to the shift in Mn(III/II) potentials of non-N-alkylated systems caused by electron withdrawing porphyrin ring substituents.[109]

The peaks for the oxidation and reduction of the ligands of Mn(N-RTPP)Cl (Table XVIII) are much clearer than those found for iron complexes The $WE_{1/2}$ (ox-red), $WE_{1/2}$(ox) and $WE_{1/2}$(red) of Mn(N-RTPP)Cl complexes are 2.09-2.29v, 0.20 - 0.21v and 0.21-0.29v respectively. Once again as in iron, it is easier to reduce the porphyrin ligands of Mn(N-RTPP)Cl compared to its non-N-alkyl analog and the reverse is true in the oxidation of the ligands.

The most reasonable explanation for the large change in the $Mn^{III/II}$ potential is the difference in geometry caused by the alkyl or aryl group bound to the nitrogen atom. The crystal structure of Mn(N-CH_3TPP)Cl shows it to be square base pyramid.[47b] Its magnetic moment, determined by nmr spectroscopy[84] and magnetic susceptibility measurements, is

5.9 B.M.;[82] consistent with a high spin system. Mn(II)TPP is also a high spin complex.[110] Although the μ_{eff} of the oxidized state, MN(N-CH_3TPP)Cl,$^+$ has not been determined, the Mn(III) non-N-alkylated porphyrins are known to be high spin complexes.[109,111] So, Mn-(N-CH_3TPP)Cl^+ is most probably a high spin system. We can extend these properties, high spin nature and distorted square base pyramid geometry, of Mn(N-CH_3TPP)Cl and Mn^{III}(N-CH_3TPP)Cl^+, to the other two N-substituted manganese porphyrins, in their +2 and +3 oxidation states.

As described in the case of iron, the large change in $Mn^{III/II}$ redox potential caused by different N-substituents (a difference of ~1.1 volt) is also clearly due to the large reduction in σ and d- π metal-ligand bonding interaction.[84]

Copper: I have studied the electrochemistry of Cu^{II}(N-RTPP)$^+$ X^- ((R=CH_3, C_2H_5 and C_6H_5 X=Cl, ClO_4 and CF_3SO_3) for two reasons: a) to determine how each compares with analogous complexes of other metal ions and b) because there is a peak for $Cu^{II/I}$ for N-alkyl complexes which is not found in the copper complexes of non-N-alkylatedporphyrins.[112]

In the electrochemistry of Cu(N-RTPP)$^+X^-$, the solvent has been held constant (acetonitrile) and the axial ligands and the N-substituent have been varied to see their effects on the $Cu^{II/I}$ potential.

In the cyclic voltammograms of Cu(II) non-N-alkylporphyrins, no peaks due to oxidation or reduction of the metal center are observed.[112] Whereas it is possible to reduce

the metal center of $Cu(N\text{-}RTPP)^+X^-$. The Cu(II)-Cu(I) process of $Cu(N\text{-}RTPP)^+X^-$ is reversible (peak separations of ~75mV) with peaks at -Ø.29 V, -Ø.25 V and -Ø.32 V (vs. Ag/AgCl) for R=CH_3, C_2H_5 and C_6H_5 and X= ClO_4 respectively (Table XVII). A large change in Cu(II)/Cu(I) potential occurs on addition of triphenylphosphine (-Ø.29 V for $Cu(N\text{-}CH_3TPP)^+ClO_4^-$ to -Ø.Ø4 V upon addition of PPh_3, Fig. 22). This change reflects the higher stabilization of Cu(I) over Cu(II) by PPh_3. Cu(I), a $d^{1Ø}$ system, is a soft acid compared to Cu(II) and can be stabilized by a soft base like triphenylphosphine. In contrast, chloride ion, a hard base stabilizes Cu(II) over Cu(I) (of all the chloro complexes of copper) by ~1ØØmV more than ClO_4^-, which is a very weak base (Table XVII, Fig.22). (The visible spectra and the cyclic voltammograms are unaffected by the addition of additional chloride).

The peaks for the oxidation and reduction of the ligands of $Cu(N\text{-}RTPP)^+ClO_4^-$ are well defined. The first oxidation potentials of the ligands are 1.29V for $Cu(N\text{-}CH_3TPP)^+ClO_4^-$, 1.31V for $Cu(N\text{-}C_2H_5TPP)^+ClO_4^-$ and 1.24V for $Cu(N\text{-}PhTPP)^+ClO_4^-$ respectively. The corresponding first reduction potentials are -1.15V, -1.14V and -1.Ø1 V (vs. Ag/AgCl) respectively. (Table XVII). The $\Delta E_{1/2}$ (ox-red), $\Delta E_{1/2}$(ox) and $\Delta E_{1/2}$(red) of $Cu(N\text{-}RTPP)^+ClO_4^-$ are 2.25-2.44 V, Ø.21-.24V and Ø.21-Ø.27V respectively. The oxidation potentials of the ligands and, hence, $\Delta E_{1/2}$ (ox-red) of the respective chloro complexes (prepared <u>in situ</u> by using excess tetraethylammonium chloride) can not be determined because

the oxidation of chloride ion (as well as other halides) occurs before that of porphyrin (Table XV) It is easier to reduce the ligands of $Cu(N\text{-}RTPP^{+})ClO_4^{-}$ than that of CuTPP. The reverse is true for the oxidation of the ligands. The ease for reducing the ligands of $Cu(N\text{-}RTPP)^{+}ClO_4^{-}$ suggests that less electron density is supplied to the metal ion (i.e. Cu(II)) from the porphyrin core. A corollary of this higher electron density at the porphyrin core is less covalent interaction between the metal ion and the N-substituted porphyrin.

The fact that it is possible to reduce $Cu^{II}(N\text{-}RTPP)^{+}X^{-}$ but not CuTPP, to a Cu^{I} species, is obviously due to the geometry of $Cu^{II}(N\text{-}RTPP)^{+}X^{-}$complexes. The crystal structures of Cu(II) N-substituted porphyrins are not known. But the great similarity in the structures of $N\text{-}CH_3TPP$ complexes of different metal ions (Mn(II), Fe(II), Co(II) and Zn(II) Table XXI)[83] suggests that Cu(II) has a distorted square base pyramid geometry. Also the same environment around the zinc atom in the structures of $Zn(N\text{-}CH_3TPP)Cl$ and Zn(N-PhTPP)Cl[99] (Ch 5) predicts a similar geometry in Cu(II) complex of N-phenylporphyrin. The Cu(I) complexes formed by reduction of $Cu(N\text{-}RTPP)^{+}X^{-}$will probably have same geometry as in the Zn(II) complexes and would have a longer bond (or weak interaction) between Cu(I) and the substituted nitrogen atom and hence Cu(I) is stabilized by PPh_3. In fact, the reversibility and the shift in $E_{1/2}$ values on addition of Cl^{-} and PPh_3 to $Cu(N\text{-}RTPP)^{+}ClO_4^{-}$ supports the assignment of pentacoordinate geometry for the Cu complexes in its both oxidation

states.

So, the metal-centered reduction of $Cu(N\text{-}RTPP)^{+}X$ is possible due to the geometry of the Cu(II) complexes of N-substituted porphyrins and the lower oxidation state of copper can be stabilized by soft bases.

Future work: The cyclic voltammetry of Cu(II), Mn(II) and Fe(II) complexes of N-substituted porphyrins opens the new horizons to chemistry of N-alkylporphyrins. So far, there has been only one report[97] of the chemistry of these metal complexes at other than +2 oxidation state. The dealkylation of Fe(II) N-methylporphyrin complexes by nucleophiles results in the removal of iron(II).[61] It is not known whether it would be possible to eliminate the alkyl group by the assistance of Fe(III) and that in turn would help us to understand whether the same thing would be possible in the green pigments formed in vivo. The Cu(I) chemistry can also be fascinating. The Cu(I) is greatly stabilized by PPh_3. So, it might be possible to take Cu(I) out by adding a soft ligand like thiols. These are all speculative but nevertheless they are very interesting. Future work only can answer some of these questions.

CHAPTER 5 .

THE MOLECULAR STRUCTURE AND PROPERTIES OF CHLORO-N-PHENYL-5,10,15,20-TETRAPHENYLPORPHINATOZINC(II)

INTRODUCTION

In the earlier chapters, I have described how the kinetics of dealkylations reactions of metallo-N-alkylporphyrins are influenced by alkyl groups bound to the nitrogen atom, the solvent and nucleophiles. In the previous chapter (ch. 4), I have discussed the possible mechanism for the formation of green pigments, especially that of N-phenylporphyrins. I have mentioned the properties and different features of free base, N-alkyl (or N-aryl)porphyrins and their metal complexes. These features are their stability, redox potentials geometry and nmr spectra etc. In this chapter, I shall describe in detail the geometry, determined by x-ray diffraction techniques, and the nmr spectrum of a zinc(II) complex of an N-phenyl-porphyrin. I shall compare this structure with that of N-methyl analog, which has been determined previously.[43] I will also discuss the basicities of free bases N-methyl and N-phenyl-5,10,15,20-tetraphenylporphyrin and the nmr spectra of free base N-substituted porphyrins.

An N-phenylporphyrin has been isolated from Heinz-bodies formed on treatment of erythrocytes of animals with phenylhydrazine.[22,23,25,68,73] It is reasonable to assume that an iron complex of N-phenylporphyrin is formed and the iron atom removed to form the free base N-phenylporphyrin that is observed. The geometry of an iron complex of N-phenylporphyrin had not been previously reported. Although

it has not yet been possible to crystallize the iron complex of an N-phenylporphyrin, the corresponding zinc complex can be obtained very easily. As described in detail later in this chapter, the molecular structure (environment) of Fe(N-PhTPP)Cl can be deduced from that of Zn(N-PHTPP)Cl because of the following similarities: (a) The crystal structures of N-methyl complexes of Fe(II),[83] Zn(II),[43] Co(II),[47b,113] and Mn(II)[47] are very similar (b) The Zn(N-CH_3TPP)Cl and Zn(N-PhTPP)Cl have similar structures [99] and (c) the visible spectra of Zn(N-PhTPP)Cl and Fe(N-PhTPP)Cl closely resmble each other.[99]

EXPERIMENTAL

General: Solvents, CH_2Cl_2 and CH_3CN were purified as mentioned in the previous chapters. Spectro grade DMSO (dimethylsulfoxide, Fisher) and 2,6-lutidine (Aldrich) were used as such without further purification. A Beckman Du-8 spectrophotometer was used for spectrophotometric titrations. The visible absorption spectra were recorded using Cary-14, Varian-635D and Beckman DU-8 spectrophotometers. Buffer solutions at pH 4.0 and 7.0 were used respectively for the titration of N-CH_3HTPP and N-PhHTPP and the pH values were measured with Radiometer Model 84 pH meter. Fisher grade hydrated zinc chloride was used for the preparation of the zinc complex. The crystal data were collected using a Nicolet R3m/E diffractometer(Mo K_α radiation).

Synthesis: The synthesis of different N-alkyl and N-aryl porphyrins have been described in the previous chap-

ters. The Zn(N-PhTPP)Cl was synthesized in the following way: 48 mg. of N-PhHTPP dissolved in 5mL (dry) CH_2Cl_2 were mixed with about 5 fold excess (>50mg) of hydrated zinc chloride dissolved in CH_3CN. I added 14 mL 2,6- lutidine to keep the solution non-acidic. The completion of the complex formation was checked by the visible spectrum. The formation of the complex was quantitative at this point. The solution was filtered and allowed to evaporate to dryness. The residue was dissolved in CH_2Cl_2 and repeatedly filtered with Whattman #42 filter paper. An equal volume of CH_3CN was added each time. On successive filtration, it was possible to eliminate the white precipitate of $ZnCl_2$. After several tries, without 2,6 lutidine I added 1-2 drops of 2,6-lutidine to the solution of Zn(N-PhTPP)Cl in CH_2Cl/CH_3CN and good crystals of Zn(N-PhTPP)Cl were obtained. It was important to take the purple crystals out before they got dried completely (the crystals are very brittle). Also, I rinsed the crystals with few drops of absolute ethanol before I took them out of the centrifuge tube.

Crystal Data: For $ZnCl(C_{50}H_{33}N_4)$: Formula Wt = 790.63, orthorhombic, $P2_12_12_1$; a = 15.078(5)Å, b =15.272(5)Å, c = 17.268(5)Å, Z = 4; ρ_{calcd}=1.32gm cm $^{-3}$, ρ_{obsd} = 1.30 gm cm^{-3}. No absorption correction was performed (the data collection crystal measured 0.37mm x 0.47m x 0.15mm. Mo K_α radiation, λ_1 = 0.70930 Å, μ (Mo K_α) = 7.4cm^{-1}).

Data Collection and Reduction: The crystal structure determination was done by Cynthia K. Schauer and Prof. Oren P. Anderson of Colorado State University. The dark purple

crystals first examined by Weissenberg and Precession Photography revealed only Laue symmetry 222, consistent with the orthorhombic crystal system. The crystals are fairly brittle. A number of attempts were required to get good crystals. The space group of the crystal is $P2_12_12_1$.

The chosen crystal for data collection was mounted on the Nicolet R3m/E diffractometer and intensities of 2928 unique observed ($I>2\sigma(I)$) reflections were determined by θ-2θ scans using Mo K_α radiation. Data collection and all crystallographic computations were performed with the Nicolet computation package.

Refinement of the Structure: In the primitive orthorhombic unit cell idealized rigid phenyl rings and hydrogen atoms are placed in fixed positions. In calculating the scattering factors for zinc, chlorine, nitrogen, carbon and spherically bonded hydrogen, data were taken from ref.115. The anomalous dispersion coefficients $\Delta f'$ and $\Delta f''$ used for all nonhydrogen atoms were also taken from ref.115.

The final structure model involved anisotropic thermal parameters for all non-hydrogen atoms. This model gave $R(=\Sigma||Fo|-|Fc||/\Sigma|Fo|)$ value 0.055, while the final $Rw(=[\Sigma w(|Fo|-|F_c|)^2/\Sigma w(Fo^2)]^{1/2}$ and GOF (good of fit) values were 0.057 and 1.20 respectively (the initial values of R and Rw were 0.051 and 0.070). The least-squares refinement program in the Nicolet R3m/E structure determination computing package minimizes $\Sigma w/Fo-(F_c)^2$, where Fo and F_c are the observed and calculated structure factor amplitudes, respec-

tively and w is the weight (= $4Fo^2/\sigma^2$ (Fo^2). The final atomic positional parameters for all nonhydrogen atoms of Zn(N-PhTPP)Cl are given in Table XXIII.

NMR Spectra: The nmr spectra of the free bases and the zinc complexes were recorded in CD_2Cl_2 or $CDCl_3$, using Varian 200 MHz or 300MHz spectrometers. The low temperature studies with Zn(N-PhTPP)Cl were done in 300MHz nmr spectrometer with a probe for the adjustment of temperature by the flow of N_2 and evaporation of liquid N_2. The sample was equilibrated to the desired temperature for five to ten minutes. At very low temperature i.e., below -56°C, broadening occurs due to the change in the viscosity of the solvent (The f.pt of CD_2Cl_2 is - 98° C).

Spectrophotometric Titrations of N-CH_3HTPP and N-PhHTPP: The N-methyl-5,10,15,20-tetraphenylporphyrin (N-CH_3HTPP) and N-phenyl-5,10,15,20-tetraphenylporphyrin(N-PhHTPP) were not soluble in water. So the titrations were done in a mixture of dimethyl sulfoxide (DMSO) and water (buffer solutions) The titrations were done as follows: N-CH_3HTPP was dissolved in DMSO (1mL) and then mixed with 1mL of $5.5x10^{-3}$M tetrabutylammonium perchlorate (TBAP) in DMSO followed by addition of 0.4 mL of pH = 4.00 buffer (potassium biphthate buffers, 0.05M, Fisher grade). The solution was then titrated with a dilute solution of perchloric acid (doubly distilled) in water. The acid was added with the help of a microtitrator and pH of the solution was measured

Table XXIII. Atom coordinates ($x10^4$) and temperature factors ($\AA^2 x10^3$).

atom	x	y	z	U
Zn	4805(1)	6017(1)	1365(1)	39(1)*
Cl	5035(1)	5580(1)	2579(1)	62(1)*
N(1)	4715(4)	5107(3)	519(3)	48(2)*
N(2)	3443(3)	6276(3)	1215(3)	38(2)*
C(1)	5407(4)	4723(4)	160(4)	51(2)*
C(2)	5098(5)	3927(5)	-235(5)	63(3)*
C(3)	4223(5)	3895(4)	-133(5)	68(3)*
C(4)	3966(4)	4646(4)	335(4)	48(2)*
C(5)	3111(4)	4904(4)	482(4)	46(2)*
C(6)	2876(4)	5716(4)	836(4)	43(2)*
C(7)	1985(4)	6047(4)	859(4)	53(2)*
C(8)	2016(4)	6796(4)	1269(4)	53(2)*
C(9)	2914(4)	6935(4)	1513(4)	45(2)*
C(10)	3193(4)	7570(4)	2037(4)	42(2)*
C(11)	4078(4)	7776(4)	2181(4)	39(2)*
C(12)	4470(5)	8104(4)	2853(4)	50(2)*
C(13)	5363(4)	8134(4)	2751(4)	45(2)*
C(14)	5582(4)	7829(4)	2014(4)	42(2)*
C(15)	6425(4)	7721(4)	1668(4)	41(2)*
N(3)	4781(4)	7619(3)	1635(3)	40(2)*
N(4)	6047(3)	6375(3)	933(3)	39(2)*
C(16)	6591(4)	7092(4)	1096(4)	44(2)*
C(17)	7360(5)	7068(5)	620(5)	59(3)*
C(18)	7344(5)	6318(5)	216(5)	59(3)*
C(19)	6525(4)	5883(4)	412(4)	44(2)*
C(20)	6259(4)	5050(5)	108(4)	50(2)*
C(31)	7452(5)	3937(4)	76(3)	110(5)*
C(32)	8093(5)	3447(4)	-314(3)	152(7)*
C(33)	8206(5)	3550(4)	-1110(3)	107(5)*
C(34)	7678(5)	4144(4)	-1517(3)	145(7)*
C(35)	7038(5)	4633(4)	-1127(3)	117(5)*
C(30)	6925(5)	4530(4)	-330(3)	60(3)*
C(51)	2521(3)	8922(3)	2620(3)	69(3)*
C(52)	1851(3)	9341(3)	3036(3)	96(4)*
C(53)	1166(3)	8851(3)	3365(3)	88(4)*
C(54)	1152(3)	7943(3)	3278(3)	77(3)*
C(55)	1823(3)	7525(3)	2862(3)	64(3)*
C(50)	2507(3)	8014(3)	2533(3)	50(2)*
C(61)	8008(3)	7921(3)	2080(3)	65(3)*
C(62)	8702(3)	8465(3)	2312(3)	93(4)*
C(63)	8548(3)	9354(3)	2439(3)	94(4)*

Table XXIII. --- continued

C(64)	7700(3)	9699(3)	2335(3)	84(4)*
C(65)	7006(3)	9155(3)	2103(3)	57(2)*
C(60)	7160(3)	8266(3)	1976(3)	52(2)*
C(71)	4678(4)	8058(4)	869(4)	37(2)*
C(72)	4665(4)	7616(4)	192(4)	47(2)*
C(73)	4633(5)	8071(5)	-521(4)	57(2)*
C(74)	4633(5)	8967(5)	-521(5)	65(3)*
C(75)	4658(5)	9420(5)	192(5)	69(3)*
C(76)	4677(4)	8980(4)	871(4)	51(2)*
C(45)	2011(4)	3729(4)	737(3)	107(5)*
C(44)	1320(4)	3183(4)	501(3)	149(7)*
C(43)	995(4)	3236(4)	-253(3)	100(5)*
C(42)	1361(4)	3835(4)	-773(3)	122(5)*
C(41)	2052(4)	4382(4)	-537(3)	116(5)*
C(40)	2377(4)	4328(4)	218(3)	48(2)*

* Equivalent isotropic U defined as one third of the trace of the orthogonalised U_{ij} tensor

at different intervals with the pH meter standardized against pH = 4.Ø aqueous buffer. The addition of small amount of tetrabutylammonium perchlorate (TBAP) increases the ionic strength of the solvent. This consequently affects the hydrogen ion activity, however this effect is normally small in comparison to the potential error without the salt.[118] The pH values measured in this way are not quantitative.[118] The pH shown on the meter can also be obtained by using the following equation:

$$pH_x = pH_s - (E_x - E_s)/S$$

Where pH_x is the pH of the sample (x), pH_s is the pH of the standard (s). E_x (in millivolt) value of the sample displayed by the pH meter. E_s the corresponding values of the standard (throughout this study it has been kept at 4.ØØ).

S the slope, normally 59mv/pH unit at 25°C.

I think the value of pH_x obtained by using the above equation is probably more precise than obtained directly from the pH meter.

Results: The structures of Zn(N-CH_3TPP)Cl and Zn(N-PhTPP)Cl determined by x-ray diffraction, are shown in Figures 26-29. The data on nmr spectra of different N-alkyl and N-aryl porphyrins and the zinc complexes of two N-substituted porphyrins are presented in Table XXIV. Fig. 3Ø shows the great resemblance in the visible spectra of Zn(N-PhTPP)Cl and Fe(N-PhTPP)Cl. The nmr spectra of a free base N-alkyl porphyrin, Zn(N-CH_3TPP)Cl and Zn(N-PhTPP)Cl are

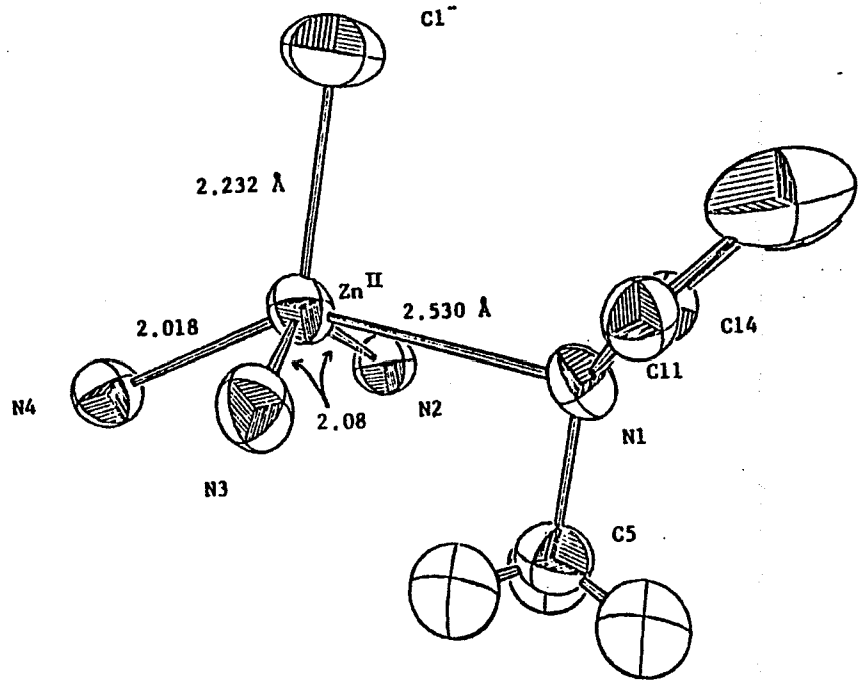

Figure 26a. The coordination sphere of Zn(N-CH_3TPP)Cl. Note the rehybridization of the nitrogen with the methyl bound pyrrole ring.

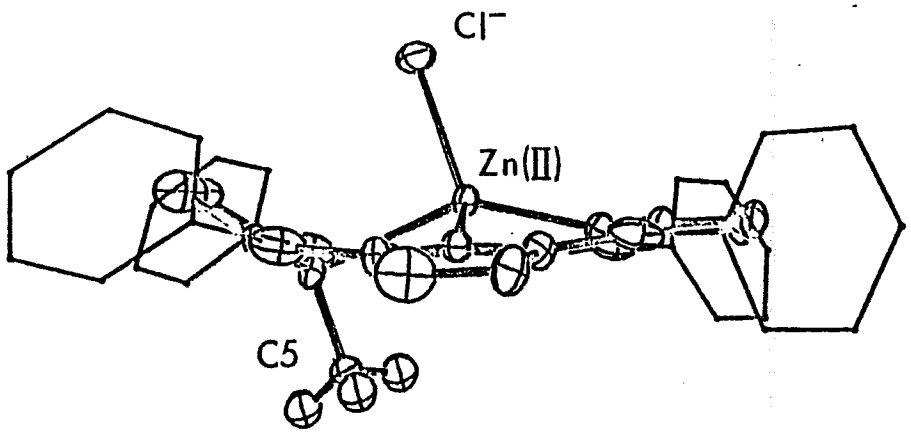

Figure 26b. A side-on view of Zn(N-CH_3TPP)Cl.

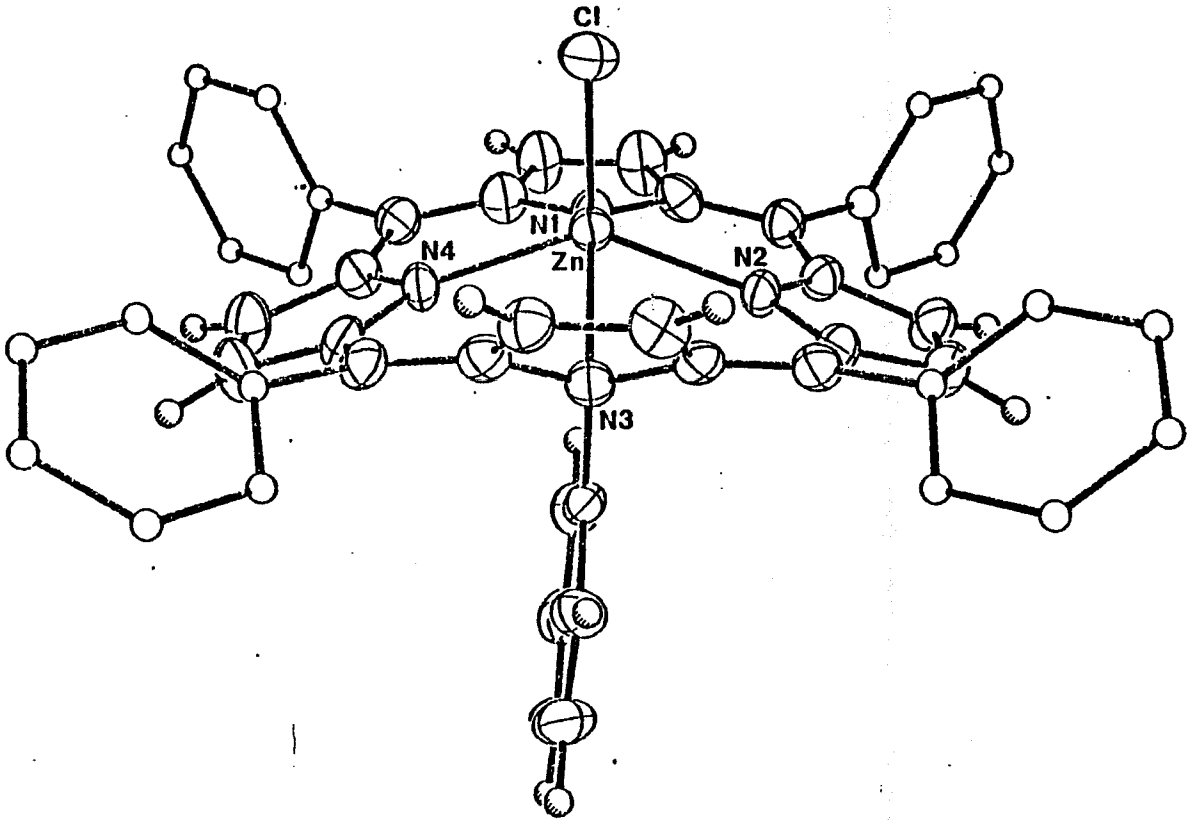

Figure 27. A view of the Zn(N-PhTPP)Cl complex which shows that the structure is almost bilaterally symmetric.

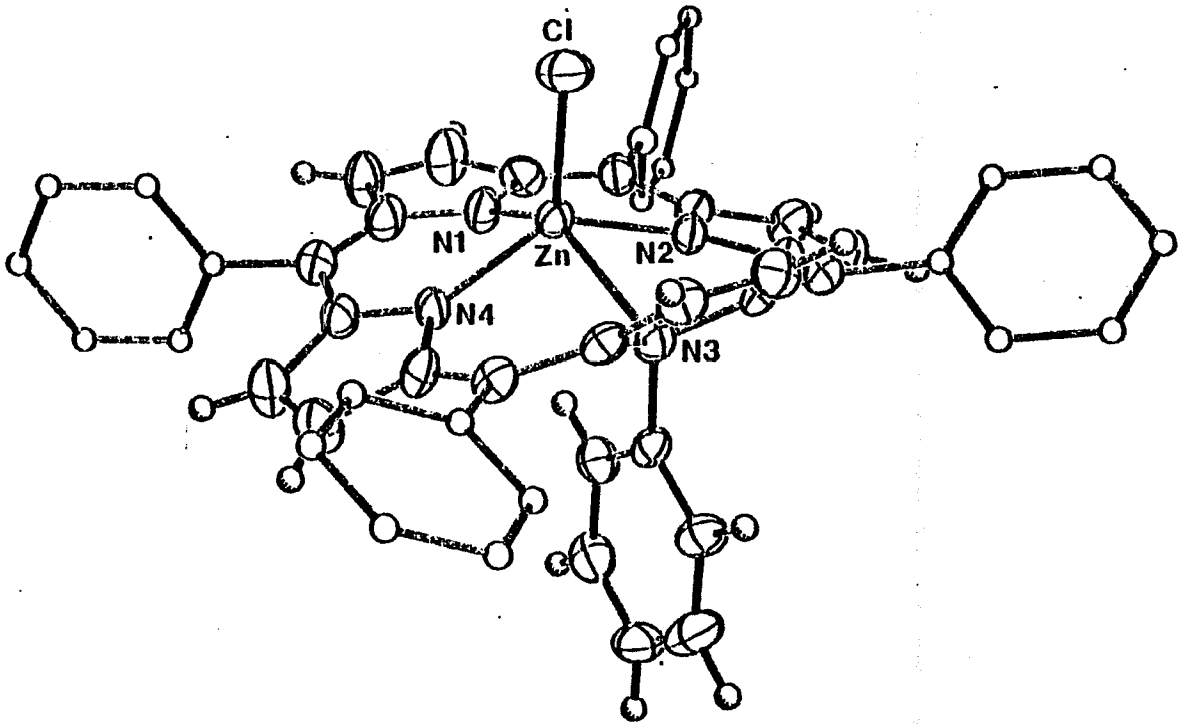

Figure 28. A view of the Zn(N-PhTPP)Cl complex. Hydrogen atoms on the phenyl rings have been omitted for clarity and the thermal ellipsoids have been drawn at the 50% probability level. This view shows the orientation of the N-phenyl ortho-hydrogen atoms.

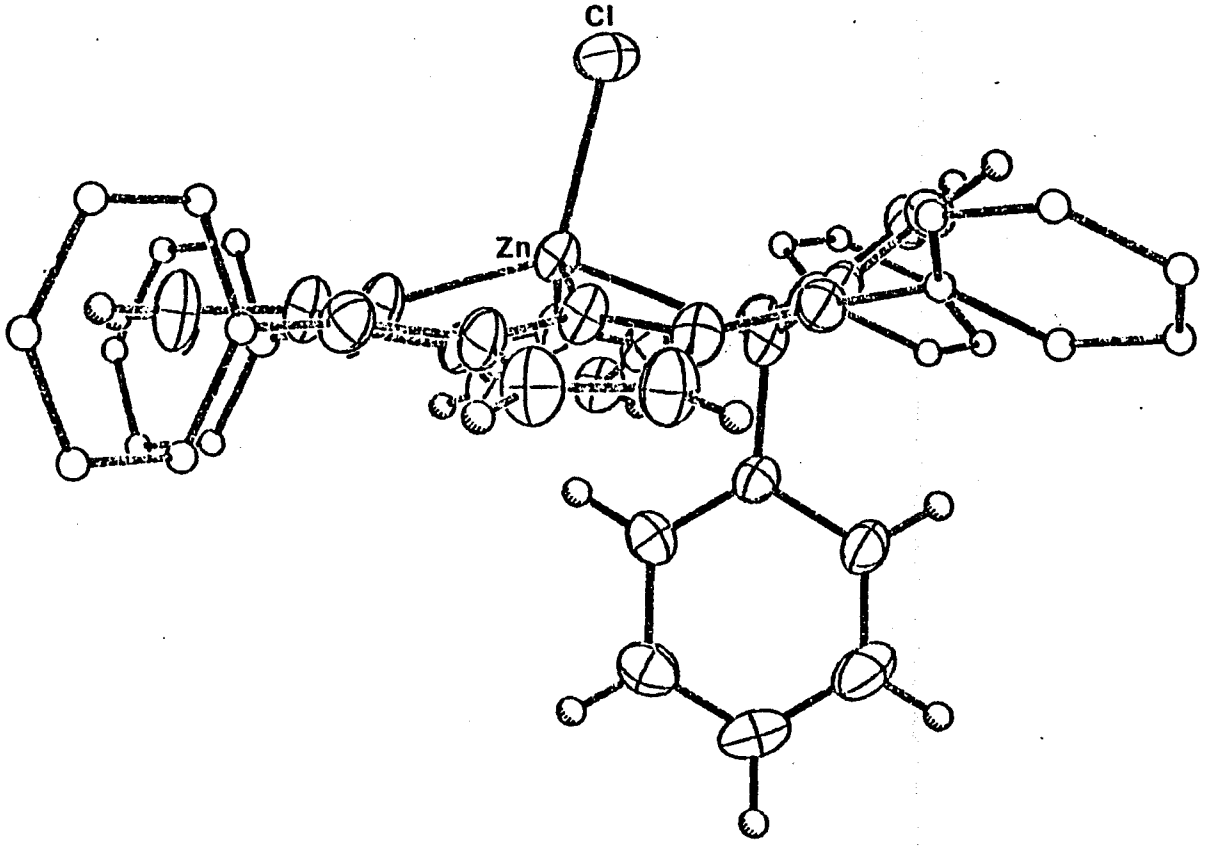

Figure 29. Another view of the Zn(N-PhTPP)Cl complex. This view shows the non-equivalency of the two ortho hydrogen atoms of the phenyl group bound to the nitrogen atom(in the solid state).

Table XXIV. Proton NMR Chemical Shifts of some N-Alkyl and N-Phenyl-5,10,15,20-tetraphenylporphyrins and Complexes in the β-Pyrrole Region[a].

Species	δ (ppm from TMS)[b]				Species	δ (ppm from TMS)[b]			
	s(2H)	d(2H)	d(2H)	s(2H)		s(2H)	d(2H)	d(2H)	s(2H)
$N\text{-}CH_3TPP$[c]	8.86	8.60	8.52	7.48	$Zn(N\text{-}CH_3TPP)Cl$[d]	8.80	8.97	8.90	8.36
($N\text{-}CH_3$, -4.16)					($N\text{-}CH_3$, -3.98)				
$N\text{-}C_2H_5HTPP$	8.81	8.70	8.49	7.50					
$N\text{-}CH_2CO_2C_2H_5HTPP$	8.78	8.66	8.46	7.64					
$N\text{-}p\text{-}CH_2C_6H_4NO_2HTPP$	8.87	8.61	8.51	7.59					
N-PhHTPP	8.70	8.33	8.16	7.35	Zn(N-PhTPP)Cl[d]	8.92	8.74	8.66	8.48
($N\text{-}C_6H_5$ o,2.99; m,5.20; p,5.67)					($N\text{-}C_6H_5$ o,2.36; m,5.22; p,5.76)				

a. In $CDCl_3$, using Varian 200 MHZ instrument unless cited

b. For assignments, see text.

c. Reference 28.

d. In CD_2Cl_2.

Figure 30. The Visible Absorption Spectra of Zn(N-PhTPP)Cl (in CH_2Cl_2) and Fe(N-PhTPP)Cl (in THF). Notice the great similarity in the two spectra.

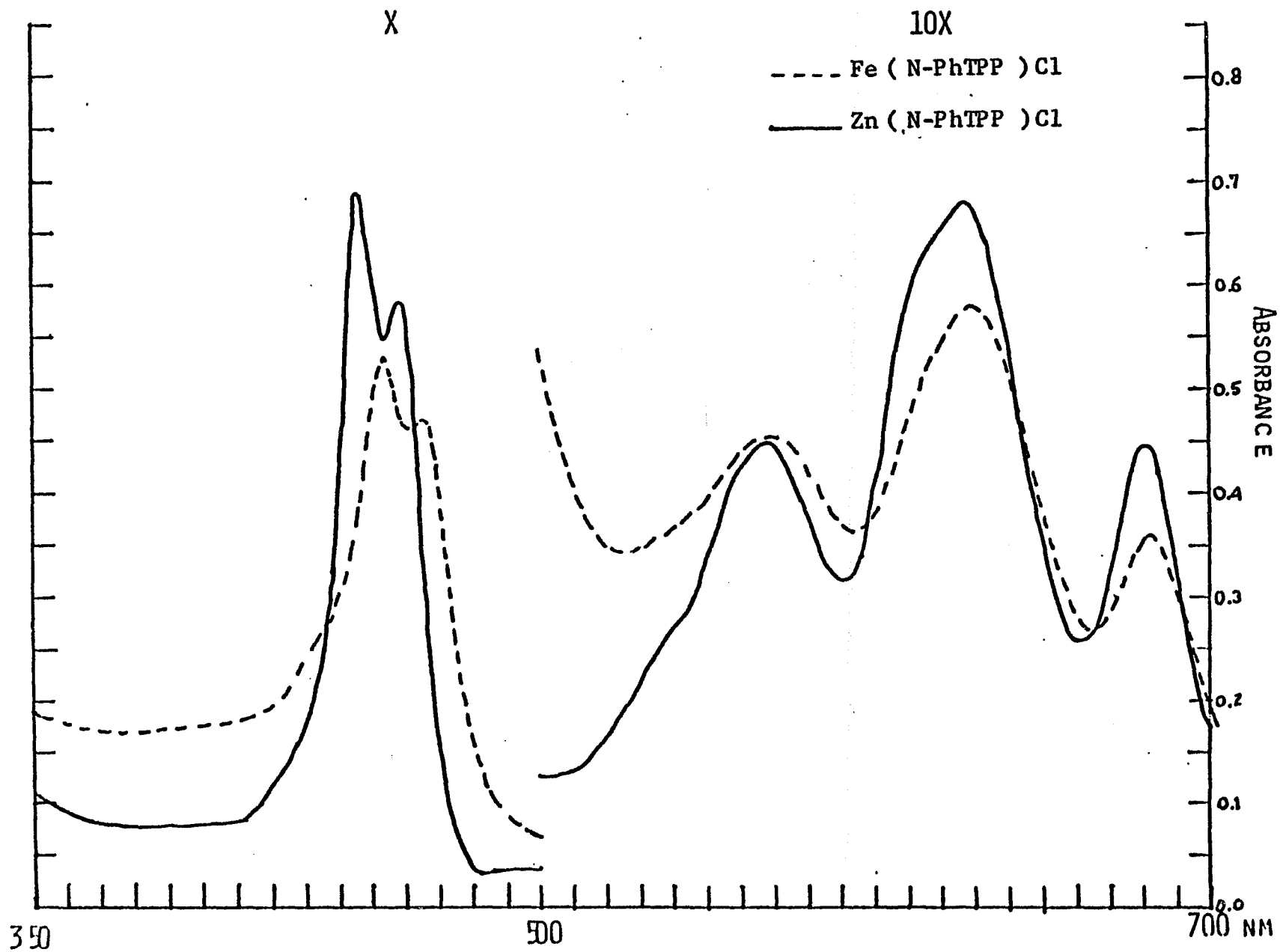
X
10X
Fe (N-PhTPP) Cl
Zn (N-PhTPP) Cl
0.8
0.7
0.6
0.5
0.4
0.3
0.2
0.1
0.0
ABSORBANCE
350
500
700 NM

shown in Fig. 31-33 and the data containing the visible spectra of different free base N-alkyl or N-arylporphyrins and their metal complexes are presented in Table XXV.

Discussion: The previous reports on the molecular structures of N-methyl-5,10,15,20-tetraphenylporphyrin complexes of Mn(II),[47a] Fe(II),[83] Co(II)[47b,113] and Zn(II)[43] show striking similarities to one another. The differences between their structures can be predicted from bond lengths known from other metalloporphyrin structures[119] and the ionic radius of the particular metal ion.[83] The visible absorption spectra of these metallo-N-alkylporphyrin complexes are very similar in comparison to those complexes of non-N-alkylated porphyrins.[58] This high similarity in the spectra of N-alkylporphyrin complexes can be attributed to the insensitivity of the $\pi \longrightarrow \pi^*$ electronic energy level difference on filling the metal 'd' orbitals.[58] (The visible absorption spectra of metalloporphyrins are generally described by $\pi \longrightarrow \pi^*$ transitions as shown below[120]).

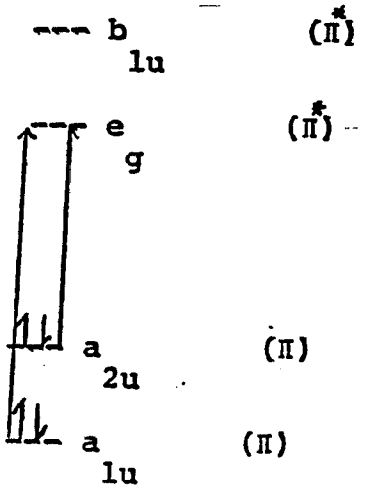

Similarly, the visible absorption spectra of the complexes

Figure 31. The 200 MHZ ^{1}H NMR spectrum of a solution of N-p-nitrobenzyl-5,10,15,20-tetraphenylporphyrin (N-p-$CH_2C_6H_4NO_2$HTPP) in $CDCl_3$ (100%, from δ = -6 to +9 ppm. The line with a mark, x, corresponds to the $CHCl_3$ peak at 7.25 ppm.).

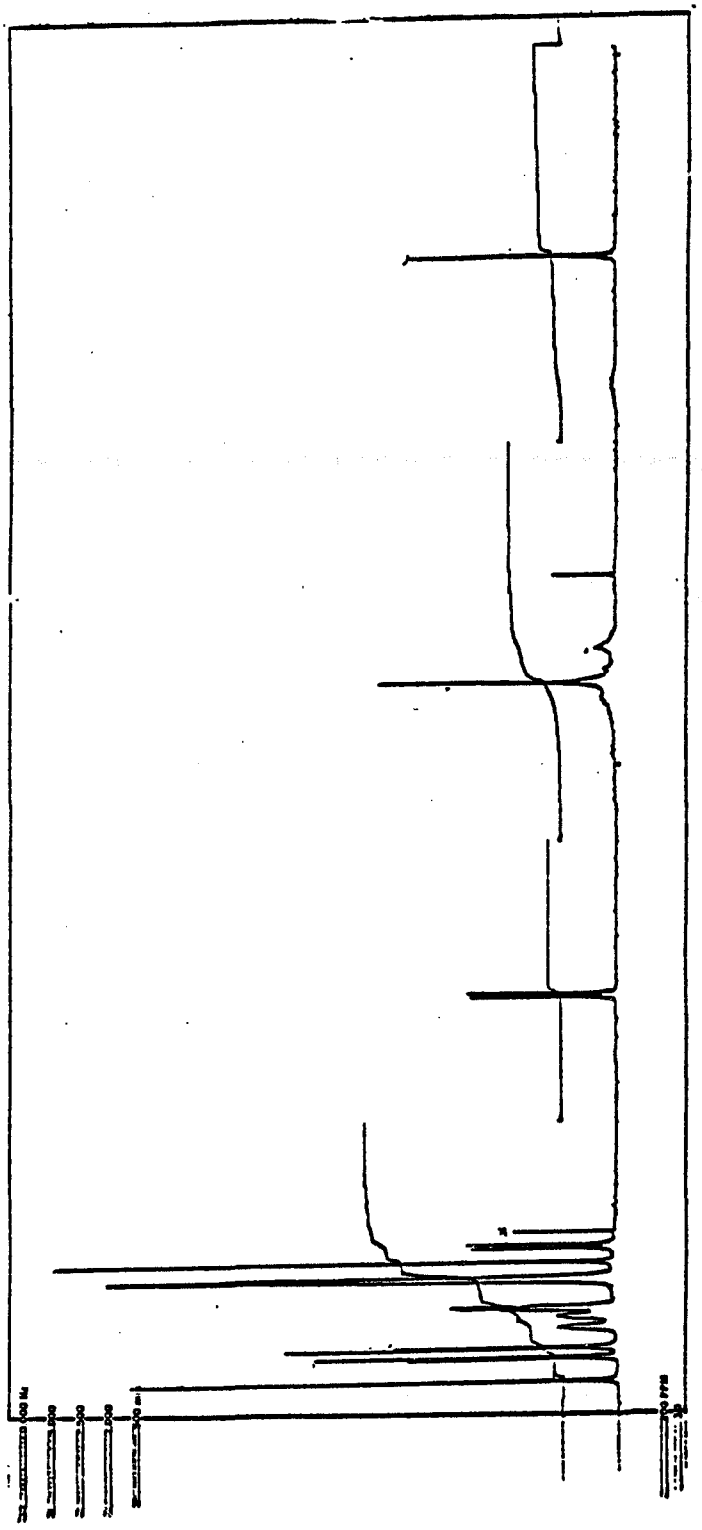

Figure 32. The 200 MHZ ^{1}H NMR spectrum of a solution of (chloro-N-methyl-5,10,15,20-tetraphenylporphinato)-zinc(II) (Zn(N-CH_3TPP)Cl) in CD_2Cl_2 (at ambient temperature).

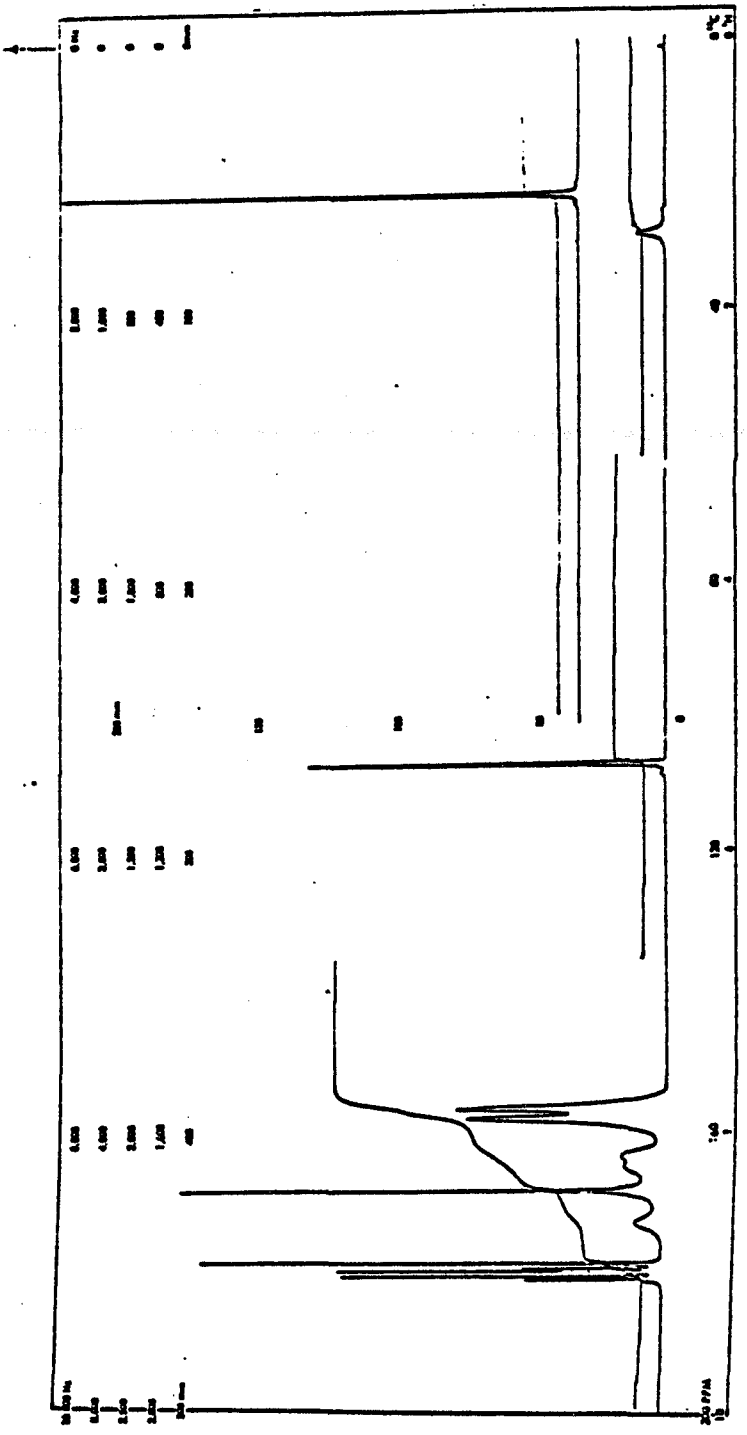

Figure 33. The 300 MHZ ^{1}H NMR spectrum of a solution of (chloro-N-phenyl-5,10,15,20-tetraphenylporphinato)-zinc(II) (Zn(N-PhTPP)Cl) in CD_2Cl_2 at 25°C. The ortho protons of the N-phenyl group (Figure 29) are equivalent up to -56°C. The noticeable feature occurs for the meso-phenyl protons at low temperature (not shown in this Figure).

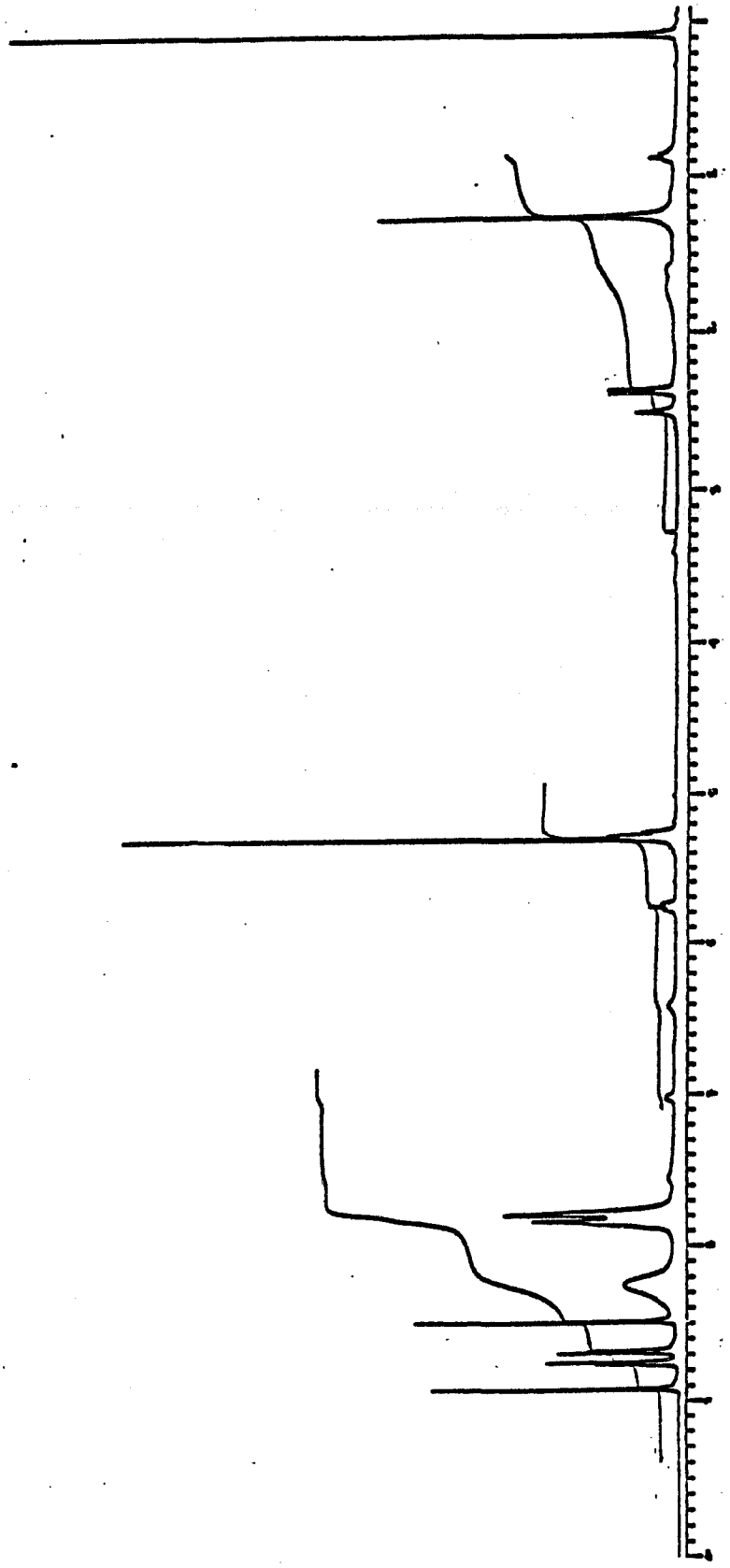

Table XXV. Visible Absorption Spectra of some N-Alkyl and N-Phenylporphyrins and their Complexes[a].

Species	Absorption Maxima (in nanometers)	Species	Absorption Maxima (in nanometers)
N-PhTPP	442,550,596,635,703	Zn(N-PhTPP)Cl	447,459,567,628,680
N-CH_3HTPP[b]	432,534,575,613,676	Zn(N-CH_3TPP)Cl	439,448,561,611,658
N-CH_2CH_3HTPP[b]	432,531,573,613,675	Zn(N-PhPP)Cl[c]	442,550,606,648
N-$CH_2CO_2C_2H_5$HTPP[b]	432,531,572,615,676	Zn(N-CH_3PP)Cl[c]	429,546,591,633
N-p-$CH_2C_6H_4NO_2$HTPP[b]	432,529,570,613,675	Fe(N-PhTPP)Cl[d]	454,465,570,630,681
N-PhHPP[c]	430,518,550,613,670	Fe(N-CH_3TPP)Cl[d]	447,459,564,610,662
N-CH_3HPP[c]	417,510,546,594,650	Fe(N-C_2H_5TPP)Cl[d]	446,457,563,612,662

a. At ambient temperature in CH_2Cl_2 except as noted. See text for abbreviations.
b. These free bases also show a prominent shoulder at 497 nm.
c. These species consist of isomers with similar but not identical spectra, see ref.11c.
d. In tetrahydrofuran.

of the naturally occurring N-alkylporphyrins, N-methyldeuteroporphyrin IX dimethyl ester(N-CH_3HDP)[54a] and N-methylprotoporphyrin IX dimethylester are similar compared to their non-N-alkylated analogs.

The chloro-N-ethoxycarbonylmethyloctaethylporphynatocobalt (II)[98] has the same coordination geometry and topology of the porphyrin ring as those of Co(N-CH_3TPP)Cl. The visible absorption spectra of Cu(II) N-alkyl-5,10,15,20-tetraphenylporphyrin (alkyl = CH_3, $-C_2H_5$, p-$CH_2C_6H_4NO_2$) complexes with $CF_3SO_3^-$ as counter ion are very similar (ch-2 and 3). The visible absorption spectra of Chloro-N-alkyl-5,10,15,20-tetraphenylporphinatocopper(II) also resemble each other (ch-4). It is then reasonable to deduce from these features that the porphyrin ring topologies for meso and non-meso substituted N- alkylporphyrin complexes are very similar.[99]

The visible absorption (Table XXV) and nmr spectra (β-pyrrolic hydrogen atoms, Table XXIV) of N-phenylporphyrins as well as their complexes are different from those of the N-alkylporphyrins. There is a red shift of 10-25nm in the visible absorption spectra of N-PhHTPP and their metal complexes in comparison to those with N-alkyl analogs (Table.XXV). Another important property of N-phenyl-5,10,15,20-tetraphenylporphyrin is its somewhat greater basicity than the corresponding N-methyl analog. [The protonation of N-PhHTPP and N-CH_3HTPP can be represented by the following equations:

$$\text{N-RH}_2\text{TPP}^+ \rightleftharpoons \text{N-RHTPP} + \text{H}^+ \qquad (1) \quad K_3$$

$$N\text{-}RH_3TPP^+ \rightleftharpoons N\text{-}RH_2TPP^+ + H^+ \qquad (2) \quad K_4$$

(R = CH_3 and Ph)

]

The pK_3 and pK_4 for N-phHTPP are 9.7 and 3.5 respectively, while the corresponding values for N-CH_3HTPP are 7.7 and 2.6. The values obtained by this method are not quantitative.[118] Nevertheless, these qualitative values are good enough to ascertain the slightly greater basicity of N-PhHTPP. (In 20% buffer solution of pH 7.0/H_2O (V/V), the N-PhHTPP gives a spectrum of its monocation. The N-CH_3HTPP does not seem to be protonated under similar conditions).

A basis for the observed differences can be predicted from the structural parameters of chloro-N-phenyl-5,10,15,20-tetraphenylporphinatozinc(II). From Figures 28 and 29, it can be seen that one ortho hydrogen of the phenyl group is very close (2.52Å) to the zinc atom and comparable to zinc-chloride distance of 2.224(2) Å. The other hydrogen atom is below the substituted pyrrole ring. In addition to the position of the phenyl group, another important thing to notice is the cant of the substituted pyrrole ring relative to the plane of three non-alkylated pyrrole rings. In Zn(N-PhTPP)Cl this angle is 42.0°, while in the N-CH_3TPP complexes the angle is 29.2° (Mn(II),[47a] 28.9°(Fe(II),[83] 31.6°-(Co(II))[47b,113] and 38.5°(Zn(II)).[43] The order of increase in this angle in the case of N-methyl complexes is consistent with the increase in length of the M-N(CH_3) bond.[83] In free base N-CH_3HTPPBR$_4$[8] and protonated-21-(ethoxycarbonylmethyl) octaethylporphyrin hydrogen iodide[121] the alkylated

pyrrole rings are tilted in the same direction as in the metal complexes of N-CH_3TPP and they are 27.7° and 19.1° respectively. The molecular structure of Zn(N-PhTPP)Cl is similar to that of Zn(N-CH_3TPP)Cl; the distance of the zinc atom from the plane of the three nitrogen atoms not bearing the alkyl group (0.65 and 0.67 Å respectively), the deviation of the zinc atom from the plane of the substituted pyrrole ring (2.04 vs. 2.12Å) and the zinc-nitrogen bond distances (Zn-N-R 2.530 vs. 2.499 Å, Zn-N-(adjacent rings), 2.089 vs. 2.086Å and 2.081 vs. 2.1021Å and Zn-N-(opposite ring), 2.018 vs. 2.015Å) (the first values in the parenthesis are for Zn(N-CH_3TPP)Cl).

The nmr spectroscopy also gives a wealth of information consistent with the geometry of N-alkyl(N-aryl)porphyrins and their complexes.[122,123] The nmr spectra of the N-substituted porphyrins and their complexes are different from their non-N-substituted analogs. The nmr spectra of the former are interpreted in terms of the geometry[8] imposed on the macrocycle by the alkyl group bound to the nitrogen atom (Fig. 2.).[123] The changes in chemical shifts are attributable to three different effects (steric distortions): a) decrease in the ring current, b) change of local shielding patterns due to conformational changes, c) an increased 'sp^3' hybridization at the nitrogen atom bearing the alkyl group.[124] For example, in contrast to a single peak (β-pyrrole protons in H_2TPP at 8.75 ppm) at 30°C (at -80°C two signals are observed at 8.90 and 8.60 ppm; the peak at 8.90 ppm has been assigned to opposite rings containing

hydrogen bound to nitrogen atoms.), there are four distinct regions for the β-pyrrole protons of N-RHTPP and their zinc complexes (Table XXIV. Notice that ring current is decreased only to a small extent on changing the geometry from H_2TPP[125] to N-RHTPP[8]).

The alkyl(-3.2 to -5.0 upfield to TMS) or phenyl group (Table XXIV) attached to the nitrogen atom in free base N-alkyl(aryl)porphyrins and their zinc complexes is highly shielded (by the aromatic ring current) due to the presence of the alkyl(aryl) groups in the center of the macrocycle (not in the plane of the macrocycle). The proton on the opposite pyrrole ring also appears in the upfield to TMS but is not observed in most cases. The N-alkylated (arylated) β-pyrrole hydrogen of the free bases N-CH_3HTPP and N-PhHTPP appear at a high field region (7.48 and 7.35 ppm respectively with respect to TMS) compared to the other three. The plane of the alkylated or arylated ring deviates more than the other pyrrole rings. (In N-CH_3HTPP Br_4[8] the N-methylated ring is tilted the greatest by 27.7°). This deviation accounts for the β-protons of the alkylated(arylated) ring to be away from the plane of the ring current and hence they are least deshielded. On complexation of Zinc(II), the spectra in theβ-pyrrolic hydrogen region becomes quite different (Table XXIV) but the differences between the complexes are comparable to the differences between the free bases,[99] which suggests a similar effect is exerted by the phenyl group relative to the methyl group in both cases.

The large change in the β-hydrogen signal of the alkylated or arylated pyrrole ring of the zinc complexes cannot be rationalized by an increase in ring current in the rigid zinc complexes as suggested by Jackson.[123b] The crystal structures of Zn(N-CH_3TPP)Cl[43] and N-CH_3HTPPBr_4)[8] show that the cant of the methylated or arylated pyrrole ring in the former (38.5°) is larger than the latter (27.7°). So, an increase in ring current should place the β-pyrrole hydrogens of the alkylated ring at least in the same region if not upfield to the previous values. What one sees is the deshielding of the β-pyrrole protons (7.48 to 8.36 on complexing with Zn(II) in the case of methyl and 7.35 to 8.48 in the case of phenyl, Table XXIV)

The deshielding of the β-pyrrole protons in the zinc complexes can probably be best explained in the following way. The zinc atom is close to the plane of the substituted pyrrole ring of zinc complexes (2.Ø4 and 2.14Å) and a large through-space effect is possible to deshield the β-hydrogens of alkylated pyrrole ring by >/Ø.9 ppm. Doublets due to the adjacent pyrrole rings (one assigned to protons 7 and 18, the other to 8 and 17) are also shifted on complexation with zinc(II) (Table XXIV). The singlet assigned to the opposite rings to the one alkylated or arylated, are much less shifted, possibly due to the change of orientation of the ring upon complexation,[8] which can lead to a cancellation of effects. In Zn(N-CH_3TPP)Cl, the methyl group is also deshielded by Ø.18 ppm. Though small, it is probably due to greater cant of methylated pyrrole ring, which sets in less

shielding of the methyl group. On the contrary, in Zn(N-PhTPP)Cl, the ortho protons are shielded more (Ø.63) presumably due to their presence in the field of increased ring current (or zinc affects the aromatic hydrogens only).

Another interesting aspect of solid state geometry of Zn(N-PhTPP)Cl (Figures 28 and 29) is the non-equivalence of two ortho hydrogens; one hydrogen is very close to Zn and the other one is below the pyrrole ring. The nmr spectra of this complex recorded from 3Ø°C to -56°C in CD_2Cl_2, (2.36 ppm (d,2H 5.22(d,2H) and 5.76(t,1H)) shows that the two ortho hydrogens are equivalent. Fig. 28 shows that a free rotation is possible for the phenyl group bond to the nitrogen atom to account this equivalency of two ortho hydrogens.

Here I have not mentioned the geometry of Fe(N-PhTPP)Cl, which is more closely related to the actual system in vivo. However the visible absorption spectra of Fe(N-PhTPP)Cl and Zn(N-PhTPP)Cl are similar. The crystal structure of Zn(N-PhTPP)Cl[99] is very similar to that of previously reported Zn(N-CH_3TPP)Cl.[43] The crystal structures of N-CH_3TPP complexes of Mn(II),[47a] Zn(II),[43] Co(II)[47b,113] and Fe(II)[83] are similar. So, it is probably safe to say that Fe(N-PhTPP)Cl has a similar environment that found in Zn(N-PhTPP)Cl.[99]

Conclusion: The structure of the N-phenylporphyrin complex, Zn(N-PhTPP)Cl, shows a strong bond (1.491Å) between the nitrogen and the carbon atom of the phenyl group, consistent with the high stability of Cu(N-PhTPP)$^+CF_3SO_3^-$ with

respect to nucleophiles (Chapter 3). The great similarity in the structures of Zn(N-CH_3TPP)Cl[99] and Zn(N-PhTPP)Cl suggest that the metal-nitrogen bond lengths and the cant of the pyrrole rings are governed by the metal ion rather than the alkyl or aryl group bound to the nitrogen atom and the structure of Fe(N-PhTPP)Cl can be predicted from the knowledge of the geometry of Fe(N-CH_3TPP)Cl.[83] The crystal structure of Zn(N-PhTPP)Cl shows the possibility of free rotation of the N-phenyl group as supported by nmr spectra recorded up to -56°C. The bathochromic shift (by 10-20 nm) in the visible spectra of N-phenylporphyrins and their complexes are probably due to electronic instead of the structural differences.[99]

CHAPTER 6

a) XPS OF N-SUBSTITUTED PORPHYRINS AND THEIR Mn(II) COMPLEXES

b) EPR OF Cu(II) N-SUBSTITUTED PORPHYRINS: COMPARISON WITH NON-N-SUBSTITUTED PORPHYRINS

INTRODUCTION

A variety of spectroscopic techniques such as uv-visible spectroscopy (UV-VIS), nuclear magnetic resonance spectroscopy (NMR), infrared spectroscopy (IR), x-ray photoelectron spectroscopy (XPS), electron paramagnetic resonance spectroscopy (EPR), extended x-ray absorption fine structure spectroscopy (EXAFS), penning ionization electron spectroscopy (PIES) etc., are used in the fields of chemistry and physics. In this chapter, I shall describe how two of these techniques, electron paramagnetic resonance spectroscopy (EPR) and x-ray photoelectron spectroscopy (XPS), can provide information about N-substituted porphyrins and their complexes.

X-ray photoelectron spectroscopy (XPS, also called electron spectroscopy for chemical analysis, ESCA) is the study of the core binding energies or the energy distribution of the electrons emitted from x-ray irradiated compounds. In this chapter, the way that XPS can be used to differentiate between two non-equivalent nitrogen atoms of N-substituted porphyrins and their metal complexes will be described. Before proceeding with applications to the N-substituted porphyrins, a brief summary of the fundamentals of XPS will be presented.

Fundamentals of Electron Spectroscopy. In gaining information on atomic and molecular structure, x-rays can be

used in different ways as depicted in scheme-6. The lower branch of scheme-6 is the concern of XPS (For review

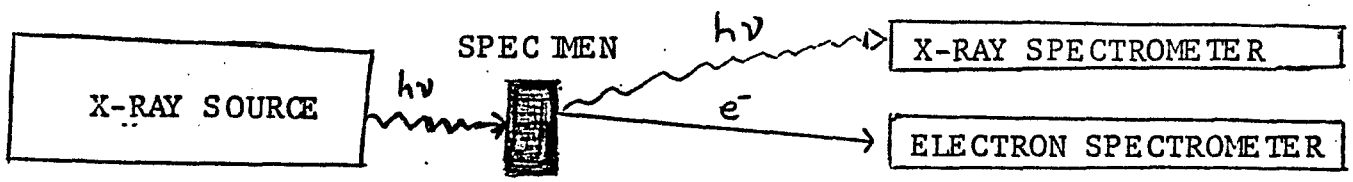

articles on XPS, see ref. 126). A typical arrangement for XPS measurements is shown in Figure 34. The sample under high vacuum (10^{-8} - 10^{-9} torr) is irradiated with X-rays (generally Mg K_α, 1253.6 ev). The kinetic energy of the ejected electron is measured with high resolution and precision. In a photoelectron spectrum, the number of detected electrons vs. their kinetic energy are plotted. The kinetic energy of the photoelectron is governed by the energy of the incident photons and the energy with which the electron is bound to its nucleus. The core electrons are generally monitored in XPS experiments. Though the inner shell electrons are not directly involved in the formation of a chemical bond, their energies are slightly shifted as the chemical or crystallographic environments of the atom are changed. The binding energy of the electrons is calculated from the energy of the incident x-ray radiation and the kinetic energy of the escaped electrons (without significant energy loss) using Einstein's photoelectric equation:

$$E_{BE} = E_{X\text{-ray}} - E_{KE}$$

Thus the changes in chemical bonding around an atom in a

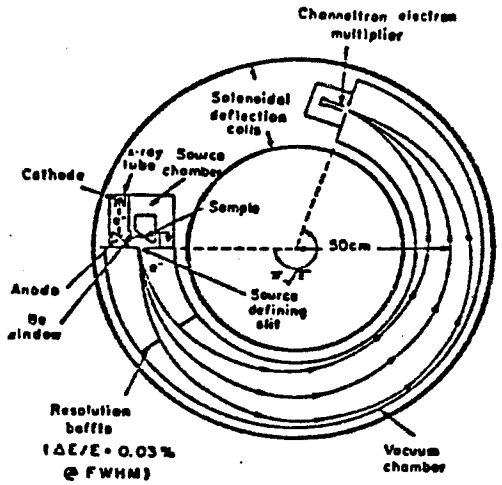

Figure 34. The components of a X-ray Photoelectron Spectrometer (Taken from Hollander, J. M. and Jolly, W.L., Acc. Chem. Res. 1970, 3, 193-200).

molecule (i.e. the change in binding energy) can be readily measured (with in 1-10 eV) although they are small relative to the total kinetic energy.

In contrast to XPS, very low energy electromagnetic radiation is used in electron paramagnetic resonance spectroscopy (EPR) of systems with one or more unpaired electrons. As this is a very common technique in chemistry laboratories, the basic principles can be found readily.[127]

In metalloporphyrins, the chemically important electrons belong to the conjugated π-electron system of the porphyrin core. They occupy orbitals that transform of the D_{4h} (in some cases, square pyramidal, C_{4v}) point group.[128] Bonding can occur only between e_g orbitals and d orbitals (d_{xz}, d_{yz}) of the metal, but the overlap is small (It is especially small in N-substituted metal complexes, chapter-4). Thus the isolation of two electronic systems, one belonging to the metal and the other to the ligand, led Fuhrhop[129] to assign either a metal or ligand reaction to a givenoxidation or reduction step of a non-N-substituted metalloporphyrin. In the electronic spectra of metalloporphyrins and metallo-N-alkylporphyrins, the $\pi \longrightarrow \pi^*$ transitions of the ligand mask the d-d transition of the metal and hence the uv-visible electronic spectroscopy is often useless for studying the electronic structure of the metal atom. Thus epr emerges as the best choice in understanding the electronic structure of the metal.

This work on the electron paramagnetic resonance of

metallo-N-substitutedporphyrins has been undertaken in order to gain further information on the properties of metallo-N-alkylporphyrins. The structures (ch-5) and potentials (ch-4) of metallo-N-substitutedporphyrins are significantly different from their non-N-alkylated analogs. Their visible absorption spectra are also different from the non-N-substituted metalloporphyrins (ch-5).[54a,58] The epr spectra of the latter have been reviewed by Lin in 1979.[130] But so far there is no report on the epr of metallo-N-alkylporphyrins. Among the metals, copper (II) is a convenient choice, because it is simple to interpret the electronic structure of a d^9 system theoretically. Besides, there are quite a few papers which concern the epr spectra of CuTPP[44-46] CuPC[131-37] (PC = pthalocyanine). There are reports on epr spectra of natural porphyrins of copper(II) also.[138-40]

EXPERIMENTAL (XPS)

The synthesis of N-p-nitrobenzyl-5,10,15,20-tetraphenylporphyrin (N-p-$CH_2C_6H_4NO_2$HTPP), N-ethylacetato-5,10,15,20-tetraphenylporphyrin (N-$CH_2CO_2C_2H_5$HTPP), N-phenyl-5,10,15,20-tetraphenylporphyrin (N-PhHTPP) have been reported previously (chapter 3). The synthesis and analysis of Mn(II) complexes, Mn (N-PhTPP)Cl and Mn(N-p-$CH_2C_6H_4NO_2$TPP)Cl, have been described in chapter 4.

The XPS spectra were taken by Lisa Delouise and Professor N. Winograd of the Pennsylvania State University, University Park. The spectra were recorded on a Leybold-

Heraeus (NOVA, 4X) spectrometer utilizing monochromatized Mg K_a (1253.6 ev) x-ray radiation. The solution (in dichloromethane) of the free base N-substituted porphyrin, Mn(N-PhTPP)Cl or Mn(N-p-$CH_2C_6H_4NO_2$TPP)Cl was spread on an indium foil and introduced into the vacuum chamber at pressure of 10^{-9} torr. All binding energies are referenced to carbon 1s binding energy. The steps involved in getting the final form of spectra involve a) collection of raw data b) subtraction of a constant c) subtraction of linear background d) smoothing e) gaussian fitting.

Results: The N 1s portion of the XPS spectra of different free bases and the complexes of Mn(II) are listed in Table XXVI. The Figure 35 shows the XPS spectra of Mn(N-$CH_2C_6H_4NO_2$TPP)Cl and N-p-$CH_2C_6H_4NO_2$HTPP. The visible spectra taken before and after the XPS experiments agree very well.

Discussion: The most sensitive probe for measuring charge distribution in porphyrins is the N 1s binding energies.[37] There are three reasons for this assertion: 1) In a metalloporphyrin the nitrogens are bound to both metal and the carbon ring skeleton. 2) There are only four nitrogens compared to 44 or more carbons to dilute the single-electron effects. 3) In many cases, the metal ion binding energy is insensitive to the small changes in the charge distribution between the macrocycle and the metal orbitals.[37]

In this chapter, I explore the effect of phenyl and alkyl groups other than the methyl group on the N 1s binding energies. In the previous report, the N 1s binding energies

Figure 35. The N 1s region of the x-ray photoelectron spectra of N-p-nitrobenzyl-5,10,15,20-tetraphenylporphyrin (Top) and chloro-N-p-nitrobenzyl-5,10,15,20-tetraphenylporphinatomanganese(II) (Bottom).

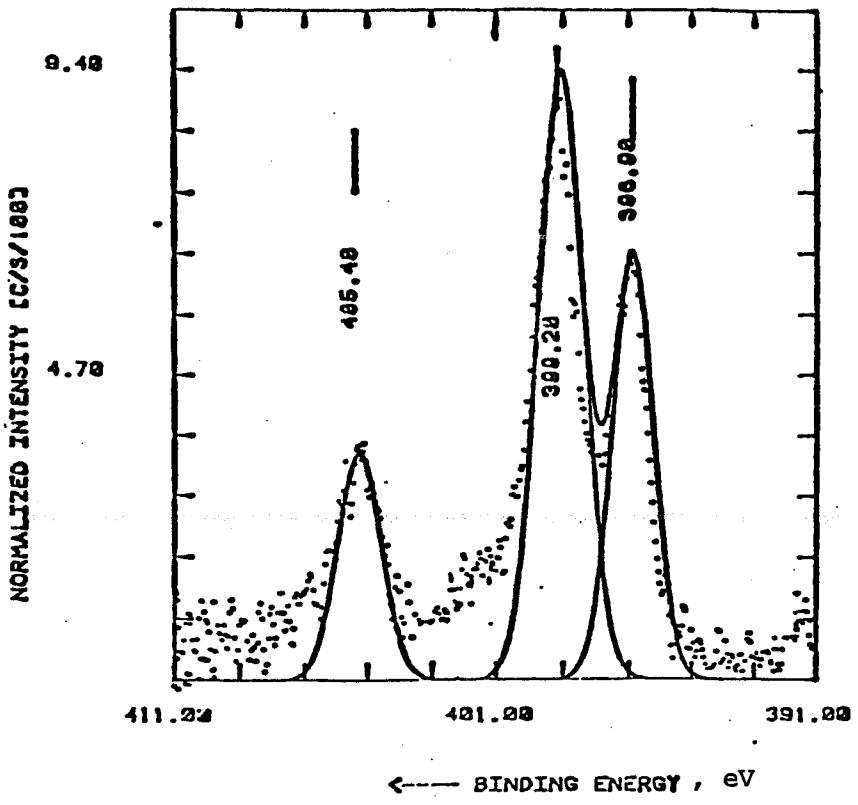
9.40
4.70
NORMALIZED INTENSITY (C/S/100)
405.40
398.20
396.00
411.00
401.00
391.00
BINDING ENERGY, eV

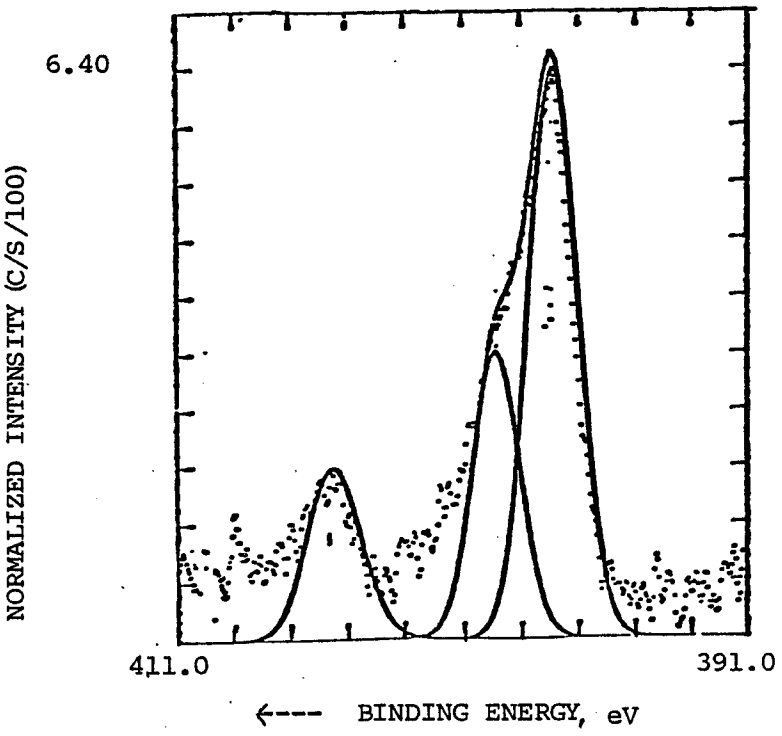
6.40
NORMALIZED INTENSITY (C/S/100)
411.0
391.0
BINDING ENERGY, eV

for Mn(N-CH_3TPP)Cl, Fe(N-CH_3TPP)Cl, Co(N-CH_3TPP)Cl, Zn(N-CH_3TPP)Cl N-methyl5,10,15,20-tetraphenylporphyrin and its dicationic salt have been examined.[42] There are two types of nonequivalent nitrogen atoms in these species. One corresponds to N-CH_3 and N-H (in free bases and protonated species) nitrogen atoms and the other type belongs to the other nitrogen atoms. The metal atom of the complexes perturbs the nonmethylated nitrogen atoms to a greater extent than the methylated one. The difference in core binding energies (the difference between the N 1s binding energies of the methylated and non-methylated nitrogen atoms) correlates in a linear fashion with differences in distances between the metal atom and the nitrogen atoms of metallo-N-methylporphyrin[42] (the metal to the nitrogen bearing the methyl group bond length minus the average metal to nonmethylated nitrogen bond lengths) determined by x-ray diffraction technique. The least difference in binding energies for Zn(N-CH_3TPP)Cl indicates very little interaction between zinc(II) and the methylated nitrogen atom consistent with its greatest bond length difference.[42] In Mn(N-CH_3TPP)Cl, however, the greater difference in binding energies is indicative of relatively strong interaction between the metal atom and the methylated nitrogen atom supported by lesser bond length difference in the manganese (II) complex. But the effect of different N-substituents in the Mn(II) complexes have not been investigated yet. So, I have used a phenyl (sp^2 carbon bound to the nitrogen atom) and a N-p-nitrobenzyl substituent to explore their effect in the man-

ganese (II) complexes. The XPS of free base N-substituted porphyrins have also been included to compare their binding energies with those of metal complexes.

The N 1s binding energies for N-methyl porphyrins[42] and non-N-substituted porphyrins[37,38] are comparable to those of other nitrogen compounds. The 1s binding energies of piperidine and piperidine hydrochloride are 397.8 and 400.4ev respectively[141] [Δ BE, (binding energies) = 2.6 eV] and for the aromatic analogs, pyridine and pyridine hydrochloride, they are 398.0 and 400.2 eV respectively (ΔBE = 2.2eV).[142] The previous work [37-41] on XPS studies of porphyrin free bases, such as tetraphenylporphyrin, show that there are two nitrogen atoms, with the higher binding energy assigned to the two nitrogen atoms those are bound to hydrogen atoms. the results of this XPS experiment clearly ruled out a symmetric structure in which hydrogen atoms are bridged between two nitrogen atoms. The N 1s portion of the XPS spectrum of N-methyl-5,10,15,20-tetraphenylporphyrin[42] shows peaks at 397.6 and 399.9 eV(based on Au $4f_{7/2}$ at83.8 eV). The peak at higher energy, 399.9ev, has been assigned to the hydrogen and methyl bearing nitrogen atoms and the binding energy differences are similar to those found in the nitrogen containing charged salts with and without hydrogen atoms (mentioned above). The binding energy differences in N-methyl-5,10,15,20-tetraphenylporphyrin (ΔBE = 2.3 eV) is also similar to that found in 5,10,15,20-tetraphenylporphyrin (ΔBE = 2.0ev).[37,38] It was established as in tetraphenylporphyrin

that the hydrogen atom does not bridge two or more nitrogen atoms.[42] The metal Mn(II), Fe(II), Co(II) and Zn(II) complexes of N-methyl-5,10,15,20-tetraphenylporphyrin[42] showed the binding energies of three "sp^2" nitrogen atoms to be in the same range of "porphyrin" N 1s energies while the substituted nitrogen is very similar in energy to the "chlorin"-type energies[37] (which comes in the higher energy region).

In N-PhHTPP, N-p-$CH_2C_6H_4NO_2$HTPP and N-$CH_2CO_2C_2H_5$HTPP, there are two different peaks as in N-CH_3HTPP[42] (Table XXVI, Figure 35 for the XPS spectrum of N-p-$CH_2C_6H_4NO_2$HTPP). By analogy with N-CH_3HTPP, the peak at higher binding energies for the free base N-substituted porphyrins (of this report) corresponds to two different types of nitrogen atoms (N-R and N-H) which have very similar binding energies.[42] The areas for these two peaks are not equal (with R = C_6H_5, p-$CH_2C_6H_4NO_2$ and -$CH_2CO_2C_2H_5$).

The higher energy N 1s peak of N-CH_3HTPP[42] is some what larger (intensity ratio 1.2:1) than the lower energy peak. Niwa et al. also found that the peak at higher binding energy is more intense (a ratio of 1.1:1).[40] The greater peak height was attributed to a satellite peak occurring at nearly the same energy as the peak at higher binding energy (N 1s). In the present case, the possibility of a satellite peak appearing at the same energy as the peak at higher binding energy (N 1s) can also account for the larger area at the higher binding energy (The experiments were repeated an the visible absorption spectra were taken before and after the experiment to ensure that free base porphyrins did not get

protonated. Protonation of porphyrins can explain a larger area of the peak for N 1s at higher energy than the one at lower binding energy). The satellite peak (if we consider the satellite peak as the contributor to cause a larger area) contributes significantly in certain cases as shown by the ratios in Table XXVI.

The full width at half maximum (fwhm) of the peaks at two binding energies can help in distinguishing two kinds of N 1s peaks of the N-substituted porphyrins. The widths of the peaks at two binding energies are clearly different in all cases (Table XXVI). The peak at higher binding energy consists of two different types of nitrogen atoms (N-R and N-H, which have very similar binding energies) similar to that found in the case of $N\text{-}CH_3HTPP$ by Lavallee et. al.[42] The peak widths for the two pairs of nitrogen atoms in 5,10,15,20-tetraphenylporphine are equal (about 0.95 eV).[143] In the case of $p\text{-}CH_2C_6H_4NO_2HTPP$ and $Mn(N\text{-}p\text{-}CH_2C_6H_4NO_2TPP)Cl$ there is another peak in the higher binding energy region (405.4 and 405.1 eV respectively due to the nitrogen atom of the nitro group. The decrease in N 1s binding energy of the nitro group by 0.3 eV in going from the free base to the manganese (II) complex is presumably due to lattice packing or an intermolecular effect between manganese (II) and the nitro group.

The significant difference between the free base N-substituted porphyrins and some of their Mn(II) complexes is the change in the "sp^2" N 1s binding energies compared to

Table XXVI. X-ray Photoelectron Spectroscopy Data (ev) for some N-substituted Porphyrins and porphyrin complexes of Mn(II).

Species	Ratio (for the area of two peaks)	BE[a] "sp^2" N 1s	BE[a] "sp^3" N 1s	ΔBE	FWHM[a] "sp^2" N 1s	FWHM[a] "sp^3" N 1s
Mn(N-PhTPP)Cl	1.2 : 1	397.7	399.7	2.0	1.16	1.77
N-PhHTPP	1 : 2.77	397.1	399.3	2.2	1.30	1.66
Mn(N-p-$CH_2C_6H_4$-NO_2TPPCl)	2.1 : 1	397.4	399.2	1.9	2.0	1.9
N-p-$CH_2C_6H_4NO_2$HTPP	1 : 1.52	396.9	399.2	2.3	1.5	1.6
N-$CH_2CO_2C_2H_5$HTPP	1 : 2.59	397.1	399.3	2.2	1.33	1.67
Mn(N-CH_3TPP)Cl[b]	-	398.3[b]	400.4[b]	2.1		
N-CH_3HTPP[b]	-	397.6[b]	399.9[b]	2.3	0.92[b]	1.09[b]

a. All the energies are reported in ev, BE, Binding Energy, ΔBE, difference in binding energies (All reported in ev); fwhm, full width at half maximum. Binding energies are reproducible to ± 0.1 ev. b. Values taken from Lavallee et al. Inorg. Chem. 1979, 18 , 1776-80.

that of the substituted nitrogen atom ("sp^3" N 1s) (Table XXVI). An important point regarding the absolute values of all the N 1s binding energies is that they differ from one laboratory to another. For example, Hayes and Zeller reported values of 399.1 and 397.2ev for the N 1s binding energies of H_2TPP;[38] Karweik and Winograd reported values of 399.Ø and 397.Ø eV[37] and the values reported by Niwa et al. are 4ØØ.2 and 398.2 eV - but with a consistent peak to peak difference in each spectrum of 2.Ø eV. Indeed this seems to be true in the present context also. In $N\text{-}CH_3HTPP$[42], the binding energies reported were 399.9 and 397.6ev respectively with a difference of 2.3 eV. In $N\text{-}p\text{-}CH_2C_6H_4NO_2HTPP$, they are 399.9 eV respectively with a difference of 2.3 eV. Though the magnitude of the N 1s binding energies are different, the differences between the binding energies in the free base N-substituted porphyrins and their complexes are consistent with those of $N\text{-}CH_3HTPP$ and $Mn(N\text{-}CH_3TPP)Cl$ (Table XXVI) reported earlier.[42]

Thus the sp^2 or sp^3 carbon atom bound to the nitrogen atom does not seem to affect the N 1s binding energies in their free bases or their complexes even though there is a distinct difference in the visible absorption spectra of N-phenyl porphyrin and its manganese complex compared to those with and sp^3 carbon atom bound to the nitrogen atom.

EXPERIMENTAL (EPR)

Purification of acetonitrile has been described in

chapter 2. Spectrograde chloroform (Aldrich) was used as such without further purification. The preparation and purification of $Cu(CF_3SO_3)_2.6H_2O$ has been described in chapter 2. The $Zn(ClO_4)_2.6H_2O$ was used as such for the preparation of the Zn complex (see below). The non-coordinating base 2,2,6,6-tetramethylpiperidine (Aldrich) was used as such in the preparation of the copper(II) complexes.

The 5,10,15,20-tetraphenylporphinatocopper(II) was prepared by the method of Adler et al.[51b] CuTPP (3-5 mg) was dissolved in less than 1 mL of $CHCl_3$ containing H_2TPP. The mixture was filtered through glass wool and transferred to the epr tube. The N-methyl-5,10,15,20-tetraphenylporphinatocopper(II) trifluoromethanesulfonate, $Cu(N\text{-}CH_3TPP)^+CF_3SO_3^-$, was prepared by mixing excess of $Cu(CF_3SO_3)_2.6H_2O$ with N-CH_3HTPP in the presence of non-coordinating base, 2,2,6,6-tetramethylpiperidine, in CH_3CN. The completion of the complex formation was checked by visible absorption spectroscopy. The solvent was removed and the residue was used as such for the epr experiments. About 8 mM $Cu(N\text{-}CH_3TPP)^+CF_3SO_3^-$ in $CHCl_3$ (spectrograde) was used for recording the epr spectrum. Similarly, the spectrum of $Cu(N\text{-}CH_3TPP)^+CF_3SO_3^-$, 10mM, in CH_3CN with excess of free ligand, was obtained. The epr spectra were also recorded for $Cu(N\text{-}CH_3TPP)^+CF_3SO_3^-$ in CH_3CN and $CHCl_3$ respectively in the absence of free ligand, N-CH_3HTPP. A non-coordinating base, 2,2,6,6-tetramethylpiperidine, does not affect the epr spectra of the complexes described here.

The Zn complex, $Zn(N\text{-}CH_3TPP)^+ClO_4^-$, was prepared by

mixing $Zn(ClO_4)_2.6H_2O$ and N-CH_3HTPP (40 and 16 mg respectively) in CH_3CN with the addition of excess non-coordinating base. The mixture was then evaporated to dryness. UV-VIS (CH_3CN): 434, 456, 559, 606 and 655 nm. The Zn complex was then mixed with Cu(N-CH_3TPP)$^+CF_3SO_3^-$ through glass wool and transferred to the epr tube. The ratio of Zn:Cu was 4:1. The sample of N-p-nitrobenzyl-5,10,15,20-tetraphenylporphinatocopper(II) was prepared by mixing an excess of $Cu(CF_3SO_3)_2.6H_2O$ with N-$CH_2C_6H_4$HTPP in the presence of 2,2,6,6-tetramethylpiperidine in acetonitrile and the formation of the complex was confirmed by visible absorption spectroscopy. Excess free ligand was added when the spectrum was recorded in the presence of free base. In all cases the mixtures were filtered.

Measurements: All the epr spectra were measured with the help of Dr. William Sweeney using an X-band spectrometer at 77° K. The spectra were simulated by Dr. Sweeney using the QCPE program NO. 265 written by Lozos, Hoffman and Franz of the Northwestern University.

Results: The epr spectrum of CuTPP in chloroform at 77° K is shown in Figure 36. The experimental and simulated spectra of Cu(N-CH_3TPP)$^+CF_3SO_3^-$ in $CHCl_3$ with free base, N-CH_3HTPP, are shown in Figure 37. The epr spectra of Cu(N-CH_3TPP)$^+CF_3SO_3^-$ in $CHCl_3$ (with free ligand N-CH_3HTPP) and $CH_3CN/CHCl_3$ mixture as well as that of the mixture of Zn and Cu N-methylporphyrin complexes (4:1) are presented in Figure 38. Figure 39 shows the effect of solvents ($CHCl_3$ and

Figure 36. The epr spectrum of CuTPP in $CHCl_3$(6 mM) at 77 ^{o}K. Microwave power = 10 mw, frequency = 9.295 GHZ, modulation amplitude = 1 Gauss.

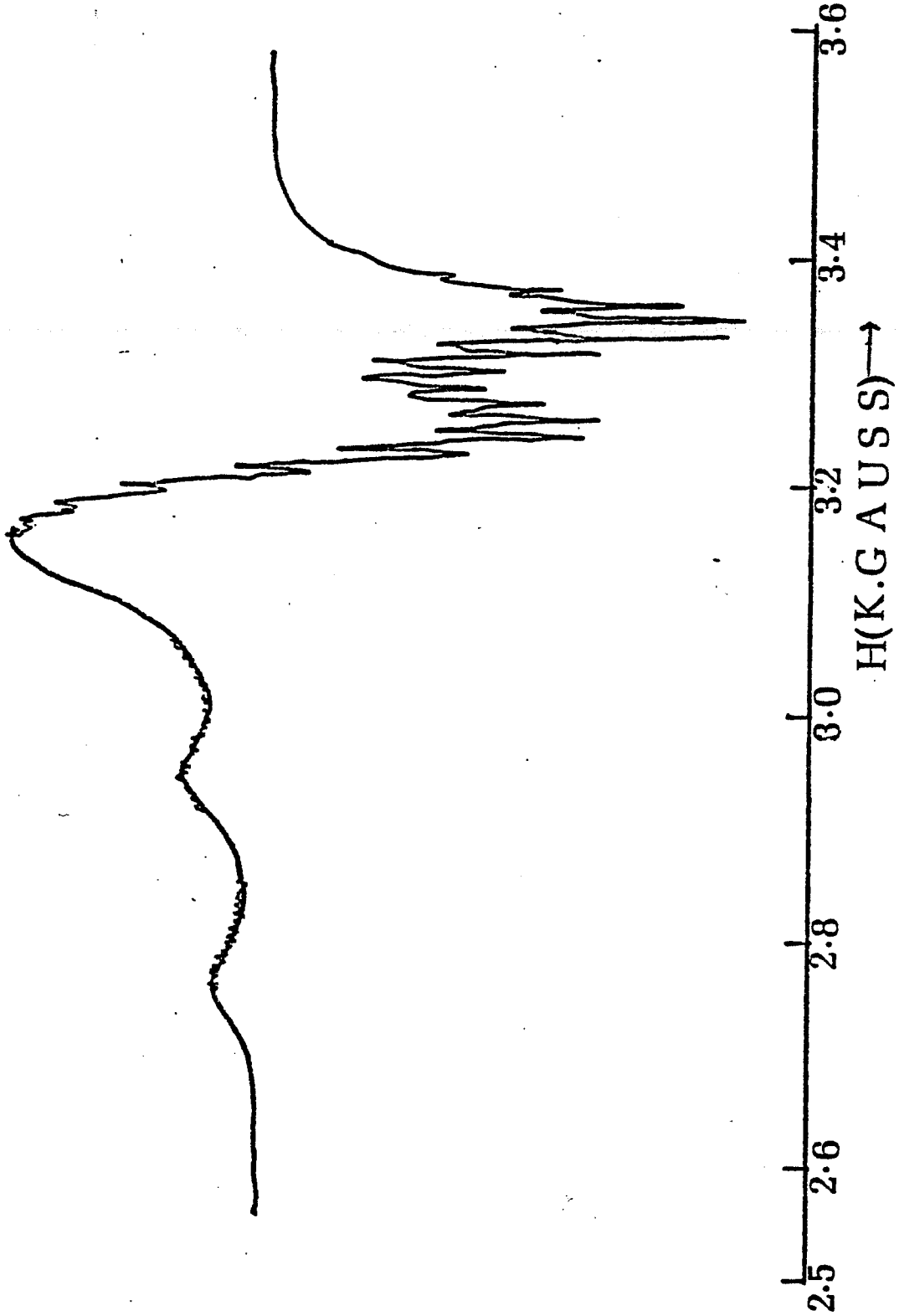
2.5
2.6
2.8
3.0
3.2
3.4
3.6
H(K.GAUSS)⟶

Figure 37. The epr spectrum of $Cu(N\text{-}CH_3TPP)^+CF_3SO_3^-$ in $CHCl_3$(5-7 mM, with excess free ligand, $N\text{-}CH_3TPP$. experimental —— simulated -----) at 77°K. Power = 10 mw, ν = 9.295 GHZ, modulation amplitude = 2 Gauss.

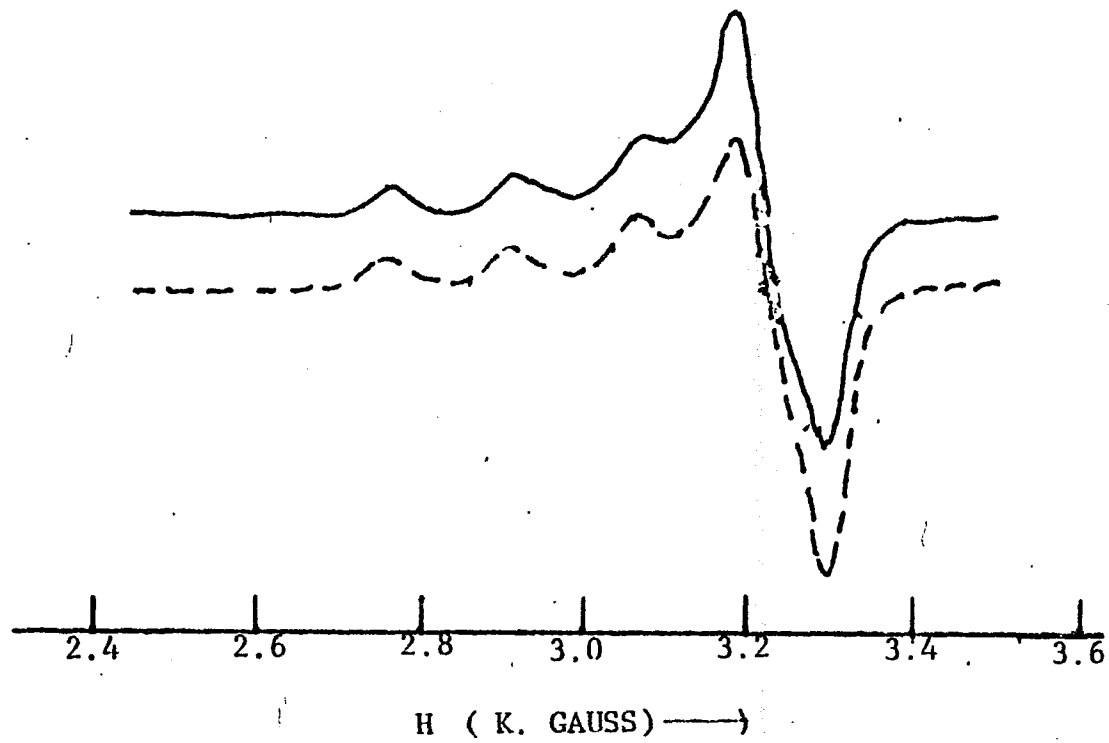
2.4
2.6
2.8
3.0
3.2
3.4
3.6
H (K. GAUSS) ⟶

Figure 38. The epr spectra of a) Cu/Zn complex of $N\text{-}CH_3HTPP$ (..... Zn : Cu = 4:1, concentration of the Cu complex 7-8 mM). Frequency = 9.295 GHZ, microwave power = 10 mw, modulation amplitude = 1.25 Gauss. b) $Cu(N\text{-}CH_3TPP)^+CF_3SO_3^-$ in CH_3CN with 20% (V/V) of $CHCl_3$ (6-7 mM, ν = 9.295 GHZ, power = 10 mw, modulation amplitude = 1.25 Gauss. c) $Cu(N\text{-}CH_3TPP)^+$-$CF_3SO_3^-$ in $CHCl_3$ in the presence of free base, $N\text{-}CH_3HTPP$ (5-7 mM, ν = 9.295 GHZ, power = 10 mw, modulation amplitude = 2 Gauss). All spectra were recorded at 77^oK.

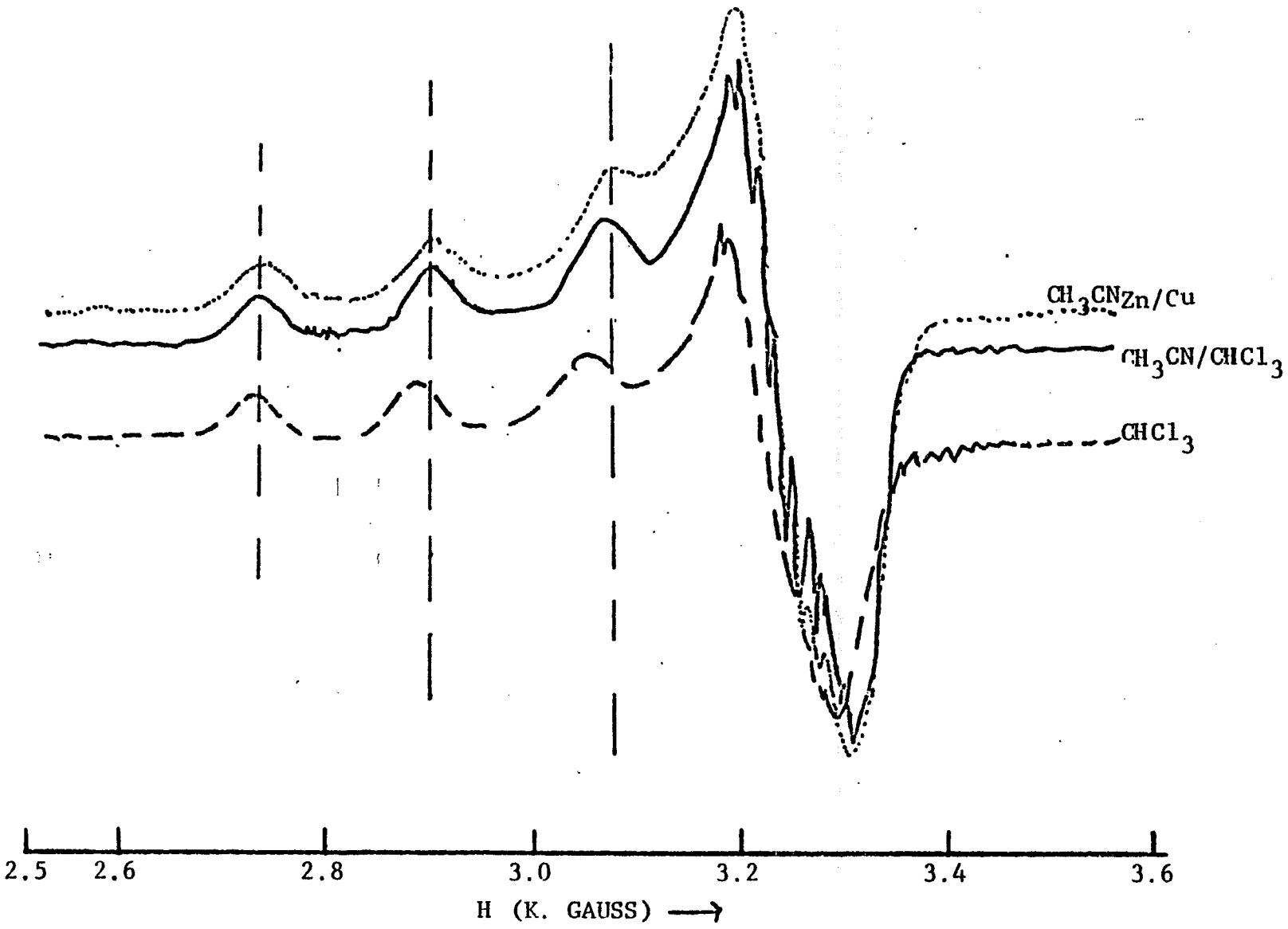
CH_3CNZn/Cu
$CH_3CN/CHCl_3$
$CHCl_3$
2.5
2.6
2.8
3.0
3.2
3.4
3.6
H (K. GAUSS) ⟶

Figure 39. The epr spectra of $Cu(N\text{-}CH_3TPP)^+CF_3SO_3^-$ a) with excess free ligand, $N\text{-}CH_3HTPP$ (The spectrum is not affected even in the absence of free ligand) in CH_3CN. ν = 9.298 GHZ, power = 10 mw, modulation amplitude = 0.0625 Gauss, 5-7 mM. b) with out free base, $N\text{-}CH_3HTPP$ in $CHCl_3$. ν = 9.299 GHZ, modulation amplitude = 0.8 Gauss, power = 10 mw, 5-7 mM. c) with free base, $N\text{-}CH_3HTPP$ in $CHCl_3$, ν = 9.295 GHZ, modulation amplitude = 2 Gauss, power = 10 mw, 5-7 mM. a) solid line b) ------- c) ..... All the spectra were recorded at 77^oK.

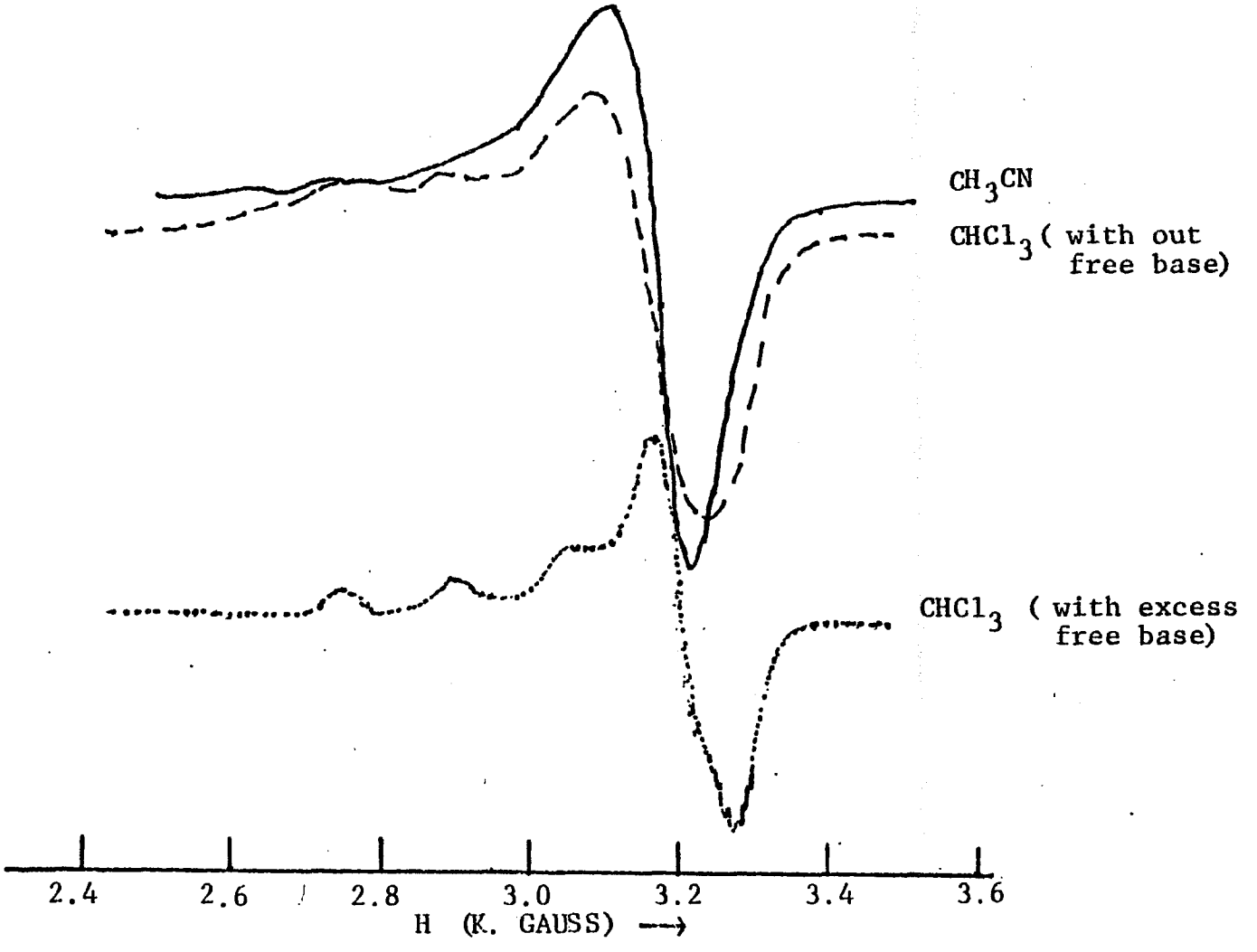
CH_3CN
$CHCl_3$ (with out free base)
$CHCl_3$ (with excess free base)
2.4
2.6
2.8
3.0
3.2
3.4
3.6
H (K. GAUSS) ⟶

CH_3CN) and free base, N-CH_3HTPP, on the epr spectra of Cu(N-CH_3TPP)$^+CF_3SO_3^-$. The experimentally observed and simulated epr spectra of Cu(N-p-$CH_2C_6H_4NO_2$HTPP) are shown in Figure 40.

Discussion: The frozen solution of 6 mM CuTPP with H_2TPP in $CHCl_3$ at 77° K is consistent with those reported in literature.[45,46] The spectrum consists of metal hyperfine lines corresponding to the g_{11} and g_1 tensors. There is a further split due to the superhyperfine interaction by the nitrogens of the pyrrole group (Figure 36). Bleany interpreted the epr spectrum by writing the spin Hamiltonian for axial symmetry[143], using the coordinate system shown below.

$$H_{sp} = g_{\parallel}\beta H_z S_z + g_{\perp}\beta(H_x S_x + H_y S_y) + A_{\parallel} S_z I_z + A_{\perp}(S_x I_x + S_y I_y) + Q[I_z^2 - 1/3\ I(I+1)] + \Sigma_n S A_n I_n$$

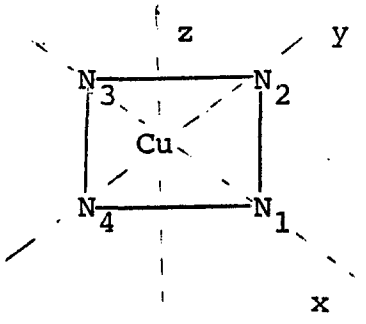

The coordinate system for CuTPP.

The fifth term in this expression is the quadrupolar term and the superhyperfine interaction is described by the last term (for 4 nitrogen nuclei).

A good analysis of the epr spectrum of CuTPP in $CHCl_3$ has been made by Manoharan and Rogers.[46] They concluded

Figure 40. The epr spectra of $Cu(N\text{-}p\text{-}CH_2C_6H_4NO_2TPP)^+$ $CF_3SO_3^-$ in CH_3CN at 77°K : a) with excess free ligand (top) b) simulated (power = 20 mw, ν = 9.291 GHZ, modulation amplitude = 8 Gauss, 3-4 mM). c) without free ligand, $N\text{-}p\text{-}CH_2C_6H_4NO_2HTPP$, solid line (bottom, 1-2 mM), ν = 9.295 GHZ, power = 10 mw, modulation amplitude = 8 Gauss.

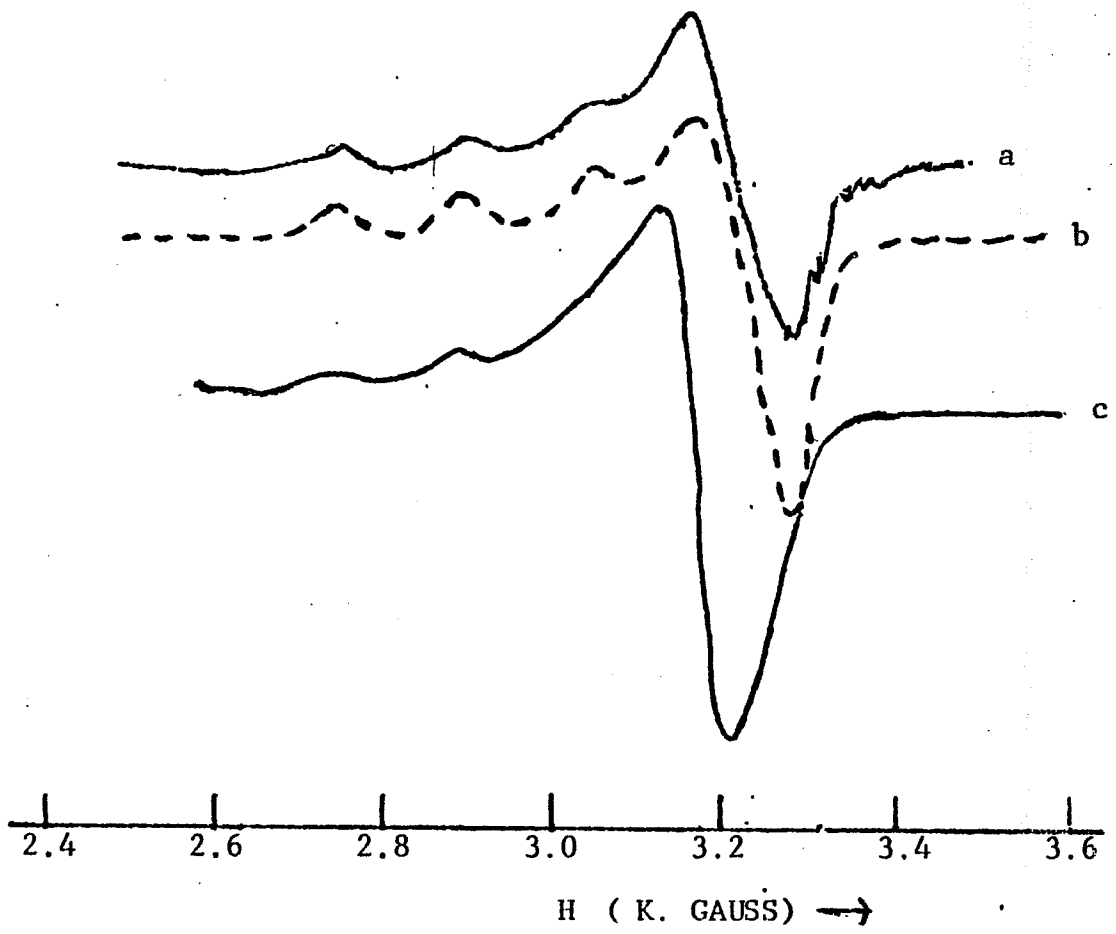
a
b
c
2.4
2.6
2.8
3.0
3.2
3.4
3.6
H (K. GAUSS) →

from their studies (as Assour did from his[45]) that two species are present and the relative amounts depend upon the experimental conditions. They further added that it is not correct to assume that the ^{63}Cu and ^{65}Cu lines can not be resolved. The reason for repeating the epr spectrum of CuTPP, in our case, is to compare it with the N-substituted complexes of copper(II) under same conditions.

The epr spectrum of $Cu(N\text{-}CH_3TPP)^+CF_3SO_3^-$ in $CHCl_3$ in the presence of free base, $N\text{-}CH_3HTPP$, at 77°K shows hyperfine due to copper but no noticeable superhyperfine due to the interaction of nitrogen atoms with copper (Figure 37) is observed. The values of g_{11} and A_{11}, 2.213 and 150 respectively, are significantly different from that of CuTPP in $CHCl_3$[45,46,144] (Table XXVII). In the absence of free base, $N\text{-}CH_3HTPP$, at 77°K the g values do not change significantly but the lines become very broad (Figure 39).

Addition of few drops of acetonitrile to the chloroform solution of $Cu(N\text{-}CH_3TPP)^+CF_3SO_3^-$ in the presence of free base, $N\text{-}CH_3HTPP$, gives superhyperfine splitting not observed in pure $CHCl_3$. Some change in g-values and copper hyperfine constants are also observed. Similar effects have been noted for addition of piperidine or 1,3,5-trinitrobenzene to a toluene solution of octaethylporphinatocopper(II).[145]

The epr spectra of $Cu(N\text{-}CH_3TPP)^+CF_3SO_3^-$ in pure CH_3CN at 77°K (with or without $N\text{-}CH_3HTPP$) are rather interesting. The spectra are significantly altered in going from pure $CHCl_3$ to pure CH_3CN (Figure 39). The fact that the observed

Table XXVII. EPR parameters for $Cu(N\text{-}RTPP)^{+}CF_3SO_3^{-}$ and CuTPP.[a]

Complex	Solvent	Free ligand	$g_{\|\|}$	$g_{\perp}$	$A_{\|\|}$	$A_{\perp}$
CuTPP	$CHCl_3$	H_2TPP	2.185	2.045	204.5	30
$Cu(N\text{-}CH_3TPP)^{+}$ $CF_3SO_3^{-}$	$CHCl_3$	$N\text{-}CH_3HTPP$	2.213	2.055	150	10
$Cu(N\text{-}CH_2C_6H_4NO_2TPP)^{+}$ $CF_3SO_3^{-}$	CH_3CN	$N\text{-}p\text{-}CH_2C_6H_4\text{-}NO_2HTPP$	2.220	2.065	142	15
$Cu(N\text{-}CH_3TPP)^{+}$ $CF_3SO_3^{-}$	CH_3CN	------	2.351	2.080	120	20
$Cu(N\text{-}CH_3TPP)^{+}$ $CF_3SO_3^{-}$	CH_3CN	$N\text{-}CH_3HTPP$	2.299	2.080	163	20

a. Hyperfine solittings are in $cm^{-1} \times 10^{-4}$

spectrum of CH_3CN dissolved material could not be fit with a single set of parameters for g_{11}, g_1, A_{11} (Table XXVII) is suggestive of more than one species present in the solution. The addition of few drops of $CHCl_3$ (20% in CH_3CN) to the above solution gives an epr spectrum similar to that observed in $CHCl_3$ (with free ligand N-CH_3HTPP, Figure 38). Besides, superhyperfine splitting is observed as in the case of addition of acetonitrile to the chloroform solution of Cu(N-CH_3TPP)$^+CF_3SO_3^-$ (mentioned above). The change in the epr spectrum of the latter is also noticed when Zn(N-CH_3TPP)$^+Cl\emptyset_4^-$ is present in the solution (Figure 38). But the superhyperfine splitting, as observed in the mixed solvents of $CHCl_3/CH_3CN$, is not clearly noticeable presumably due to some kind of weak magnetic interaction. Notice that the top two epr spectra of Figure 38 in CH_3CN (in the presence of Zn and $CHCl_3$) are more similar than that of Cu(N-CH_3TPP)$^+CF_3SO_3^-$ in $CHCl_3$ (with free base, bottom one of Figure 38). This difference suggests that acetonitrile coordinates to copper when the samples of Cu(N-CH_3TPP)$^+CF_3SO_3^-$ are prepared in acetonitrile. The trifluoromethanesulfonate counterion of the copper complex is very labile and there is other evidence which support that acetonitrile can coordinate to copper. There is a bathochromic shift of 5-10 nm when the visible absorption spectrum of Cu(N-C_2H_5TPP)$^+CF_3SO_3^-$ (very similar to Cu(N-CH_3TPP)$^+CF_3SO_3^-$) is recorded in CH_3CN instead of CH_2Cl_2. Other compounds containing nitrogen atoms, like amines, coordinate to Cu(N-RTPP)$^+CF_3SO_3^-$ readily (ch-2, Figure 10).

Thus all the information presented above suggest that there is an aggregation of the molecules of Cu(N-CH_3TPP)$^+CF_3SO_3^-$ in CH_3CN. The broadened spectrum observed in acetonitrile reflects magnetic interaction between Cu atoms in different molecules, and the interaction is disrupted by dilution with the Zn complex. Addition of few drops of chloroform to a solution of Cu(N-CH_3TPP)$^+CF_3SO_3^-$ in CH_3CN (with or without free ligand) also breaks the aggregated species present in acetonitrile (Figure 39).

In the case of Cu(N-p-$CH_2C_6H_4NO_2$TPP)$^+CF_3SO_3^-$ in CH_3CN (in the presence of free ligand, N-p-$CH_2C_6H_4NO_2$HTPP) the epr spectrum does not reveal any aggregation found for the N-methyl analog in acetonitrile (The broadening of lines occur to a small extent when the epr spectrum in CH_3CN is recorded in the absence of free ligand, Figure 40). This can be attributed to the higher solubility of N-p-$CH_2C_6H_4NO_2$HTPP compared to that of N-CH_3HTPP in acetonitrile and thus the free ligand prevents the molecules of Cu(N-p-$CH_2C_6H_4NO_2$TPP)$^+CF_3SO_3^-$ to come closer. The g_{11} and A_{11} for the latter (in CH_3CN) are different from that of CuTPP in $CHCl_3$ (2.235 and 150 compared to 2.185 and 204.5 respectively, Table XXVII) and is similar to that observed in the N-methyl complex.

The broadening of lines of Cu(N-CH_3TPP)$^+CF_3SO_3^-$ in chloroform (when no excess ligand is present) also suggest a kind of weak interaction among the molecules of Cu(N-CH_3TPP)$^+CF_3SO_3^-$. The formation of aggregates of Cu(N-

$CH_3TPP)^+CF_3SO_3^-$ in acetonitrile is comparable to those of CuPPDME and CuPP in $CHCl_3$, pyridine or piperidine.[144] Alston and Storm showed that addition of free base protoporphyrin and PPDME breaks down the aggregates of protoporphinatocopper(II). In a sense, our result is similar to their finding in that or $Zn(N\text{-}CH_3TPP)^+ClO_4^-$ or $CHCl_3$ prevent the formation of aggregates of $Cu(N\text{-}CH_3TPP)^+CF_3SO_3^-$ in acetonitrile. They also mentioned that the aggregation is absent in CuTPP due to the configuration of the phenyl groups. But there are other reports which show strong evidence for the formation of dimers in the case of tetraphenylporphyrin complexes. The epr studies of the copper(II) chelates of tetrakis(p-sulfonato)phenylporphyrin and tetrakis(p-carboxy)phenylporphyrin in water provide evidence for the process of aggregation.[146]

The g and A values of five-coordinated N-substituted Cu(II) complexes, reported here, are in accordance with those of five coordinated Cu(II)-non-N-substituted porphyrins. It has been suggested, on the basis of uv-vis and esr results, that on adding bases like 1-methylimidazole, pyridine and piperidine, the square planar complexes CuTPP, CuPP and CuPPDME form five coordinate square-pyramidal complexes.[144] However, the crystal structures of Co(II)[47b,113], Mn(II)[47a], Zn(II)[43] and Fe(II)[83] are all similar and they have a geometry with a distorted square-base pyramid. The Cu(II) N-substituted complexes probably have a similar geometry found in other complexes of N-methyl-5,10,15,20-tetraphenylporphyrin.

Conclusion: The solvents and free ligands have significant effect on the epr spectra of Cu(II) N-substitutedporphyrins. The presence of a substituent on the nitrogen atom alters the epr spectra of the complexes significantly from that of non-N-substituted complexes. The superhyperfine splitting, due to the interaction of the nitrogen atoms of the porphyrin with Cu(II), observed in CuTPP is not noticeably in $Cu(N\text{-}RTPP)^{+}CF_3SO_3^{-}$ complexes. The lack of observed superhyperfine splitting is presumably a direct consequence of the reduction of symmetry. In CuTPP, 4 nitrogens are equivalent. Whereas $Cu(N\text{-}RTPP)^{+}X^{-}$ is a system of ABC_2 type, leading to 3 different hyperfine splitting constants and loss of resolution.

APPENDIX

Treatment of Kinetic Data: All the kinetics of the dealkylation reactions of metallo-N-substitutedporphyrins were done under pseudo-first-order condition where the concentration of amine, chloride or pyridine is kept in large excess(100-fold) compared to the complex of Cu(II) N-substitutedporphyrins.

$$Cu(N\text{-}RP)^{+} + Nu \longrightarrow CuP + Nu\text{-}R^{+}$$

Where 'P' is porphyrin, 'Nu' is nucleophile and 'R' is the substituent bound to the nitrogen atom.

The rate law,

$$\frac{d[CuP]}{dt} = \frac{-d[Cu(N\text{-}RP)^{+}]}{dt} = k_1[Nu][Cu(N\text{-}RP)^{+}] \qquad .....(I)$$

As $[Nu] \gg [Cu(N\text{-}RP)^{+}]$

$\therefore k_1[Nu] \cong k$ ('k' is the observed rate constant)

(The actual expression for the rate law of the dealkylation of N-substitutedporphyrin complex of Cu(II) by amines is given on page , chapter 2). Substituting k in eq. (1)

$$\frac{-d[Cu(N\text{-}RP)^{+}]}{dt} = k[Cu(N\text{-}RP)^{+}] \qquad .....(2)$$

Let's say for simplicity $[Cu(N\text{-}RP)^{+}] = C$

$$\therefore \quad \frac{-d[C]}{dt} = k[C] \qquad .....(3)$$

Which on integration gives,

$$C_t = C_0 \exp(-kt) \qquad .....(4)$$

C_t is the concentration at time 't'

C_0 is the concentration at time 't' = 0

C_t can be replaced by $(OD_t - OD_\infty)$ and C_0 by $(OD_0 - OD_\infty)$

Substituting the values of C_0 and C_t in eq. (4)

$$(OD_t - OD_\infty) = (OD_0 - OD_\infty)\, e^{-kt} \qquad \ldots\ldots\ldots\ldots\ldots\ldots (5)$$

or, $OD_t = OD + (OD_0 - OD_\infty)\, e^{-kt}$

The form used in the PROPHET,

$$Y(x) = B_1 - (B_1 - B_2)\, \exp(-B_3 * x) \qquad \ldots\ldots\ldots\ldots\ldots\ldots (6)$$

$B_1 = OD_\infty$, $B_2 = OD_0$ and $B_3 = k$, the observed rate constant.

The non-linear least square program within the PROPHET calculates OD_t from the parameters and variables given and compares its value for OD_t to the observed value. The sum of the squares of the differences, $\Sigma(OD_t(\text{exp}) - OD_t(\text{calc}))^2$ is minimized in the process. Arbitary values for OD_0, OD (usually 1) and the observed rate constant, B_3 (k_{obsd}) were given (a value from 0.00001 to 0.1, depending upon the reactions concerned) to fit the equation (6). All the parameters are allowed to vary simultaneously. In most cases, more than five iterations were necessary to perform the fits. All the pseudo-first-order reactions are linear up to at least four half-lives.

Activation parameters were determined using the Eyring relationship with the help of the PROPHET computing system.

$k = \nu \exp (-\Delta\overset{\neq}{G}/RT)$ .....(7)

Definitions: $\nu = k_B T/h = 6.020 \times 10^{12}$ at 298^oK

$k_B = 1.381 \times 10^{-16}$ erg/^oK, $h = 6.626 \times 10^{-27}$ erg. sec

$\nu/T = k_B/h = (6.20 \times 10^{12})/298 = 2.08 \times 10^{10}$, k_B = Boltzmann's costant, h = Planck constant, R = the gas constant = 1.98716 cal/mol/^oK

Rearranging eq.(7), $\ln(k/T) = \ln(k_B/h) - \Delta\overset{\neq}{H}/RT + \Delta\overset{\neq}{S}/R$

The plot of $\ln(k/T)$ vs. $1/T$ gives the slope = $-\Delta\overset{\neq}{H}/R$

Intercept = $\ln(k_B/h) + \Delta\overset{\neq}{S}/R$

$= 23.7625 + \Delta\overset{\neq}{S}/R$

The entropy of activation can be calculated also by using the equation (8)

$\Delta\overset{\neq}{S} = R(\ln k - \ln k_B T/h) + \Delta\overset{\neq}{H}/T$ .....(8)

REFERENCES

1. Adler, A.D., Ann. N.Y. Acad. Sci., 206, 1973, pp. 7-17 and references therein.

2. "Porphyrins and Metalloporphyrins", K.M. Smith, ed.,Elsevier, New York, 1975.

3. "The Porphyrins", D. Dolphin, ed., Academic Press, New York, 1978.

4. Lever, A.B.P. and Gray, H.B., Ed. "Iron Porphyrin" Part 1 and 2, Addison-Wesley Publishing Company, Inc., Reading, Massachusetts, 1983.

5. McEwen, W.K., J. Am. Chem. Soc. 1936, 58, 1124.

6. McEwen, W.K., J. Am. Chem. Soc. 1946, 68, 711-13.

7. Ellingson, R.C. and Corwin, A.H., J. Am. Chem. Soc. 1946, 68, 1112-15.

8. Lavallee, D.K. and Anderson, O.P., J. Am. Chem. Soc. 1982, 104, 4707-08.

9a. Levin, W.; Sernatinger, E.; Jacobson, M. and Kutzman, R., Science 1972, 176, 1341-43.

b. DeMatteis, F. and Cantoni, L. Biochem. J., 1979 183, 99-103.

c. Ortiz de Montellano, P.R.; Mico, B.A. and Yost, G.S.Biochem. Biophys. Res. Commun. 1978, 83 132-37.

10. De Matteis, F.; Gibbs, A.H.; Jackson, A.H. and Weerasingle, S., FEBS Lett. 1980, 119 109-12.

11a. Ortiz de Montellano, P.R.; Bailan, H.S.; Kunze, K.L. and Mico, B.A., J. Biol. Chem. 1981, 256, 4395-99.

b. Ortiz de Montellano, P.R.; Kunze, K.L.; Beilan, H.S. and Wheeler, C. Biochem. 1982 21, 1331-39.

c. Ortiz de Montellano, P.R.; Kunze, K.L.; Mico, B.A., Mol. Pharmacol., 1980, 18, 602-5.

12a. Ortiz de Montellano, P.R.; Beilan H.S. and Mathews, J.M.J. Med. Chem., 1982, 25, 1174-79.

b. Frank, B. Angew. Chem. Int. Ed. Eng., 1982, 21, 343-53.

c. Meyer, V.A. and Schmidt, R. in Stanburg, J.B. Wyngarden, J.M.; Fredrickson, D.S., The Metabolic Basis of Inherited Disease, McGraw Hill, New York, 1978, 1166.

d. Tschudy, D.P. in Bondy, P.K. and Rosenberg, L.E., Diseases of Metabolism Saunders, W.B., London 1974, 775.

e. Battle, A.M. et al. "Porphyrins and Porphyrias, Ethiopathogenesis, Clinics, and Treatment", Pergamon Press, Oxford, 1980.

f. Silber, B.; Mico, B.A; Ortiz de Montellano, P.R.; Dols, D.M. and Reigelman, S. J. Pharmacol. Ext. Ther. 1981, 219, 125-33.

13a. De Matteis, F.; Gibbs, A.H., Farmer; P.B. and Lamb, J.H. FEBS Lett., 1981, 129, 328-31.

b. De Matteis, F.; Hollands, C.; Gibbs, A.H.; Desa, N. and Rizzardini, M. FEBS. Lett. 1982, 145, 87-92.

14. Ortiz de Montellano, P.R.; Beilan, H.S. and Kunze, K.L. J. Biol. Chem. 1981, 256, 6708-13.

15. Tephly, T.R.; Coffman, B.L.; Ingall, G.; Abou Zeithar, M.S.; Goff, H.M.; Tabba, H.D. and Smith, K.M., Arch. Biochem. Biophys., 1981, 212, 120-26.

16. De Matteis, F.; Jackson, A.H.; Gibbs, A.H.; Rao, K.R.N.; Atton, J.; Weerasinghe, S. and Hollands, C. FEBS Lett. 1982, 142, 44-48.

17. Coffman, B.L.; Ingall, G.C.; Tephly, T.R. Arch. Biochem. Biophys., 1982 218(1) 220-4.

18. Tephly, T.R.; Gibbs, A.H. and De Matteis, F. Biochem. J. 1979, 180, 241-44.

19. De Matteis, F.; Gibbs, A.H. and Tephly, T.R., Biochem. J. 1980, 188, 145-52.

20. Ortiz de Montellano, P.R.; Kunze, K.L.; Cole, S.P.C. and Marks, G.S., Biochem. Biophys. Res. Commun. 1981, 103, 581-86.

21. Beale, S.I. and Foley, T., Plant. Physiol. 1982, 69, 1331-33.

22. Hoppe-Seyler, G.Z. Physiol. Chem. 1885, 9 34-39.

23. Heinz, R., Virchows. Arch. Pathol. Anat. Physiol. Klin. Med. 1890, 122, 112-16.

24a. Jandl, J.H.; Engle, L.K. and Allen, D.W., J. Clin. Invest. 1960, 39, 1818-36.

b. Beutter, E. Pharmacol. Rev. 1969, 21, 73-103.

c. French, J.K.; Winterborn, C.C. and Carrell, R.W. Biochem. J., 1978, 173, 19-26.

d. Goldberg, B.; Stern, A. and Peisach, J. J. Biol. Chem. 1976, 251, 3045-51.

25. August, O.; Kunze, K.L. and Ortiz de Montellano, P.R. J. Biol. Chem. 1982, 257, 6231-41.

26. Ortiz de Montellano, P.R.; Kunze, K.L. and Augusto, O., J. Am. Chem. Soc. 1982, 104, 3545-45.

27. Callot, H.J. and Metz, F., J. Chem. Soc. Chem. Commun. 1982, 947-48.

28. Mansuy, D.; Battioni, J.P.; Dupre', D.; Sartori, E. and Chottard, G. J. Am. Chem. Soc. 1982, 104, 6157-61.

29. Kunze, K.L. and Ortiz de Montellano, P.R. J. Am. Chem. Soc. 1983, 105, 1380-88.

30. Battioni, P.; Mahy, J.P.; Gillet, G. and Mansuy, D. J. Am. Chem. Soc., 1983, 105 1399-401.

31. Austen, J.D.; Mecond, S.; Carrano, C.J. and Tsutsui, M., Cancer Treat. Rep., 1978, 62, 511-18.

32. Doi, J.D.; Lavallee, D.K.; Srivastava, S.C.; Prach, T.; Richards, P. and Fawwaz, R.A., Int. J. of Appl. Rad. and 1981, 212, 120-6.

33. Liddane, K.; Lavallee, D.K.; Srivastava, S.C.; Prach, T.; Richards, P. and Fawwaz, R.A. work in progress.

34. Bain-Ackerson, M.J. and Lavallee, D.K. Inorg. Chem. 1979, 18, 3358-64.

35. Shah, B.; Shears, B. and Hambright, P. Inorg. Chem., 1971, 10 1828-30.

36. Hambright, P. Coord. Chem. Rev. 1971, 6, 247.

37. Karweik, D.H. and Winograd, N. Inorg. Chem. 1976, 15, 2336-42.

38. Zeller, M.V. and Hayes, R.G., J. Am. Chem. Soc. 1973, 95, 3855-60.

39. Karweik, D.H.; Winograd, N.; Davis, D.G. and Kadish, K.M., J.Am. Chem. Soc. 1974, 96, 591-92.

40. Niwa, Y.; Kobayashi, H. and Tsuchiya, J. Chem. Phy., 1974, 60 7920 and Inorg. Chem., 1974, 13, 2891.

41. Falk, M.; Hofer, O. and Lehner, H., Monatsh., Chem. 1974, 105, 366-78.

42. Lavallee, D.K., Brace, J. and Winograd, N. Inorg. Chem. 1979, 18, 1776-80.

43. Lavallee, D.K.; Kopelove, A. and Anderson, O.P., J. Am. Chem. Soc., 1978, 100, 3025-3033.

44. Ingram, D.J.E.; Bennett, J.E.; George, P. and Goldstein, J.M., J. Am. Chem. Soc. 1956, 78, 3545-.

45. Assour. J.M. J. Chem. Phys. 1965, 43, 2477

46. Manoharan, P.T. and Rogers, M.T. "Electron Spin Resonance of Metal Complexes", T.F. Yen. ed., Plenum Press, New York, 1969, 143.

47a. Anderson, O.P. and Lavallee, D.K., J. Am. Chem. Soc. 1977, 99, 1404-09.

b. Anderson, O.P. and Lavallee, D.K. Inorg. Chem., 1977, 16, 1634-40.

c. Fleisher, E.; Miller, C. and Webb, L. J. Am. Chem. Soc. 1964, 86, 2342

d. Hoard, J.L.; Cohen, G.H. and Glick, M.D., J. Am. Chem. Soc. 1967, 89 1992

48. Shears, B. and Hambright, P., Inorg. Nucl. Chem. Lett., 1970, 6, 679-80.

49. Lavallee, D.K., Inorg. Chem. 1976, 15, 691-4.

50. Lavallee, D.K. Inorg. Chem. 1977, 16, 955-7.

51. Adler, A.D.; Longo, F.R.; Finnelli, L.D.; Goldmacher, J.; Assour, J. and Korsakoff, L., J. Org. Chem. 1967, 32, 476.

52. Lavallee, D.K. and Gebala, A.F. Inorg. Chem. 1974, 13, 2504-08.

53. Lavallee, D.K.; McDonough, T.J., Jr. and Cioffi, L. Appl. Spectrosc. 1982, 36, 430-5.

54a. Lavallee, D.,K. and Bain-Ackerman, M.J. Bioinorg. Chem. 1978, 9, 311-21.

b. Bain-Ackermann, M.J., Ph.D. Thesis, Colorado State Univ., 1979.

55. Kuila, D. and Lavallee, D.K. Inorg. Chem. 1983, 22, 1095-99.

56. Perrin, D.D.; Armarego, W.L.F. and Perrin, D.R. "Purification of Laboratory Chemicals" Pergamon Press, London, 1966.

57. Cotton, F.A. and Wilkinson, G., "Advanced Inorganic Chemistry," Third Edition, Wiley, New York, 1978, p. 274.

58. Lavallee, D.K., Bioinorg. Chem. 1976, 6, 219-27.

59. Stinson, C. and Hambright, P. Inorg. Chem. 1976, 15, 3181-82.

60. The PROPHET Computing system is a multisite network, the CBIS system of NIH, which includes a wide array of statistics and structural simulation software. We are grateful to NIH for the installation of the Hunter Collge facility.

61. Lavallee, D.K. J. Inorg. Biochem. 1982, 16 135-43.

62. Clark Still, W.; Kahn, M. and Mitra, A. J. Org. Chem. 1978, 43, 2923-25.

63. Callot, H.J.; Fischer, J. and Weiss, R., J. Am. Chem. Soc. 1982, 104, 1272-76.

64. Callot, H.J. and Schaeffer, E., Nov. J. De Chimie 1980, 307.

65. Callot, H.J. and Tschamber, T. Bull. Soc. 1973, 3192-98.

66. Callot, H.J., Tet. Lett. 1979, 33, 3093-96.

67. Fleischer, E.B.; Palmer, J.M.; Srivastava, T.S. and Chatterjee, A., J. Am. Chem. Soc. 1975, 95, 3162-67.

68. Ortiz de Montellano, P.R.; Kunze, K.L., J. Am. Chem. Soc. 1981, 103, 6534-36.

69. Ortiz de Montellano, P.R.; Kunze, K.L., Biochem. Biophys. Res. Commun. 1981, 103 581-86.

70. Funahasi, S.; Yamaguchi, Y.; Ishhara, K. and Tanaka, M., J. Chem. Soc. Chem. Commun. 1982, 976-77.

71. Pasternack, R.F.; Vogel, G.C.; Showronek, A.; Harris, R.K. and Miller, J.G. Inorg. Chem. 1981, 20, 3763.

72. Turray, J. and Hambright, P. Inorg. Chem., 1980, 19, 562

73. Saito, S. and Itano, H.A., Proc. Natl. Acad. Sci. USA. 1981, 78, 5508-12.

74. Smith, A.G. and Farmer, P.B., Biomed. Mass. Spectrom., 1982, 9, 111-14, and the references there cited in.

75a. Dolphin, D.; Halko, D.J. and Johnson, J. Inorg. Chem., 1981, 20, 4348-51.

b. Ogoshi, H.; Watanbe, F., Noketzu, N. and Yoshid, Z., J. Chem. Soc., Chem. Commun., 1979, 943-44.

c. Abeysekara, A.M.; Grigg, R.; Iracha-Grimshaw, J. and King, T.J., J. Chem. Soc. Perkin Trans., 1979, 91, 2184-92.

d. Ogoshi, H.; Omura, T. and Yoshida, Z., J. Am. Chem. Soc. 1973, 95, 1666-68.

e. Ogoshi, H.; Setsuno, J.I.; Omura, T. and Yoshida, Z., J. Am. Chem. Soc. 1975, 97, 6461-66.

76. Doi, J.D.; Compito-Magliozzo, C. and Lavallee, D.K., Inorganic Chem., in press.

77a. Salas, C.E. and Sellinger, O.Z., J. Chromatog. 1977, 123, 231-36.

b. Beranek, D.T.; Weis, C.C. and Swanson, D.H. Carcinogenesis, 1980, 1, 595-606.

c. Rustum, Y.M., Anal. Biochem. 1978, 90, 288-99.

78a. Nakajima, A. and Pullman, B., Bull. Soc. Chim France, 1958, 1502.

b. Pullman, B. and Pullman, A., Biochim. Biophys. Acta., 1959, 36, 343.

79. Falk, J.E, "Porphyrins and Metalloporphyrins", Elsevier, Amsterdam, 1964.

80. Clark, W.H., "Oxidation-Reduction Potentials of Organic Systems." Williams and Wilkins, Baltimore, Md. 1960.

81. Weissberger, A. and Rossiter, B.W. Physical Methods of Chemistry, Part 11A, Electrochemical Methods, Wiley-Interscience, New York, 1971.

82. Lavallee, D.K. and Bain, M.J., Inorg. Chem. 1976, 15, 2090-93.

83. Anderson, O.P., Kopelove, A.B. and Lavallee, D.K., Inorg. Chem., 1980, 19 2101-7.

84. Kopelove, A.B., M.S. Thesis, Colorado State University 1981.

85a. Mansuy, D.; Lange, M. and Chottard, J.C., J. Am. Chem. Soc. 1979, 101, 6037 .

b. Chevrier, B.; Weiss, R.; Lange, M.; Chottard, J.-C. and Mansuy, D., J. Am. Chem. Soc. 1981, 103, 2899-2901.

c. Lange, M. and Mansuy, D., Tet. Lett. 1981, 22, 2561-64.

86. Wisneiff, T.J.; Gold, A. and Evans, S.A. Jr., J. Am. Chem. Soc. 1981, 103, 5616

87. Olson, J.M. Science, 1970, 168, 438

88. Kadish, K.M., in "Iron Porphyrins," edited by A.B.P.Lever and H.B. Gray, Reading (Massachussets), 1983. Part two P-182.

89. Buchler, J.W., P-201 of Smith, K.M., edited "Porphyrins and Metalloporpohyrins" Elsevier Amsterdam, 1975.

90. Kadish, K.M., unpublished results.

91. P-169 of ref. 88.

92a. Fuhrhop, J.H. in "Porphyrins and Metalloporphyrins", K.M. Smith, edited, Elsevier, Amsterdam, 1975.

b. Fuhrhop, J.H.; Kadish, K.M. and Davis, D.G., J. Am. Chem. Soc. 1973, 95, 5140-47.

93. David, D.G. in "The Porphyrins", D. Dolphin (ed.), Academic, New York, Vol. V, Part C pp. 127-152, 1979.

94. Zerner, M. and Gouterman, M. Theor. Chim. Acta. 1966, 4 44-63.

95. Felton, R.H., Private Communication, cited by D. Dolphin.

96a. Kadish, K.M.; Marrison, M.M.; Constant, L.A.; Dickens, L. and Davis, D.G., J. Am. Chem. Soc., 1976, 98, 8387-90.

b. Kadish, K.M.; Cheng, J.S., Cohen, I.A. and Summerville, D., ACS. Symp. Ser., 1977, 38, 65 .

97. Ogoshi, H.; Kitamura, S.; Toi, H. and Aoyoma, Y., Chem. Lett. 1982, 495-98.

98. Goldberg, D.E. and Thomas, K.M., J. Am. Chem. Soc. 1976, 98 913-19.

99. Kuila, D.; Lavallee, D.K., Schauer, C. and Anderson, O.P., J. Am. Chem. Soc., in press.

100. Brault, D. and Neta, P., J. Am. Chem. Soc. 1981, 103, 2705-10.

101a. Lexa, D.; Mispelter, J.; Savent, J.M., ibid. 1981, 103, 6806- 12.

b. Lexa, D.; Saveant, J.M., ibid. 1982, 104, 3503-04.

102. Lange, M. and Mansuy, D., Tet. Lett. 1981, 22, 2561-64.

103. Wolf, C.; Mansuy, D.; Nastainczyk, W.; Deutschmann, G. and Ullrich, V. Molecular Pharmacol 1977, 13, 698

104. Mansuy, D.; Nastainczyk, W. and Ulrich, V.; Vaunyn Schmiedeberg, Arch. Pharmacol, 1974,285-315

105. Mansuy, D.; Battioni, J.P., Chottard, J.C. and Ulrich, V., J. Am. Chem. Soc. 1979, 101, 3971-73 and the references there cited.

106. Olmstead, M.M., Cheng, R.J. and Balch, A.L. Inorg. Chem., 1982, 21 443-48.

107. Battioni, J.P.; Lexa, D.; Mansuy, D. and Saveant, M., J. Am. Chem. Soc. 1983, 105, 207-15.

108. Kelly, S.L. and Kadish, K.M., Inorg. Chem. 1982, 21, 3631-39.

109. Boucher, L.J. and Garber, H.K., Inorg. Chem. 1970, 12, 2644-49.

110. Boucher, L.J., Coord. Chem. Rev. 1972, 7, 289-329.

111. Loach, P.A. and Calvin, M. Biochem. 1963, 2, 361-71.

112. Wolberg, A. and Mannassen, J., J. Am. Chem. Soc. 1970, 92, 2982-91.

113. Anderson, O.P. and Lavallee, D.K., J. Am. Chem. Soc. 1976, 98, 4670-71.

114. Stewart, R.F., Davidson, E.R. and Simpson, W.T., J. Chem. Phys. 1965, 42, 3175-87.

115. "International Tables for X-ray Crystallography", Vol IV, Kynoch Press, Birmingham, England, 1974.

116. Worfield, P.W.R.; Doedeus, R.J. and Ibers, J.A., Inorg. Chem. 1967, 6, 197-204.

117. Anderson, O.P., Packard, A.B. and Wicholas, M., Inorg. Chem. 1976, 15, 1613-18.

118. Westcott, C.C. in "PH Measurements" Academic Press, New York, 1978, P-113.

119. Hoard, J.L. in "Porphyrins and Metalloporphyrins", K.M. Smith, Ed. Elsevier, Amsterdam, 1975, P 317-ff.

120a. Maniken, M.W. and Churg, A.K. in "Iron Porphyrins," A.B.P. Lever and H.B. Gray (eds.), Addison-Wesley, Reading, Massachussets, 1982, part one pp. 141-235.

b. Gouterman, M. in "The Porphyrins," D. Dolphin (ed.), Academic, New York, Vol. III, Part A, pp 1-156, 1979.

121. McLaughlin, G.M., J. Chem. Soc., Perkin Trans. 2, 1974, 136-140.

122. Scheer, H. and Katz, J.J. in "Porphyrins and Metalloporphyrins" K. M. Smith (Ed.), Elsevier, Amsterdam, 1973, pp. 399-535.

123a. Jackson, A.H., in "The Porphyrins," Vol. I, D. Dolphin ed., Acad. Press, New York, 1978, pp. 342-364.

b. Jackson, A.H. and Dearden, G.R., Ann.N.Y. Acad. of Sci., 206, 1973, 151-76.

c. Al-Hazimi, H.M.G.; Jackson, A.H.; Johnson, A.W. and Winter, M., J. Chem. Soc., Perkin Trans. 1, 1977, 98-103.

124. Caughey, W.S. and Ibers, P.K., J. Org. Chem. 1963, 28 269-70.

125a. Silvers, S.J. and Tulinsky, A., J. Am. Chem. Soc., 1967, 89,3331-37.

b. Silvers, S.J. and Tulinsky, A., J. Am. Chem. Soc., 1964, 86, 927-28.

126a. Jenkins, J.G.; Leckey, R.C.G. and Liesegang, J. J. Electron Spectrosc. 1977, 12, 9.

b. Siegbahn, K.; Nordling, C.; Fahlman, A.; Nordberg, R.; Hamrin, K.; Hedman, J.; Johanson, G.; Bergmark, T.; Karlsoon, S.E.; Lindgren, I. and Lindberg, B., "ESCA: Atomic Molecular and Solid State Structures Studies by Means of Electron Spectroscopy", Nova Acta Regiae Soc. Sci. Upsaliensis Ser. IV 20, Almaquist and Wiksells, Upsala, 1967.

c. Siegbahn, K.; Nordling, C.; Johansson, G.; Hedman, J.; Heden, P.-F.; Hamrin, K.; Gelius, U.V.; Bergmark, T.; Werme, L.O.; Manne, R. and Baer, Y., ESCA Applied to Free Molecules, North-Holland, Amsterdam, 1969.

d. For an example of an extensive review, see Scigbahn, K., Chapter 15 in Molecular Spectroscopy, Heyden and Sons, 1977, pp. 227-312.

e. Hollander, J.M. and Jolly, W.L. Accounts Chem. Res. 1970, 3, 193-200.

f. Carlson, T.A. (edited), X-ray Photoelectron Spectroscopy Benchmark Papers in Physical Chemistry and Chemical Physics, V. 2) Dowden, Hutchinson & Ross, Inc., Strousbourg, Pennsylvania.

127. Carrington, A. and Maclachlan, A.D., "Introduction to Magnetic Resonance, "Harper & Row, New York, 1967.

128. Lonquet-Higgins, H.C.; Rector, C.W. and Platt, J.R. J. Chem. Phys. 1950, 18 1174.

129. Fuhrhop, J.H. Structure and Bonding, 1974, 18, 12.

130. Lin, W.C. in "The Porphyrins", D. Dolphin, ed., Academic, New York, Vol. IV, Part B, pp. 355-377, 1979.

131a. Bennet, J.E. and Ingram, D.J.E., Nature (London), 1955, 175, 130.

b. Bennet, J.E. and Ingram, D.J.E., Discuss., Faraday, Soc., 1955, 19, 140.

c. Gibbson, J.I.; Ingram, D.J.E. and Schonland, D. Trans. Faraday Soc. 1958, 26 72.

132. Roberts, E.M. and Koski, W.S., J. Am. Chem. Soc. 1961, 83,1865.

133. Kivelson, D. and Neiman, R., J. Chem. Phys. 1961, 35 149.

134. Harrison, S.E. and Assour, J.M., Paramagn. Resonance, 1962, 2, 855; J. Chem. Phys. 1964, 40 365.

135. Deal, R.M.; Ingram, D.J.E. and Srinivasan, R., Proc. Colloq. Ampere, 12th, 1963, p. 239.

136. Aoyagi, Y., Masuda, K. and Yamaguchi, J., J. Phys. Soc. Jpn. 1967, 23, 1188.

137. Guzy, C.M.; Raynor, J.B. and Symons, M.C.R., J. Chem. Soc. A, 1969, 2299.

138. Roberts, E.M. and Koski, W.S., J. Am. Chem. Soc. 1960, 82, 3006.

139. Hsu, Y.C. Mol. Phys. 1971, 21, 1987.

140. Koniski, S.; Hoshino, M. and Imamura, M., J. Phys. Chem. 1982, 86, 4888.

141. Nordberg, R.; Albridge, R.G.; Bergmach, T.; Ericson, V.; Hedman, J.; Nordling, C.; Scigbahn, K. and Lindberg, B.J., Ark. Kemi 1967, 28, 257.

142. Hendrickson, D.N.; Hollander, J.M. and Jolly, W.L., Inorg. Chem. 1969, 8 2642.

143. Bleaney, B. Phil. Mag. 1951, 42, 441.

144. Alston, K. and Storm, C.B. Biochemistry, 1979 4292-4300.

145. Yokoi, H. and Iwaizumi, M., Bull. Chem. Soc., Japan, 1980, 53, 1489-92.

146. DeBolfo, J.A.;Smith, T.D.; Boas, J.F. and Pilbrow, J.R., J. Chem. Soc., Dalton, 1975, 1523-5.

AUTHOR

Debasish Kuila was born in a village of West Bengal in 1955. After the completion of his B.Sc. with Hons. in Chemistry from University of Calcutta, he went to I.I.T., Madras to do M.Sc. in Chemistry. In fall, 1979 he came to New York to do his graduate studies. He received the Mina Rees Scholarship of 1983. He will join as a postdoctoral associate in the Division of Biophysics and the Department of Biological Chemistry of The University of Michigan, Ann Arbor starting January, 1984.